A Modeling Based Approach Studying Potential for Geothermal System Regeneration

by

Gregory James Conroy Castro

Student Number:	5921538
Main Supervisors:	Dr. Ir. Martin Bloemendal
	Dr. Ir. Phil Vardon
Daily Supervisors:	Dr. Amirhossein Hashemi
	Dr. Ergin Kükrer
Committee Member:	Dr. Alexandros Daniilidis
Project Duration:	February, 2025 - November, 2025
Place:	Faculty of Electrical Engineering, Mathematics and Computer Science Delft, Netherlands
Master:	Sustainable Energy Technology
Track:	Heating and Cooling

A Modeling Based Approach Studying Potential for Geothermal System Regeneration

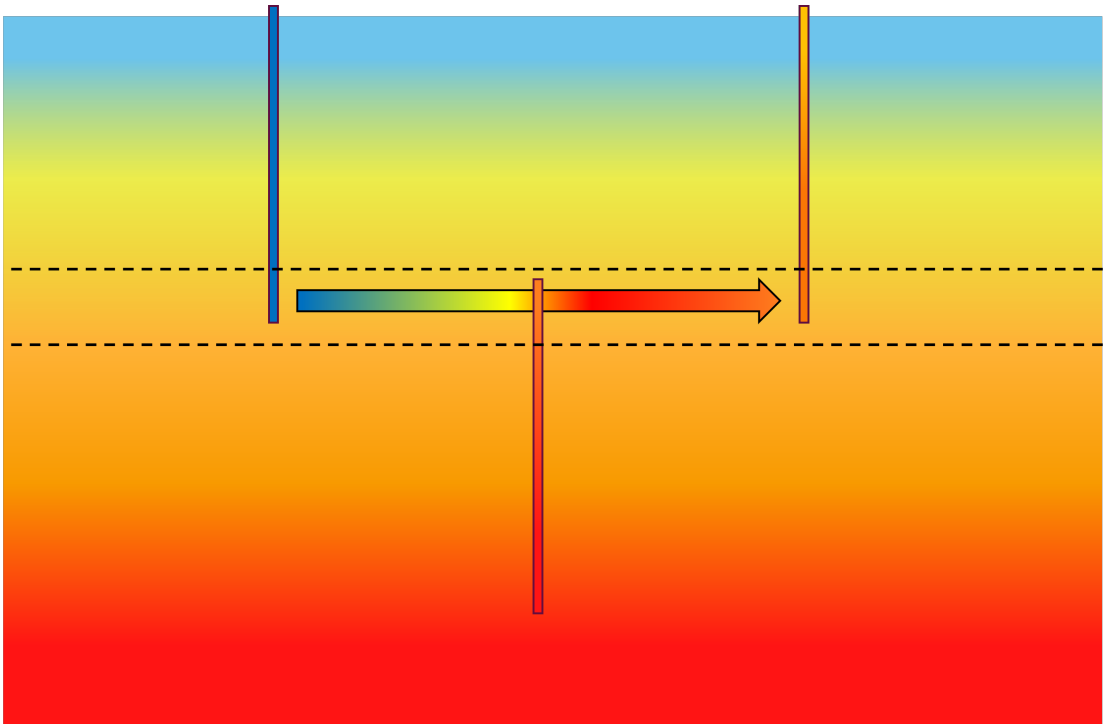

Thesis Report

by

Gregory James Conroy Castro

TU Delft

Abstract

Conduction-dominated geothermal systems are often affected by an underground phenomenon called thermal breakthrough, which limits their functionality and lifetime. This study aims to numerically explore a novel method of addressing thermal breakthrough directly, through the implementation of Geothermal Reservoir Enhancing Geometries (GREGs) within the geothermal reservoir. The aim of these GREGs is to recharge the colder thermal breakthrough plume, thereby extending the lifetime of the modeled geothermal utility through passively transferring heat from deep beneath the geothermal reservoir, into the thermal breakthrough plume. Optimization of the GREGs which include, but are not limited to, dimensioning and placement, are central to this experimentation. 200 years of simulation time is run for every trial, evaluating production temperature, heat fluxes and resultant geothermal lifetime extension due to implementation of GREGs in the geothermal system. Larger-dimensioned GREGs which are less feasible for deep subsurface implementation according to current drilling practices, benefit from increased surface area and therefore increased power output. Conversely, smaller radius GREGs, which are feasible according to contemporary drilling practices, while lower in surface area and individual power output, exhibit nonlinear increases in heat flux per unit area when compared to their larger counterparts. Results also indicate that placement of GREGs near the production well has the potential for increasing lifetime by 5 years under the most feasible GREG scenario, which would add approximately 381,000 MWh of output from the modeled geothermal system. Economics are also discussed, and find that LCoH from this added energy amounts to approximately 30.16 €/MWh. Longer GREGs reaching an additional kilometer into the subsurface did not have a significant impact on geothermal lifetime extension when compared to their shorter counterparts, and tended to see a negative impact regarding economic feasibility. Extending the lifetime of geothermal utilities however, is also practical when considering improved insulation practices of the built environment, represented by decreased heating demands per unit area of consumer floor space. These falling demands could result in a greater reach of direct geothermal heat supply. Therefore, a system integration study was also discussed, in the context of GREG implementation, resulting in significant increases in customers that could be serviced by the geothermal utility as their insulation and consequent energy efficiency improved. The implementation of GREGs was therefore determined to have significant potential in extending the lifetime of conduction dominated systems affected by thermal breakthrough by approximately 8.2%, adding energy security for an extended period of time, and advancing the role of geothermal power in the energy transition.

Preface

First and foremost, I thank God for the opportunity of a lifetime, and making this experience a reality. It is my honor to be completing my thesis under the supervision and guidance of Martin Bloemendal and Phil Vardon at TU Delft - a tremendous thank you to you guys and everything you've done, and for believing in this unorthodox idea and guiding me. Martin, I always enjoyed the lectures you taught, talking to you always put me in a good mood, and that made not just my thesis, but this entire experience in working towards my master's incredible. And to Phil, the scary guy in the room, I knew you'd come around; your feedback was instrumental in this process, and I owe most of my success in this thesis to you - thank you. I would also like to thank my daily supervisors Amirhossein Hashemi and Ergin Kukrer for offering insights and helping me in my day-to-day. Amirhossein, thank you for always being available to help me build my model. It wasn't always an easy process, in fact much of it was trial and error, but I learned to look for solutions in less obvious places and I owe that to you my friend. Ergin, you never really said much, but when you did, it was always well founded, precise and properly thought out - your guidance was reliable and I thank you for that.

A big thank you to the people in my personal life, especially my girlfriend Federica for listening to me ramble about the things that broke in my models and the things that worked, on any given day of any given week. Of course, none of this would be possible without and my parents, and their financial support, love you ma & pa - I miss you more and more each day, I know I'm at home when you guys are around. On that note, special thank you to my best friend and little sister Isabella, I want to make you laugh and smile - I hope this project is something that fulfills that objective. Juanjo, my cousin, that goes for you too - I helped you with your thesis, I'm so thankful you got to be part of mine. Mis tios, Monica y Mike, gracias por siempre recibirme, les quiero.

And this paragraph is to my friends and all the people in the library. I'd like to start with all the Coffee Star crew who saw me most days out of the year. That includes Danny, Luca, Alice, Mateush, Iris, Emma, Emile, Roland, Victoria, Sofi, Sara, Ellie, if I misspelled your names, I apologize, but you should know I wouldn't have gotten this far without all that delicious coffee you poured me. My day ones, Jasna, Josh, Endino, Felix, Deva, Ilaria, Fernando, Leti, Monica, Zohar, Pavan, Shadi, Emi, Marina love you guys, and I miss a lot of you.

To my closest roommates over all this time, Sharada, Daphone and Irati, I couldn't have asked for better roommates. I'll never forget you. Which brings me to my newest roommates, Asia and Anna - I look forward to seeing you every night I come home. Baci tutti.

To David and Alex, the ones who spoke my favorite language, thank you - if I could pack you both into a suitcase I'd bring you everywhere I go. Love you guys. Keep my spirit alive in those dances. Evi, this haircut still slaps, love you. Eric, Orpheas, Yana, talking to you was exactly what I needed some days, love you guys.

I think that's all of them.

Contents

List of Figures

1

Introduction

In a time when climate disasters are being reported with increasing frequency, humanity has adapted by shifting away from fossil fuels, in an effort to address the role it plays in this environmental adversity [1]. In the void space produced from various sectors relying less on fossil fuels, a new demand has been created for what is known as clean energy, an effect that advances a cause called the energy transition.

Decades of study into clean energy has revealed several different avenues for its production, such as wind power, photovoltaic, and hydroelectric. Another notable power source is known as geothermal energy, which works to extract heat from subsurface reservoirs, using a production well and an injection well. Energy is brought up in the form of hot water, via the production well. Once the energy has been extracted from this water, it returns to the reservoir a significant distance away as colder water, via the injection well [2].

Geothermal utilities can generally be categorized under two different scopes: for the production of electricity or the production of heat. Higher heat reservoirs are easily fitted for the production of electricity, which relies on producing steam to spin turbines, while direct-use geothermal is used for producing hot water directly, and conveying it for heating applications [3].

Many colder regions rely on space heating during significant portions of the year - in Europe alone, approximately 50% of all total final energy generation is used for this application. Much of this demand is met with gas fired boilers, or from the electricity grid, which implies additional use of fossil fuels and sustained greenhouse gas production [4]. However, a growing fraction of this demand is now being met via direct-use geothermal, reinforcing its significance in the energy transition [5].

An advantage to geothermal utilities is that they are able to consistently provide heat, and do not depend on intermittent availability of energy resources, which are disadvantages seen in wind and solar power production [6]. However, geothermal utilities come with a notable limitation, for both electrical, and direct use, known as “thermal breakthrough,” which limits both the quality of produced heat, and the lifetime of the utility. Thermal breakthrough happens as a result of the reinjected colder water, which expands in the subsurface in a plume that eventually encapsulates the production well [7]. This in turn lowers production temperature and defines the lifetime of the geothermal doublet, which is often between 30 and 60 years [8].

Ultimately, this marks thermal breakthrough as a significant problem in widespread geothermal investment, as limited operational period and profitable timeline may also make it difficult to justify the significant investment involved in these operations [9]. However, if the limitation of geothermal breakthrough is solved, or improved, the potential for both electrical, and direct-use geothermal applications could greatly increase, both in places that are thermally abundant, and regions which are considered barren in this regard.

Thus far, few methods have been developed to address thermal breakthrough. The most notable way to slow down its advance is to decrease production and injection rates, as the rate of expansion of the cold water plume around the injection well is almost exclusively a consequence of pumping rates. The main disadvantage to this method is that heat extraction also slows with it, handicapping power production. Geothermal systems known as Enhanced geothermal systems (EGSs), which induce artificial porosity and permeability through hydraulic fracturing, have attempted to delay thermal breakthrough through additional fracking, thermal stimulation, and chemical stimulation. While these approaches are often successful in freeing up more heat, and increasing permeability, they often risk opening up preferential flow pathways,

short-circuiting the flow of water within geothermal reservoirs and accelerating thermal breakthrough in these systems [10]. Additionally, they come with high risks of induced seismicity, which can cause damage to structures on the surface, and environmental concerns [11].

In essence, there are few limited interventions for thermal breakthrough, none of which are a perfect solution, as they all come with considerable environmental concerns, and risks in actually accelerating thermal breakthrough. How could the problem of thermal breakthrough be addressed directly, in a way that minimizes environmental impact?

Research Question

Thermal breakthrough is considered to be a limitation in geothermal systems due to the low temperature associated with it. The previous methods of intervention discussed for lightly addressing thermal breakthrough were successful in freeing up more heat, but are not considered successful in delaying thermal breakthrough. The cold temperature of the breakthrough front therefore remains.

Regeneration of this cold water plume to a higher temperature is an application that is less explored, and would constitute a direct intervention in solving the problem of thermal breakthrough. Evidently, deep beneath any geothermal reservoir are layers that are abundant with heat, and this applies even to places with low subsurface heat. There is a thermal gradient associated with every place, and essentially it dictates that as depth increases, so does heat.

Therefore, considering the ubiquity of this stored heat, often relatively close to any geothermal exploitation operation, one may ask the following question: **how could subsurface heat at depth be used to directly address thermal breakthrough?**

Research Objectives for Geothermal Reservoir Enhancing Geometries (GREGs)

Thus, a use-case for this deeper heat, which would be to regenerate the thermal breakthrough plume in conduction driven geothermal operations, is established. In actuality, the plume does absorb this underlain heat over time via conduction, as heat rises from the subsurface, albeit, slowly, with some estimates suggesting it would take hundreds of years for full recovery to pre-production temperatures [12]. While this rate of heat transfer by conduction may be slow, enhancement of it has the potential to accelerate the rate at which heat is transported between these layers, and makes the argument for conducting heat between layers as a theoretically viable approach for recharging the geothermal reservoir.

Therefore, the aim of this study is to introduce a novel method of addressing the thermal breakthrough plume directly, investigating the possibility of overriding its effects, by modeling the capabilities of high heat transfer structures which work passively to bring up heat from deep within the subsurface into the thermal breakthrough path, known as Geothermal Reservoir Enhancing Geometries (GREGs). The research objectives are as follows:

1. GREGs may come in all shapes and sizes. **Investigate the optimal placement and dimensioning of GREGs to maximize geothermal doublet lifetime.**
2. Plenty of heat exists within the subsurface, and becomes more ubiquitous with depth, according to a region's geothermal gradient. **Investigate the extension of geothermal lifetime under the scope of transient heat transfer through modeling the heat transfer properties and final depths of singular GREGs.**
3. The built environment and overall heating demand plays an enormous role in geothermal production rates. As better insulation practices are implemented in surface infrastructure and buildings, heat production will be more efficiently used. **Investigate how the GREGs mesh alongside a geothermal system that supplies heat to a changing built environment.**

2

GREGs

This chapter aims to describe the central idea behind GREGs, and their implementation. Section 2.1 answers the question as to what exactly a GREG is and how it functions in its capacity. Section 2.2 describes their installation process and methods used.

2.1. What are Geothermal Reservoir Enhancing Geometries (GREGs)?

Geothermal Reservoir Enhancing Geometries, otherwise known as GREGs, are sealed vessels that take advantage of natural convection to transmit heat into the geothermal reservoir of a geothermal utility. Under ideal conditions, they are filled with a working fluid, such as water, and installed at a final depth far below the geothermal reservoir, to where they can take advantage of significantly higher temperature domains, according to the thermal gradient. The bottom of the GREG is used to take up heat from lower regions, while the top of the GREG, known as the head, intercepts the reservoir. As the working fluid at the bottom heats up, natural convection takes hold, and the hotter, less dense fluid begins to rise to the top of the vessel.

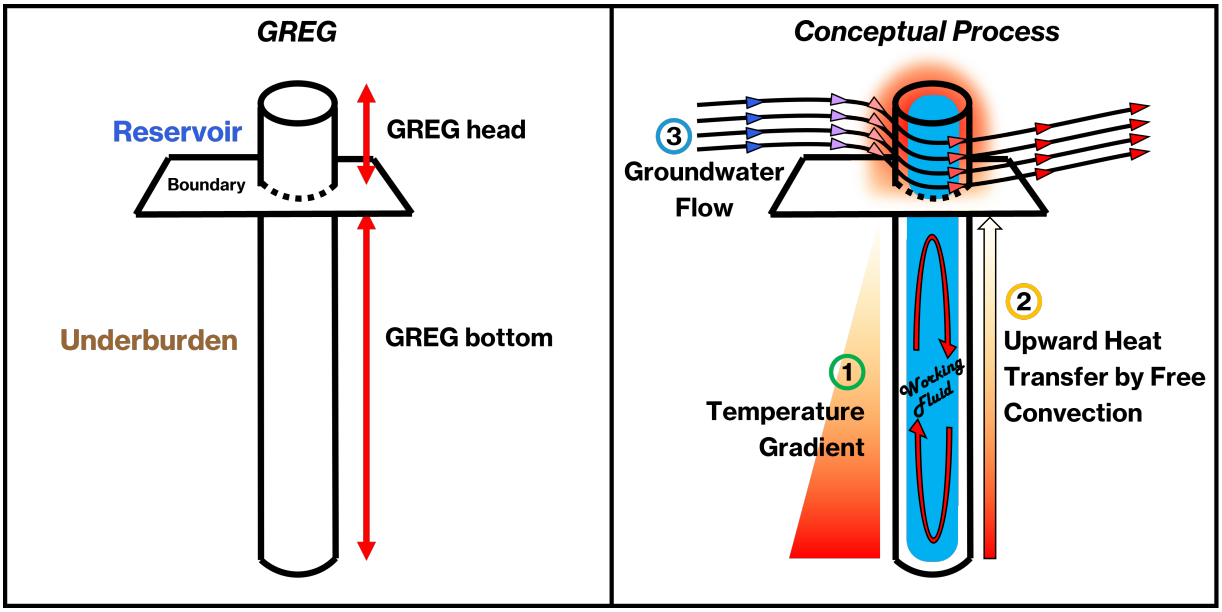

Figure 2.1: Concept of Geothermal Reservoir Enhancing Geometries (GREGs), and how they work.

Once the higher temperature water reaches the top of the vessel, heat is transferred from the fluid to the wall, via convection, and through the wall of the GREG head, via conduction. The heat then transfers from the exterior wall of the head into the geothermal reservoir, primarily via forced convection, where it is picked up by the groundwater flow driven by the geothermal utility, heating it up. This process aims to increase production temperature at the well, which helps to increase the lifetime of the geothermal utility.

2.2. How are GREGs installed?

Installation of GREGs requires drilling, and the transport of the structure down to the depth of installation. One avenue of installation is to execute a drilling scope similar to what would be required for a geothermal well. The casings that would enter the bore would be repurposed as the structure of the GREG. Figure 2.2 describes a 2km long GREG spanning from 1950m to 3950m below land surface (BLS), which was modeled as part of this study.

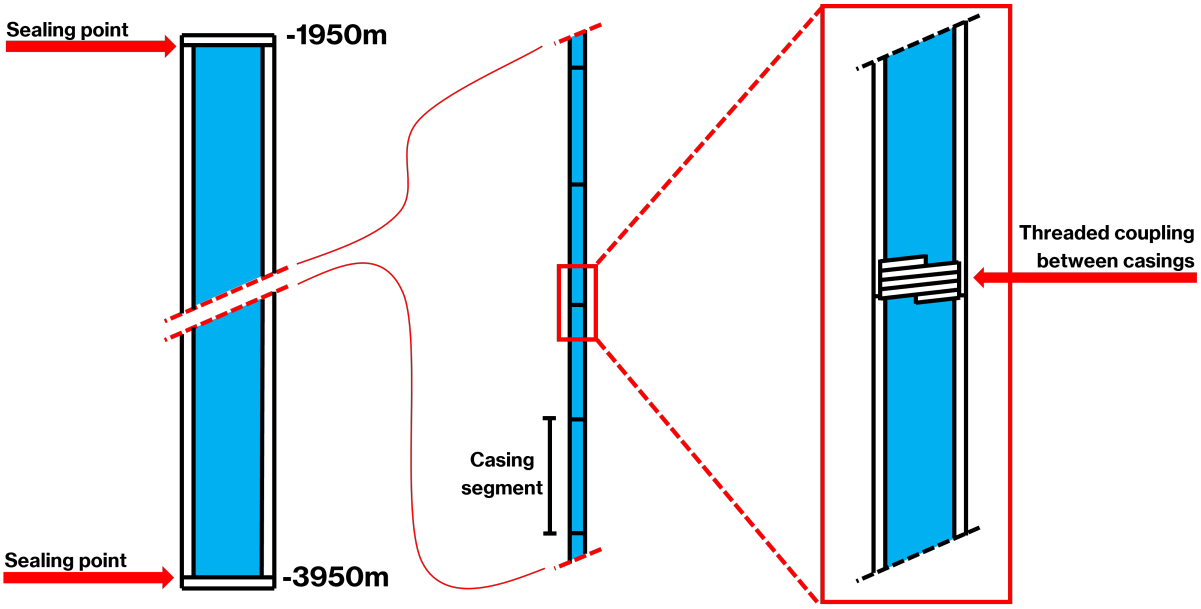

Figure 2.2: Drilling/installation Scope for Geothermal Reservoir Enhancing Geometries (GREGs).

The installation of a GREG would mainly require sealing of the whole structure to contain the working fluid. This would be applied at the top and bottom casings of the GREG, by welding a plate onto the end pieces. Threaded couplings between the casings/segments would also be necessary to seal in the working fluid, which is already a commonly executed practice in geothermal well drillings.

3

Background

In this section, a general review of geothermal systems is offered, along with an outline of the thermal breakthrough problem. Additionally, background research is presented here, addressing methods used by geothermal utilities to limit the approach of thermal breakthrough. A breakdown and categorization of the Dutch built environment energy efficiency is also presented here, as part of an analysis that will follow in the discussion which aims to fulfill the third research objective.

3.1. Geothermal Systems

Extraction potential for geothermal energy mainly depends on steep thermal gradients and adequate geological conditions, involving ample permeability, porosity, and rock matrix heat capacity. A geothermal system works by producing and injecting reservoir water through a pair of production and injection wells, which are installed within the crust of the earth, and referred to as doublets. Heat is then extracted from the produced water using a heat exchanger, cooling down the fluid, which is then reinjected into the reservoir via injection well.

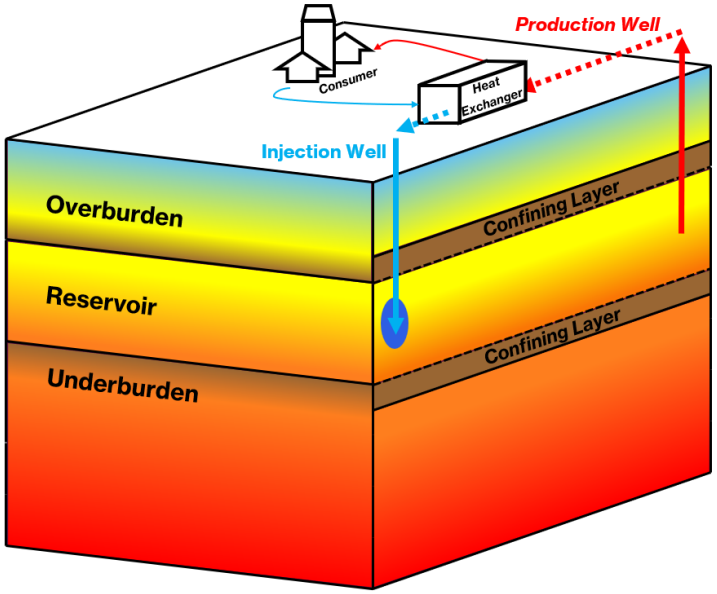

Figure 3.1: Basic concept of geothermal production, injection and use.

One of the main consequences of producing geothermal power is that the constantly injected colder water into the reservoir eventually makes its way to the production well, lowering the temperature of the produced water over time, and eventually saturating the production site entirely with cold water, in a process known as thermal breakthrough. The injected water expands radially from the injection site, pushing away the ambient temperature groundwater, forming a subterranean region of significantly cold water that grows as

time passes. Once the effects of thermal breakthrough decrease the geothermal production temperature past a certain predefined threshold, the lifetime of the geothermal doublet is effectively reached, and the wells are abandoned.

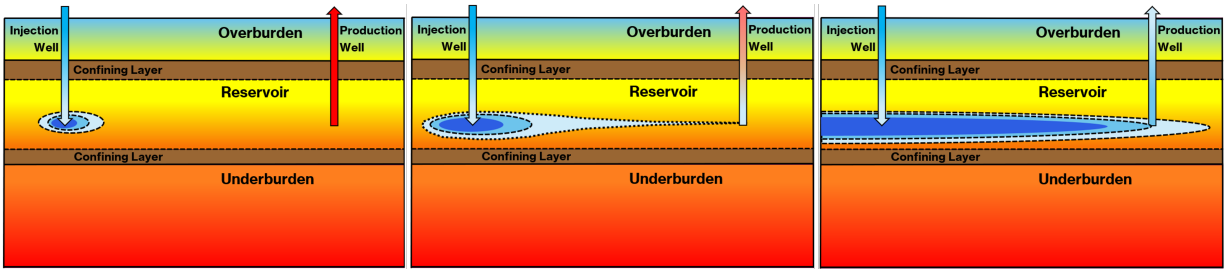

Figure 3.2: Basic concept of geothermal breakthrough. The radius of influence of the cooled injected water starts small in the beginning (left). As time passes, continuous injection of cold water begins to expand this radius of influence, slowly making its way to the production well (middle). Eventually, the thermal breakthrough front is large enough to encapsulate the production well entirely (right).

Research regarding the delay of thermal breakthrough has thus far focused on slowing of pumping rates, as this is the most immediate intervention that can be exacted to slow the advance of the thermal breakthrough plume. This is because the expansion rate of the thermal breakthrough plume is heavily dependent on geothermal injection rates, and the injection rate is dependent on the production rate of the geothermal system. Therefore, the most immediate solution to delaying the advance of thermal breakthrough is to delay heat production from the geothermal utility.

Other subterranean interventions, such as hydraulic fracturing, thermal stimulation, or chemical stimulation may also have an effect on the thermal breakthrough plume, as they are directed to open up more heat resources within geothermal reservoirs. These interventions often lead to immediately increased flow rates and thermal power production, however, often result in short-circuiting of the reservoir layer, through the opening of preferential flow paths which accelerate thermal breakthrough. Additionally, hydraulic, thermal, and chemical stimulation of the subsurface often lead to unintended consequences; outside of accelerated thermal breakthrough, these methods come with high risks of induced seismicity, or groundwater contamination, or both [11]. Therefore, slowing pump rates is essentially the least invasive and consequential course of action, with the largest disadvantage being handicapped geothermal production and lower economic return.

Interestingly, there is an abundance of heat trapped directly below geothermal reservoirs, as suggested by the geothermal gradient of a region. Essentially, subsurface heat increases with depth, and since physical laws find that energy transfers from places of high concentration to low concentration, it is observed that heat from deep within the subsurface slowly trickles upwards, at an average rate of approximately 65 mW/m^2 under normal conditions [13]. Therefore, it is also observed that over time, this heat has the capacity to regenerate the cold water inside a geothermal reservoir, restoring it to its original temperature, albeit, over a long period of time, a recovery which is often predicted over a time scale of centuries [12] [14].

Therefore, very limited research has explored effectively delaying thermal breakthrough, and the limited research which has produced avenues in solving this problem has also highlighted the steep consequences and side effects in employing these strategies. Regenerating the cold thermal breakthrough plume is therefore not deeply explored. Meanwhile, it is known that there is an abundance of heat below any layer used in geothermal exploitation. How could this heat be extracted and channeled up into the thermal breakthrough plume for the purposes of regenerating its heat to extend the lifetime of geothermal well doublets?

3.2. Surface Infrastructure

Most buildings in the Netherlands are associated with energielabels, which are qualifiers that signify a building's yearly energy consumption per square meter of floor space [15]. Much of this energy demand is

by association dependent on space heating and cooling demands, and in turn, outlines its criterion for buildings, referred to as BENG 1. Another standard, known as the BENG 2, ultimately measures maximum allowable primary fossil-fuel based energy consumption of a building [16]. This fossil-fuel based primary energy use also factors into the determination of energielabels of buildings, which are separated by levels corresponding to energy demand per square meter of usable space, spanning from A+++ (lowest energy demand) to G (highest energy demand).

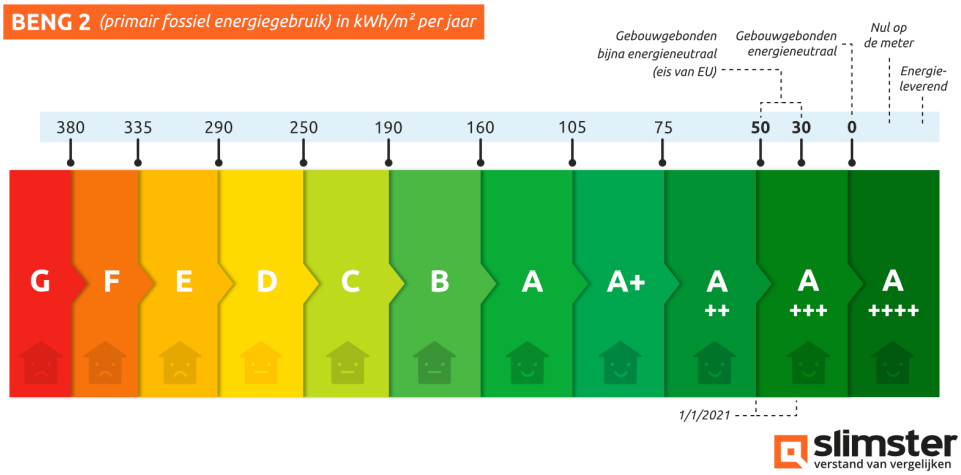

Figure 3.3: Beng-2 Energielabel Designations by kWh/m^2. *Source: https://slimster.nl/energie/energielabel/energielabel-huis/*

Much of a building's energy efficiency is largely in part due to its current level of insulation, as space heating takes up approximately 50% of primary energy usage in Europe [4]. Therefore, a building's ability to hold onto invested heat plays an important role in its ensuing heat demand, which is key to detailing and significantly improving its energy efficiency and subsequent energy label.

Currently, there is a movement to integrate better insulation into new buildings and constructions in the Netherlands, as well as old ones. Existing structures, especially those with low energielabel values of E, F, and G, are projected to integrate improved insulation methods, per the Dutch National Insulation Program (NIP), making them less energy consumptive, and helping the country achieve its goal of insulating 2.5 million homes by 2030 [17].

Buildings subjected to improvements in insulation will require lower heat supply temperatures from their respective District Heating Networks (DHNs) [18], and consequently, reduced heating demands due to higher return temperatures associated with low-temperature heating. With regard to geothermal facilities, a direct consequence of improving building insulation and therefore reducing consumer heating demands, is the reduction of necessary power production from the geothermal utility to meet those same consumers. This would result in another angle in delaying the thermal breakthrough front and extending geothermal doublet lifetime.

Therefore, it is important to review what changes can be made to surface infrastructure to be able to extend either geothermal doublet lifetime, or increase serviced consumers by geothermal heat. How will increasing efficiency of the built environment change consumer demands and result in the increased use of direct use geothermal heat under the scope of GREGs?

4

Approach & Methods

The aim of this study is to characterize the functionality and feasibility of GREGs under the operation of a modeled geothermal utility to establish a locally optimal GREG setup and operation. It is hypothesized that the implementation of GREGs across the underburden and the geothermal reservoir will result in the upward transference of heat contained in the underburden through the GREG, and the deposition of this heat into the incoming cold geothermal breakthrough plume, thereby increasing the production and resulting injection temperatures and the lifetime of the geothermal utility. Therefore, six experiments were developed to quantify the performance of the GREGs, which served to tailor a locally optimal dimensioning and setup of the GREG, which aimed to maximize geothermal lifetime, heat transfer, economic and practical feasibility, and accuracy, as shown below:

Table 4.1: Experimental Approach Summary

EXPERIMENTAL APPROACH

Static GREG Experiments	**Descriptions**
Study 1 - Temperature Analysis:	This experiment aims to answer what is possible from the GREGs under ideal conditions, by applying temperature boundary conditions with which GREG temperatures do not change over the course of the simulation, and measiring the extension of geothermal lifetime and thermal power output into the reservoir as a result.
Study 2 -Position Analysis:	This experiment aims to find an optimal placement of the GREG, which results in the longest geothermal lifetime extension, by applying a 100ºC boundary to the GREG and simulating its thermal output over different locations in the reservoir domain. GREG temperature once again does not change over the course of the simulation, and the extension of geothermal lifetime and thermal power output into the reservoir are measured as a result.
Study 3 - Radius Analysis:	This experiment aims to answer what radial dimensions of the GREG result in the longest geothermal lifetime extensions, applying a 100ºC boundary to the GREG and simulating different GREG radii and resulting surface areas. Thermal output into the geothermal reservoir dependent on varying radius of the GREG in the reservoir domain is measured, along with the extension of geothermal lifetime. GREG temperature once again does not change over the course of the simulations.
Dynamic GREG Experiments	
Study 4 - Thermal Conductivity Analysis:	This experiment aims to answer what affordability the underburden has in terms of heat resources that may be transferred into the reservoir via the GREGs. For this study, the temperature boundary condition is removed from the GREG, and high thermal conductivities are applied to it, assuming it to be a solid, spanning the entire thickness of the reservoir domain, and most of the underburden domain. This assumes that a relatively computationally inexpensive conductivity study may offer insights as to functionality and feasibility of GREGs in place of mounting a computationally expensive CFD study. Once again, thermal outputs and geothermal lifetime extensions are measured, along with the temperature of the GREG head.
Study 5 - Mesh Refinement Analysis:	This experiment aims to measure the accuracy of the previous result by rerunning the Thermal Conductivity Analysis under three different mesh resolutions. These results are compared to those of the previous study.
Study 6 - Final Depth Analysis:	This experiment aims to measure the functionality and lifetime extension of the GREGs as a function of underburden depth. As heat increases with depth, the bottom of the GREG will be exposed to higher temperatures which will affect overall transference of heat and longevity of the GREG. Once again, geothermal lifetime, thermal power output, and head temperature are recorded as the results of this study.

The six experiments are divided into two groups - the first, known as the static experiments, are executed using static temperature boundary conditions over the top 100m of the GREG which exists in the reservoir. This model is relatively computationally inexpensive as it only includes the reservoir layer, and therefore, the heat transfer through the GREG does not represent the heat resources contained in the underburden, but instead, represents a best-case scenario, in which heat does not deplete from the GREG. The dynamic experiments, on the other hand, are experiments meant to probe the heat transference through the GREG, and the heat resources that can be afforded by the underburden - with these experiments, reheating of the thermal breakthrough plume is a direct consequence of the transmittance of heat through the GREG, and the availability of heat in the underburden, and so the temperature boundary condition on the GREG is removed for these experiments. The geothermal operation modeled in both groups of experiments sustains a consistent power output of approximately 8716.7 kW, produced by the temperature difference of 25 K from the production flow, at a rate of 300 m^3/HR. This flow rate is initially produced at a temperature of 75°C, and injected at a temperature of 50°C. Once the geothermal production temperature drops under 70°C, it is assumed that the lifetime of the utility has been reached. Therefore, geothermal lifetime extension is dependent on production temperature, which is dependent, in part, on the performance of the novel Geothermal Reservoir Enhancing Geometries (GREGs). To measure the performance of the GREGs, the dimensioning, positioning, heat transference and feasibility must all be characterized according to the outlined studies.

Prior to experimentation with the GREGs, model controls and parameters which will remain constant throughout the modeling must be established, discussed in Section 4.1. Additionally, the performance indicators are reviewed here. In Section 4.2, a control model is discussed and developed, providing an expected geothermal lifetime without the influence of GREGs, and a reference point for all the GREG experimentation in this study. Section 4.3 describes the model which introduces of a singular GREG head within the reservoir, which is used to conduct the static experimentation. The independent variables probed to measure its effectiveness are also discussed. Section 4.4 discusses the application of the data from Section 4.3 for testing the GREGs in a transient scenario using feasible setups which maximized geothermal lifetime extension, known as the dynamic experiments. This portion of experimentation discusses removing the temperature boundary condition and applying high thermal conductivities to the GREG in order to measure heat transfer from the underburden into the reservoir via the GREG. The purpose of this is to gain an indication as to what rate of heat transfer may be possible from a natural convection setup in which the GREG is filled with a fluid, and to find out how the energy depletion in the underburden evolves over time. Additionally, a mesh refinement is offered after this study, and the effect of final GREG depth is also probed.

4.1. Model Design, Controls and Parameters

The modeled geothermal domain consists of two layers: the reservoir layer, and the underburden layer. In reality, geothermal reservoirs are often bound by two confining layers, known as the underburden, and an overburden, both of which have characteristically low porosities and permeabilities. Due to the nature of this study, however, the overburden is excluded in order to minimize heat transfer through layer boundaries and isolate the thermal effects of the GREGs. The study is composed using three different models:

1. **Geothermal Control Model:** known as the control model, it is only composed of the reservoir layer, which is characteristically absent of heat communication between layers. It is also absent of the GREGs, and measures the behavior of the geothermal reservoir without the influence of the GREGs, producing results that are unbiased to their effects.
2. **Static GREG Model:** known as the Static GREG model, it introduces a singular static-temperature GREG head into the geothermal reservoir, to measure its effects in a computationally inexpensive way, resulting in insights on optimality of placement as well as dimensions. The underburden is once again omitted in this model.
3. **Dynamic GREG Model:** known as the Dynamic GREG model, it introduces the underburden and extends the GREG down into it, to record its functionality under a transient setting, using the insights from the previous study. For this model, thermal insulation is applied at the boundary where the reservoir meets the underburden; this is only overridden by the areas in which the GREGs traverse both layers, so that the heat transfer from the underburden into the reservoir occurring only through the GREG material can be isolated.

It is also necessary to determine realistic geological and thermal power parameters for the models created. This would include parameters pertinent to the geothermal utility, the reservoir, and the underburden, such as production and injection rates, well distancing, temperature gradient, thermal power, layer thickness, and figures for permeability, porosity, thermal conductivity, and density applied to subterranean domains, among other things. Section 4.1.1 discusses the construction and justification of the domains that compose the models, which are the reservoir layer, the underburden layer, and the GREGs. The software used to execute the study is discussed in Section 4.1.2, along with boundary conditions, physics, and meshing parameters.

4.1.1. Domain Construction

This section aims to describe the domains that compose the models. There are three separate domains to consider:

1. Reservoir Layer
2. Underburden Layer
3. GREGs

Reservoir Construction

It has been observed that subsurface conditions for geothermal exploitation in the Netherlands are often thermally adequate between depths of 1.5km and 3km, exhibiting temperature ranges from 60°C to 100°C [19]. Specifically, at a depth of 2000m BLS, temperature ranges between 75°C and 85°C for most of the Netherlands [20]. Thus, the geothermal models in question assumed parameters matching Dutch geology - therefore, a surface temperature of 10°C was chosen, and a temperature of 75°C at a depth of 2000 meters was assumed, amounting to a thermal gradient of 32.5 degrees per kilometer of depth, which is applied to all models in the study.

One notable geothermal project in the Netherlands is located in the city of Delft, which is to produce heat from a reservoir in the Delft Sandstone Member geologic formation. Geological formations typically vary in thickness, and geological report from 2018 probing this reservoir found it to have a maximum thickness of up to 130 meters [21]. However, to simplify the model, a uniform thickness of 100m was chosen for the reservoir domain in the model, respecting the max thickness of found in the report. The reservoir was assumed to exist at a depth from 1950 m BLS to 2050 m BLS, corresponding to temperatures of 73.375°C and 76.625°C, respectively, to achieve an average initial production temperature of 75°C as previously stated. The geometry itself spans horizontally with a length of 3km along the x-axis and a width of 2km along the y-axis. Both the injection well and the production well are assumed to have a vertical screen of the same length as the thickness of the reservoir, spanning from the top of the reservoir, to the bottom. As this system is loosely based on the Delft geothermal research project, a flowrate of 300 m^3/HR is also applied to both the injection and production wells, which is below the maximum flowrate of the actual project, which is approximately 400 m^3/HR [22]. Once again, for simplicity, this rate remains constant. A study on the Delft Sandstone Member found that its porosity ranges from 8% to 25%, while permeability ranges from several tens of mD, to up to 3000 mD [23]. For this reason, a uniform porosity of 20% and a permeability of 150 mD was applied to the reservoir layer of the model.

The last parameters to be applied to the reservoir portion of the model are the density, heat capacity, and thermal conductivity of the material. Reservoir heat capacity and wet thermal conductivity values of 827 J/kgK, and 2.9 W/mK, are applied to the reservoir layer, respectively, which are applicable to a subsurface layer known as the Rotliegend Sandstone formation [24]. The Rotliegend Sandstone Formation ranges in density, between 2500 and 2700 kg/m3. Therefore, the modeled reservoir for this study assumes a density value of 2600 kg/m^3, which is the average between the two extremes of the range. Well spacing can vary many distances, however, a spacing of 1000 m was arbitrarily chosen for the study, according to what has previously been tested [24].

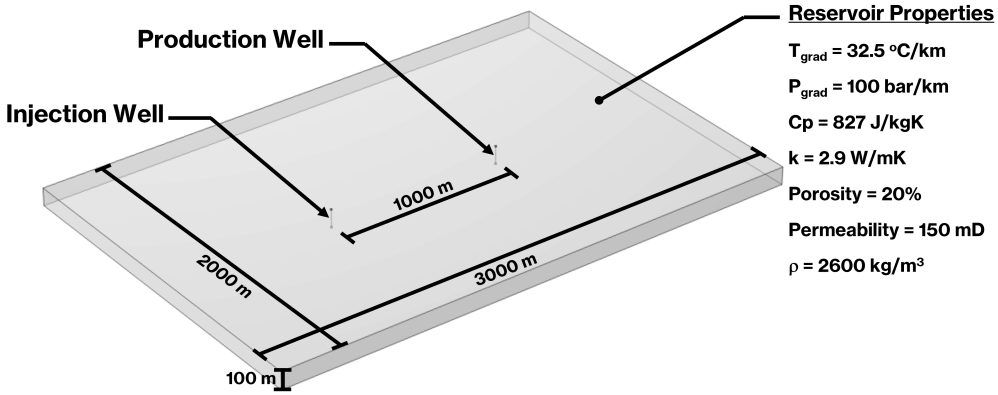

Figure 4.1: Geothermal Reservoir Layer

Underburden Construction

The underburden layer, which underlays the reservoir layer, is responsible for most of the heat resources in later dynamic model, and is initialized as a solid of zero porosity, rather than a saturated porous material. In reality, this portion of the subsurface is saturated, just as with the reservoir layer, and has a porosity and permeability associated with it. However, this model assumption helps simplify computations, as fluid flows between the layers can effectively be stopped, and the GREGs can be properly isolated to study their heat transport via conduction from the underburden. Additionally, the fluid flows in these models use COMSOL's Darcy's Law physics, which assumes non-inertial laminar flow within saturated porous media. The omission of this set of physics from the underburden layer could therefore help to improve model runtime, in a portion of a domain that is inherently there to study conduction as a heat transport mechanism rather than advective effects.

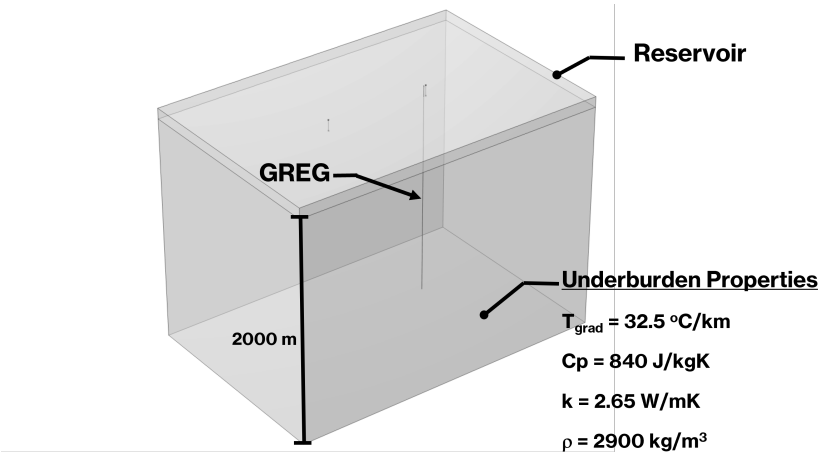

Figure 4.2: Underburden Layer along with the Geothermal Reservoir Layer.

The underburden layer bears the same x and y dimensions as the reservoir, at 3km by 2km. It initially extends down to a final depth of 4,175m BLS, however, for a later study this is changed to 5,175m BLS. The thermal gradient continues from the reservoir into the underburden at the same rate of 32.5 degrees per kilometer. The density, heat capacity, and thermal conductivity of the underburden assumed the properties of 2900 kg/m^3, 840 J/kgK, and 2.65 W/mK, which are properties that have been assumed for a confining layer known as the Limburg Group in the Netherlands [24].

GREG Construction
GREGs will vary in dimensions according to the portion of the study that is being executed. However, the general format is that the GREG is a cylindrical element, with varying radii and lengths to be tested. For the static studies, which are discussed below, the GREG is arbitrarily initialized as solid aluminum metal, at a static temperature. For dynamic studies, which measure its capacity to transfer heat, it is initialized as a solid blank material initially at 75°C, with varying thermal conductivities depending on the portion of the study, and the heat capacity and density of water. The reason for it assuming the properties of water is because the proposed GREGs ideally will be fluid filled structures that can accelerate heat transport via natural convection, and water is generally an agreeable and feasible option in terms of availability. While this approach is ineffective at capturing how water would behave in place of natural convection, it does assume the other properties of the proposed working fluid of the GREG.

4.1.2. Software, Boundary Conditions, and Governing Equations

COMSOL Multiphysics was the software chosen for running this study, not only due to its well-documented application in the geothermal field, flexibility in defining domain geometries and its ability to easily control the meshing sequence [25], but also due to its streamlined, user-friendly interface. This software employs the Finite Element Method (FEM), which works to break down model domains into relatively small, discrete geometries of constantly shifting information, according to the physics involved, to provide large scale results. This study employed COMSOL's Darcy's Law physics, as well as Heat Transfer in Solids and Fluids Physics in time-dependent studies.

Darcy's Law
Darcy's law was applied only to the reservoir layer, as prior study has demonstrated its capability for studying the fluid flows in permeable domains [25]. This set of physics is governed by the following equations:

$$\frac{\partial}{\partial t}(\epsilon_p \rho) + \nabla \cdot (\rho \mathbf{u}) = Q_m \tag{4.1}$$

$$\mathbf{u} = -\frac{k}{\mu}(\nabla p - \rho g) \tag{4.2}$$

where ϵ_p stands for porosity, ρ is the fluid density (kg/m^3), **u** stands as Darcy velocity (m/s), Q_m is the mass source term $kg/m^3 s$, k is the permeability of the porous medium (m^2), μ is the dynamic viscosity of the fluid $(Pa \cdot s)$, p is the pore pressure in Pa, and g is the gravitational constant $(9.81 m/s^2)$. The initial condition is as follows:

$$P = p_{ref} - p_{gradient} z \tag{4.3}$$

where P is pressure (Pa), p_{ref} is the reference pressure (Pa) taken at the surface as $1bar$, $p_{gradient}$ is the pressure gradient $(100bar/km)$, and z is depth (m).

Pressure gradient is applied to the reservoir domain as a whole, and the vertical walls assume a pressure boundary equal to the gradient at that depth [25]. Furthermore, the ceiling, the floor, and the GREG walls have the No Flow boundary condition applied to them. No flow is applied to the floor to omit any outside influence which may interfere with the measure of heat output via the GREG. Additionally, there is no overburden layer, so the no flow boundary is already applied here, and since the GREGs are solid, non-porous structures, Darcy's Law does not apply to them.

Heat Transfer in Solids and Fluids
Due to the nature of this study, Heat Transfer in Solids and Fluids was applied across all domains, which includes the reservoir, underburden and GREGs, as the models aim to measure production well heat in the reservoir, which is dependent on heat transfer out of the GREGs, and consequently, the heat transfer into them from the underburden. This module is described by the following equations:

$$\rho c_p \frac{\partial T}{\partial t} + \rho c_p \mathbf{u} \cdot \nabla T + \nabla \cdot \mathbf{q} = Q + Q_{ted} \tag{4.4}$$

$$\mathbf{q} = -k\nabla T \tag{4.5}$$

where ρ stands for material density (kg/m^3), c_p stands for material heat capacity (J/kgK), **u** stands as Darcy velocity (m/s), T represents temperature (K), **u** represents the Darcy velocity (m/s), **q** represents heat flux (W/m^2), Q represents additional heat sources (W/m^3), Q_{ted} stands for thermo-elastic damping (W/m^3), and k represents the material's thermal conductivity. The initial condition takes surface temperature and temperature gradient according to depth as follows:

$$T = T_{ref} - T_{gradient}z \tag{4.6}$$

where T represents temperature (K), T_{ref} stands for surface temperature, which is assumed to be 10°C, $T_{gradient}$ is the temperature gradient $(32.5K/km)$, and z is depth (m).

A temperature gradient is indiscriminately applied to the reservoir domain and the underburden layer, which relates increases in heat with increases in depth. Thermal insulation is applied to the ceiling of the reservoir, the floor of the reservoir (which coincides with the ceiling of the underburden), and the floor of the underburden. The floor of the underburden and the ceiling of the reservoir do not neighbor any other domains, so these insulation layers are native to the design of the study. The thermal insulation boundary between the reservoir and underburden however, is applied to limit heat transfer between the layers only through the GREGs, so that this data may be isolated, measured, and compared to the control model, which is also isolated from any other layers, which is discussed in 4.2. Additionally, thermal insulation is also applied to the vertical walls of the underburden, because it is assumed that no additional heat outside of these boundaries will make significant changes to the end results. The walls of the reservoir layer on the other hand, assume the open boundary boundary condition, with the same initial condition according to the temperature gradient serving as the upstream temperature, primarily to allow lower heat from the injection to escape along the sides of the model, mirroring what would happen in a more realistic setup, in which the subsurface is not bounded by walls.

Meshing and Tolerance
Within the COMSOL solver module, absolute tolerance was set to 0.001. Relative tolerance was set to be controlled by the physics of the models. A total of four nodes were used for building the mesh:

1. Free Quad - applied to the cylindrical faces of GREGs, using maximum element size of equal to the GREG radius, and a minimum element size of GREG radius divided by 2.5, for a final 32 elements per face - later to be changed in the mesh refinement study.
2. Swept Mesh - applied along the length of the cylindrical GREG domains, which takes from the free quad node previously described, at a maximum element size of 0.5m.
3. Free Tetrahedral No.1 - applied to the reservoir layer, at maximum and minimum element resolutions of 60m and 0.5m, respectively - maximum element growth rate, curvature factor and narrow region resolution are set at 1.3, 0.2 and 1, respectively, along with Distribution nodes applied to the injection and production well line elements, for a total of 14 nodes per line element.
4. Free Tetrahedral No.2 - applied to the underburden layer, with maximum and minimum element resolutions of 60m and 0.5m, respectively - maximum element growth rate, curvature factor and narrow region resolution are set at 1.3, 0.2 and 1, respectively.

4.2. Geothermal Control Model

This model only employs the reservoir layer, as well as the injection and production wells, as seen on Figure 4.2. It serves to probe the natural evolution of the production temperature without the influence of the GREGs which are the objective of this study. The performance indicator of this study is therefore the production temperature and resulting geothermal lifetime.

4.3. Singular Static GREG Model

This model introduces the conceptual cylindrical GREG elements within the reservoir layer only, effectively spanning the thickness of the reservoir layer (100m). The performance indicators in this study are the

production temperature, and additionally, the heat flux, which provides insights as to their effectiveness per unit surface area, as well as in their totality, only within the reservoir. Omitting the underburden layer also makes this study less computationally expensive, and is used to determine and fine-tune favorable setups for consequent transient studies. A visualization of the Static GREG model is offered in Figure 4.3 below, along with parameters which will be changed:

- Static temperature, assuming position at x = 0m, radius = 5m.
- Position, assuming Temperature = 100°C, radius = 5m.
- Radius, assuming x = -475m and +475m, Temperature = 100°C.

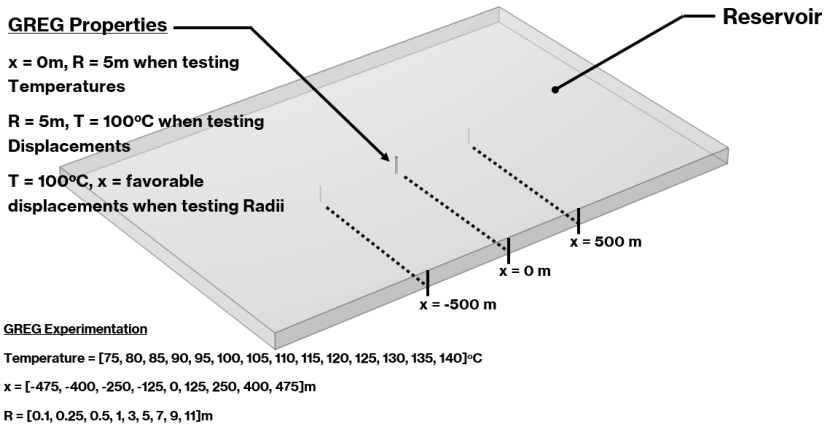

Figure 4.3: Static Model - Geothermal Reservoir with Static GREG

This model is used to answer the first research objective, which is to find an optimal GREG setup which maximizes geothermal lifetime, taking into consideration GREG temperature, positioning and dimensions as independent variables for this study. Based on the results seen here, a model is produced, which aims to measure the rechargeability of the thermal breakthrough plume and dynamic performance of the GREGs, according to the heat resources stored in the underburden.

4.4. Dynamic GREG Model

In this study, the underburden is introduced, along with the full length of the GREG. Once again, the GREG traverses both the reservoir and the underburden, conducting higher temperature heat from the deeper underburden, and transmitting it upward into the thermal breakthrough plume, which is lower in temperature. The objective of this portion of the experiment is to assess this transmittance of heat across the length of the GREG up into the reservoir, and evaluate the deposition of heat, by measuring the increased sustained production temperatures at the production well. Therefore, the static temperature boundary condition along the surface of the GREG is removed, and its temperature becomes dynamic, changing with time.

The initial idea was to model the performance of the dynamic GREG as a fluid filled vessel, to study the upward heat transfer through natural convection. Low computational affordability however, along with the relatively high computational requirements to perform this computational fluid dynamics (CFD) study at this scale rendered this option chronologically impossible. Therefore, in place of mounting this CFD study, a range of thermal conductivities was applied to the GREG as a material characteristic, in order to simplify the case of natural convection, mirroring what provisions may be possible from the underburden, through the GREG and into the reservoir. Thus, the primary performance indicator for this study is once again production temperature and ensuing geothermal lifetime. Heat flux is also examined, and the evolution of the GREG head temperature is also recorded.

The thermal conductivity study is then repeated under different mesh sizes, to conduct a mesh refinement analysis. This helps to ensure the precision of the results. Lifetime extension, production temperature, head temperature and power output are once again observed in this portion of the study.

The next portion of the study is to measure performance indicators according to the final depth of the GREG. This is done by extending both the underburden and the GREG downwards by an additional kilometer, effectively extending the length of the GREG by 50%, and increasing its capacity to take up heat. A bulleted list of these analyses is presented below, along with a visualization of the model used to study dynamic properties of the domain, as Figure 4.4:

- Thermal Conductivity
- Mesh Size
- GREG Depth

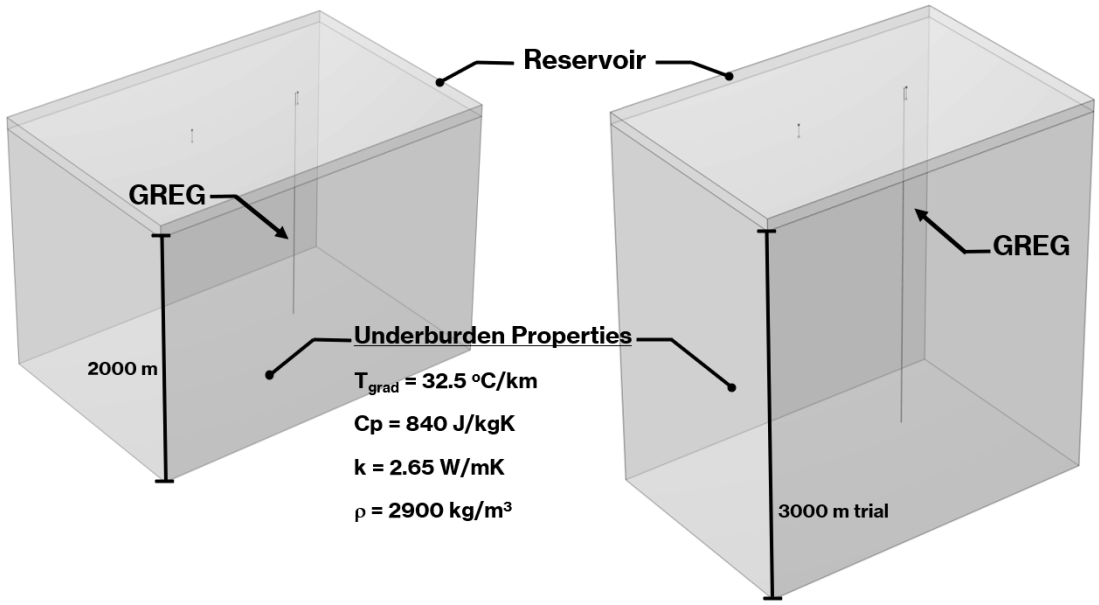

Figure 4.4: Dynamic Model - Geothermal System used to experiment on dynamic GREGs with varying thermal conductivities and final depths, along with a mesh refinement study.

The dynamic studies aim to fulfill the second research objective using this extended model, which will measure not only the underburden's capacity to transfer heat, and extend the lifetime of the geothermal utility, but also the rate at which this heat transfer is sustained. This will conclude the experimental chapter.

5

Results

In this section, the results of the models will be presented. Section 5.1 discusses the control model and its standard project lifetime without the influence of GREGs. Section 5.2 discusses the results from the static experiments, which includes the temperature, proximity, and radius analyses. Section 5.3 discusses the results from the dynamic studies, which includes the thermal conductivity analysis, mesh refinement study, and depth analysis.

5.1. Geothermal Control Model Results

The results suggest that under the control setup, the geothermal lifetime is 61 years, which is marked upon crossing the temperature threshold of 70°C. By year 200, the injection temperature has dropped to 36.291°C, and the production temperature has dropped to 61.291°C, always reflecting the 25-degree temperature difference for the sustained power production, as shown in Figure 5.1.

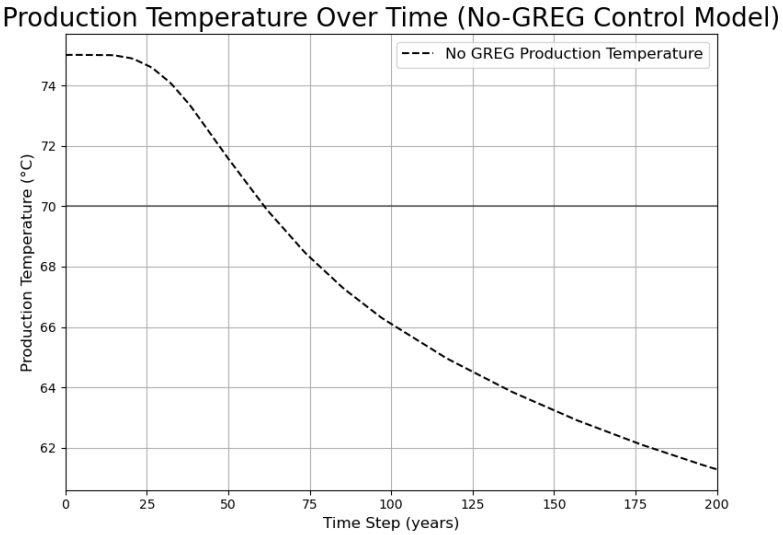

Figure 5.1: Production Temperature evolution of control model (no GREG).

This geothermal lifetime value of 61 years is representative of the reservoir setup and characteristics outlined in the reservoir construction section, without the implementation of GREGs. The aim in the subsequent studies is to see how this value changes upon introducing the GREG into the reservoir domain, and changing its parameters and characteristics.

5.2. Singular Static GREG Model Results

As a reiteration, this model applies the same reservoir conditions as the control model, but introduces the GREG. The study begins with the cylindrical GREG initialized at x = 0m, equidistant from both the injection well, and production well, at a radius of 5 meters. The simulation time was once again set for 200 years. These serve as controls for the first leg of this study, which tests static temperature settings of the GREG.

The analysis of GREG position follows this study, setting the GREG to a temperature of 100°C across all trials, and retaining the 5 meter radius. From here, the simulation is re-run for various positions between the injection well and production well.

Finally, an analysis on GREG radius is done, taking the positions which maximize geothermal lifetime from the previous study, and testing a range of radii on these positions, retaining the temperature setting of 100°C Celsius.

The insights from these studies are used to run the following portion of the study, which addresses the model as a dynamic system.

5.2.1. GREG Temperature Analysis

The temperature analysis will test the GREG at a static temperature boundary condition for each simulation, from 75°C, to 140°C in 5-degree increments, assuming that under real transient conditions and natural convection, the head of the GREG may stabilize near the average temperature of the subsurface between the top and bottom of the GREG for a sustained period of time. Therefore, these tested temperatures are meant to represent possible final lengths/depths of the GREG; for example, a 1km GREG starting from 2km BLS, at 75°C would average around 90°C, and a 4km GREG starting from 2km BLS and reaching a depth of 6km BLS would average around 140°C. This list of tested temperatures then provides insights as to how final depth of the GREG may relate to final thermal power output, and geothermal lifetime extension. For the purposes of later studies, the temperature contour of 100°C is outlined in black due to this being a conservative reference result used in later experimentation to represent a 2km long GREG.

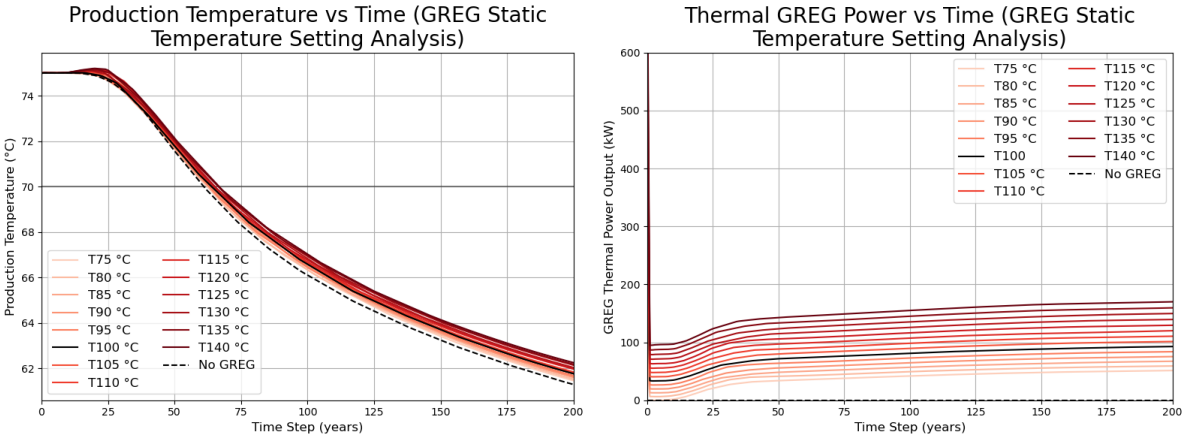

Figure 5.2: Static GREG Temperature Results for production temperature (left), and GREG power output over simulation time (right).

Compared to the control scenario, the GREG temperature that resulted in the lowest geothermal doublet lifetime was the one with the lowest temperature setting out of the trials, which was 75°C, raising the lifetime of the geothermal doublet by only 1 year compared to the control model, for a total of 62 years. The GREG temperature that resulted in the highest geothermal doublet lifetime was the one set at the highest tested temperature, which was 140°C, raising the lifetime of the geothermal doublet by 5 years more than the control, for a total of 66 years; furthermore, an end-of-simulation (EOS) temperature increase of 0.959 degrees is recorded for this trial, when compared to the control, while the 75°C GREG saw an EOS temperature increase of 0.169 degrees. Additionally, the 100°C scenario saw geothermal lifetime increase to 64 years, or 3 years more than the control.

Final power productions for 75°C, 100°C, and 140°C set GREGs were 35.74, 74.21, and 146.60 kW by lifetime, respectively, and 51.31, 92.72, and 169.93 kW by EOS, respectively. It is important to note that these thermal power outputs were not at equilibrium, as injection temperature consistently drops with production temperature, therefore increasing the influence of the static-temperature set GREGs throughout ever decreasing temperature of the thermal breakthrough plume.

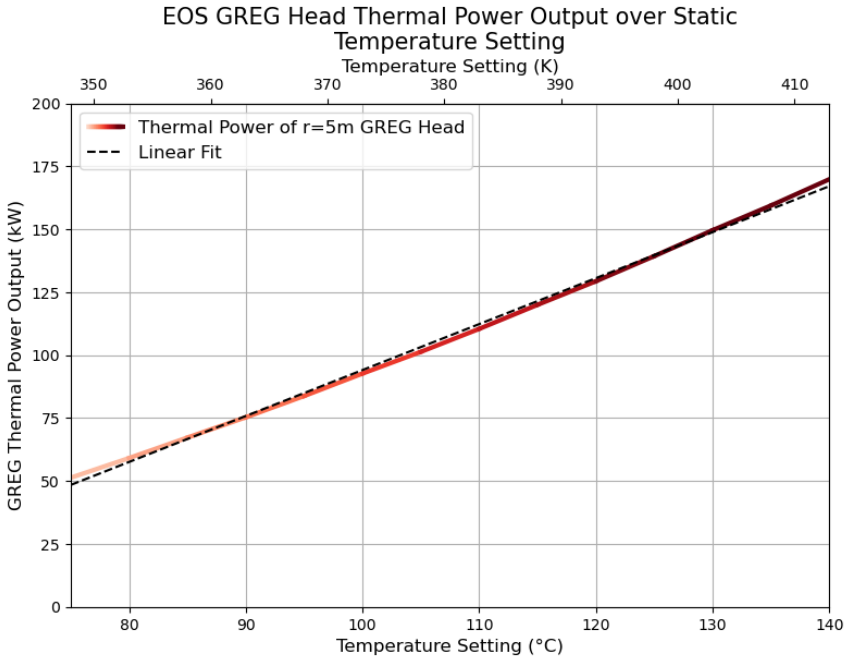

Figure 5.3: EOS GREG Power as static temperature setting increases.

A linear relationship is observed in both the production temperature, and power production as static temperature of the GREG rises, due to a larger temperature difference between the GREG and reservoir temperature, and could be described by the following equation:

$$P_{output}[W] = (1826.5[\frac{W}{K}])T_{GREG}[K] - 587439.2[W] \tag{5.1}$$

$$R^2 = 0.9981 \tag{5.2}$$

The data suggests that increases in head temperature result in longer geothermal lifetimes, and higher heat outputs. A maximization of GREG head temperature is hypothesized to be achieved via deeper GREGs, however, economic feasibility may limit deeper implementations. For now, a temperature setting of 100°C is assumed for the following studies, assuming a slightly lower equilibrium temperature than what would be expected from a 2km GREG, which is considered the standard length for GREGs in later portions of the study.

Table 5.1: Temperature Analysis Summary of Results.

GREG Temperature	Lifetime (yr)	Lifetime Change (yr)	Lifetime Heat Flux Output (W/m^2)	Lifetime Power Output (kW)	Lifetime Energy Output (MWh)	EOS Power Output (kW)	EOS Production Temperature (°C)	EOS Production Temperature Change (°C)
No GREG (control)	61	NA	NA	NA	NA	NA	61.291	NA
75 °C	62	1	11.4	35.7	11697	51.3	61.46	0.169
80 °C	62	1	13.6	42.9	16149	59.1	61.52	0.233
85 °C	62	1	16.0	50.3	20118	67.3	61.60	0.307
90 °C	63	2	18.5	58.1	25035	75.3	61.63	0.335
95 °C	63	2	21.0	65.8	30062	83.8	61.68	0.389
100 °C	64	3	23.6	74.2	35024	92.7	61.77	0.476
105 °C	64	3	26.3	82.6	39979	101.4	61.80	0.507
110 °C	64	3	28.9	90.8	45188	110.5	61.84	0.548
115 °C	64	3	31.7	99.5	50436	120.0	61.97	0.679
120 °C	64	3	34.5	108.4	55728	129.4	61.98	0.687
125 °C	65	4	37.5	117.9	61645	139.4	62.04	0.745
130 °C	66	5	40.7	127.7	68191	149.7	62.14	0.849
135 °C	66	5	43.6	136.8	74169	159.5	62.18	0.891
140 °C	66	5	46.7	146.6	79917	169.9	62.25	0.959

**EOS: End of Simulation (200 years)*

5.2.2. GREG Position Analysis

The purpose of this portion of the study is to measure the influence of GREG position on production temperature and geothermal lifetime extension. There is 1 km between the injection well and production well. It is hypothesized that the middle region which has been tested thus far (at x = 0m, known as the origin) may have the lowest groundwater velocity in the line between the injection well and production well, and therefore, longest amount of contact time between the thermal breakthrough plume and the GREG. However, higher groundwater velocities are expected close to the injection well and production well (x = -500m, and x = 500m from the origin, respectively), and are expected to offer different results. Therefore, GREG positions tested were -475m, -400m,-250, -125m, 125m, 250m, 400m, and 475m from the origin, along the x-axis. To clarify, distances are defined according to the origin, which is the center of the domain, and the midpoint between the injection well and the production well. Negative distances approach the injection well, which is at x = -500m, and positive distances approach the production well, which is at x = 500m. Trial results are from GREG placement directly in line between the injection and production wells, with no deviations in the negative or positive y direction. Once again, GREG radius is maintained at 5 meters, and the GREG is set at a static temperature of 100°C. The result from the GREG temperature setting of 100°C and position at x = 0m from the previous study is therefore used as a reference point and is represented as a black contour, shown in the following results (Figure 5.4):

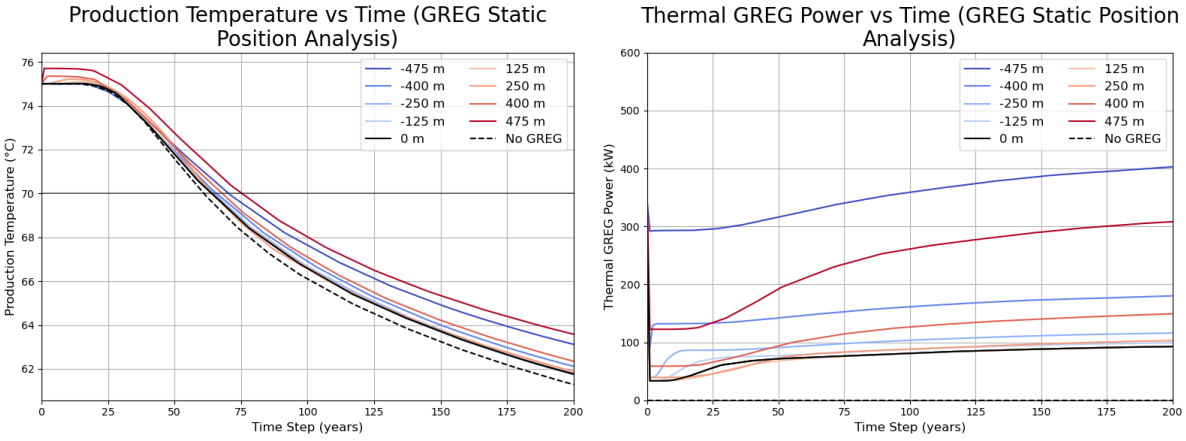

Figure 5.4: Static GREG Position Results for production temperature (left), and GREG power over simulation time (right).

As a reiteration, the results from the static temperature analysis saw a geothermal lifetime increase of approximately 3 years when placing the static 100 degree Celsius GREG at an equal distance from both

the injection well and the production well, represented by the solid black contour in Figure 5.4. The results indicate that the production temperature, and geothermal lifetime sees significant increases as the GREG placement approaches either the injection well, or the production well, seeing final geothermal lifetimes of 70 years, and 75 years, respectively. This is a 9 year increase in geothermal lifetime compared to the control study when the center of the GREG is placed close to the injection well (at x = -475m), and a 14 year geothermal lifetime increase when it is placed close to the production well (at x = 475m). This finding also highlights an asymmetry in the model, showing a lifetime increase difference of 5 years between the two opposing placements.

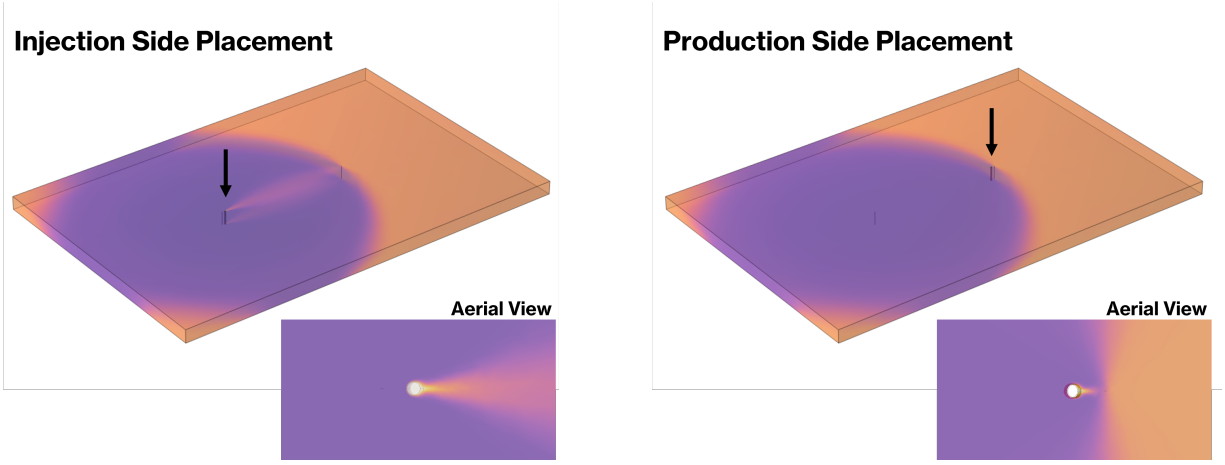

Figure 5.5: Model visualization showing injection well side placement of 5m radius GREG (left) compared to GREG placement near production well (right).

While the placement of the GREG results in higher production temperatures and longer lifetime when placed near the production well, it also results in decreased fluxes and thermal output when compared to the placement near the injection well at the same distances. This result reflects a converse asymmetry from what was previously seen in the production temperature analysis, showing that thermal output is significantly increased at the injection side placement (x = -475m), at 402.9 kW by EOS, rather than the production side placement (x = 475m), at 308.1 kW. However, the general conclusion is that the production side placement achieves favorable results between the two opposites, as it adds 5 additional years to geothermal lifetime over the injection side placement, with only 70% of the power output by lifetime, setting it up as a significantly more efficient placement.

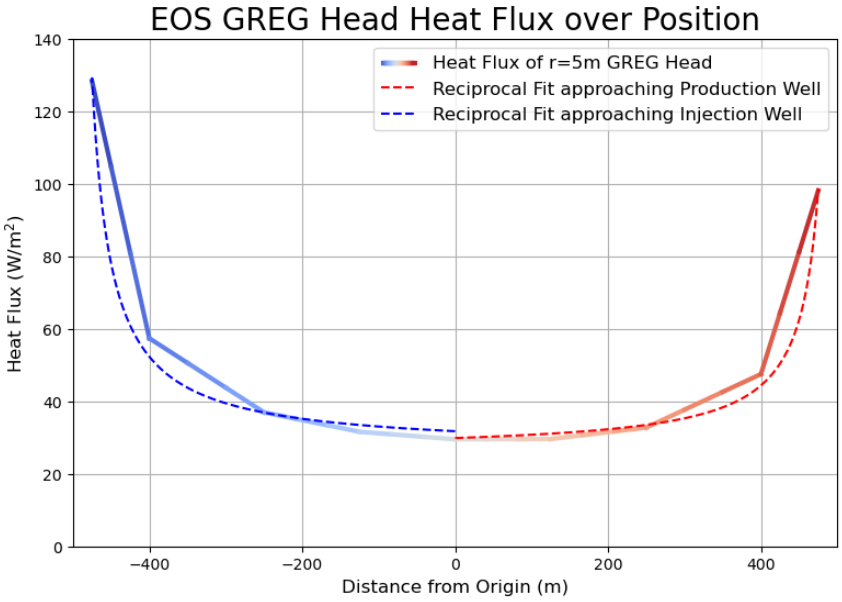

Figure 5.6: Final EOS heat flux of GREG compared to different tested proximities to wells.

The relationship between heat flux and GREG distance from the origin by end of simulation can be represented using the reciprocal relationship offered below, for both, production side, and injection side (for injection side, convert all x-values to positive):

$$q_{Production}[\frac{W}{m^2}] = \frac{1811.52[\frac{W}{m}]}{x_{Prod.Well}[m] - x_{GREG}[m]} + 26.25[\frac{W}{m^2}] \tag{5.3}$$

$$R^2 = 0.9962 \tag{5.4}$$

$$q_{Injection}[\frac{W}{m^2}] = \frac{2568.10[\frac{W}{m}]}{x_{Inj.Well}[m] - x_{GREG}[m]} + 26.62[\frac{W}{m^2}] \tag{5.5}$$

$$R^2 = 0.9949 \tag{5.6}$$

Based on these results, the most favorable placement of the GREG appears to be at the production side, as it maximizes the geothermal doublet lifetime, and it does so with less energy output when compared to the injection side placement. This could also prove beneficial in the transient simulations, as slowed depletion of energy from the GREG could better preserve the heat in the underburden, making it last longer. However, the injection side placement remains as a point of interest, as thus far it is unclear as to how this asymmetry in results would behave under changing GREG dimensions.

Table 5.2: Position Analysis Summary of Results

GREG Position from origin (m)	Lifetime (yr)	Lifetime Change (yr)	Lifetime Heat Flux (W/m²)	Lifetime Power Output (kW)	Lifetime Energy Output (MWh)	EOS Heat Flux (W/m²)	EOS Power Output (kW)	EOS Production Temperature (°C)	EOS Production Temperature Change (°C)
No GREG (control)	61	NA	NA	NA	NA	NA	NA	61.291	NA
-475	70	9	107.0	336.0	191281	128.3	402.9	63.12	1.832
-400	65	4	47.4	148.8	80456	57.4	180.2	62.12	0.828
-250	64	3	30.2	94.7	49666	37.0	116.0	61.83	0.538
-125	64	3	25.5	80.0	40216	31.6	99.2	61.75	0.454
0	64	3	23.6	74.2	35024	29.5	92.7	61.77	0.476
125	63	2	23.2	73.0	31891	29.6	93.0	61.84	0.552
250	63	2	25.5	80.0	33367	32.8	102.9	61.88	0.590
400	67	6	34.6	108.6	48594	47.5	149.1	62.35	1.061
475	75	14	74.9	235.1	113014	98.1	308.1	63.58	2.290

5.2.3. GREG Radius Analysis

The previous results suggest that placing the GREG close to the production and injection wells results in an increase in production temperature, geothermal lifetime, and power output, when compared to placements farther away from either well. Furthermore, production temperature as well as geothermal lifetime is boosted when the GREG is placed close to the production well in comparison to placement near the injection well, while also resulting in lower heat output. Conversely, while GREG placement close to the injection well results in a higher thermal output, it does not increase lifetime as much as production well placement. This asymmetry in the system merits additional probing into the positioning close to the injection well. Therefore, the control positions determined for the analysis of varying radii of the GREG are -475m, and 475m from the origin. This study once again retains the static GREG temperature of 100°C.

The radii being tested in this study are 0.1m, 0.25m, 0.5m, 1m, 3m, 5m, 7m, 9, and 11m, both at the position close to the injection well, and the position close to the production well. Previously, the 5 meter radius GREG was used for study at a position of 475m away from the origin. This meant that the outer edge of the GREG was at a distance of 480m from the origin, or 20m away from the well. Therefore, it was necessary to adjust the positions of the GREGs such that their outer edge also coincided with a 20m distance from the well. In this case, the central position of the GREG varies between x = +/- 479.9m for GREG of R = 0.1m, to x = +/- 469m for GREG of R = 11m. The results are set up so that a negative radius is significative of GREG placement close to the injection site, while positive radii correspond to GREG placement near the production site. The blue contours in Figure 5.7 represent GREG placement near the injection site, with color intensity increasing with GREG radius. The red contour represents the GREG placement on the production side, once again, with color intensity increasing with GREG radius. In this case, the reference data are those of the 5 meter radius GREGs, at x = -475m and x=475m from the previous study, colored in blue (near injection) and red (near production), represented by dash-dotted lines. The 5 meter radius GREG at x=0m is also present, represented by the black dash-dotted line. Finally, the black dashed line represents the control model results without influence of GREGs.

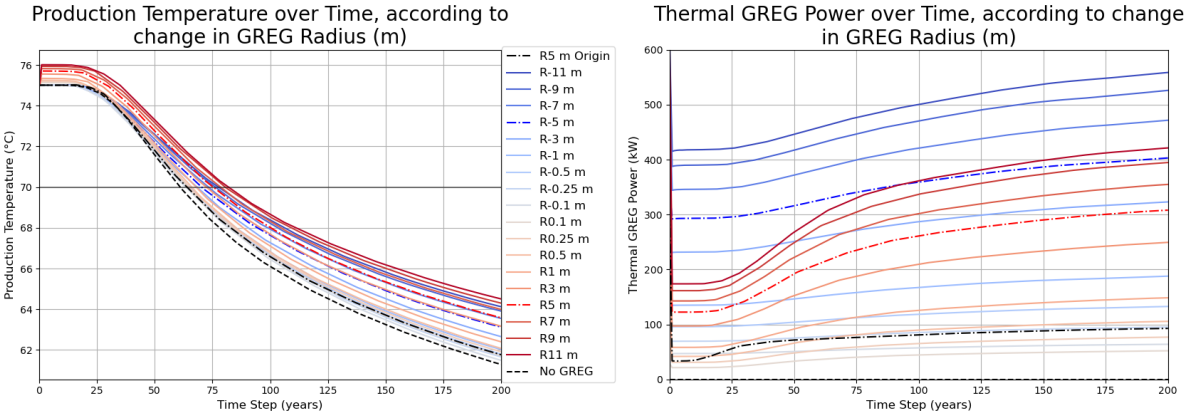

Figure 5.7: Static GREG Radius Results for production temperature (left), and GREG power over simulation time (right).

The results indicate that production temperature and geothermal doublet lifetime increase with GREG radius. This is likely due to the additional surface area provided by structures of larger radius, lending themselves to a higher total power output than their smaller-dimensioned counterparts. This is also reflected in the power charts, as power output increases significantly with every increase in GREG radius. Once again, the results show higher geothermal production temperatures when GREGs are placed on the production well side rather than on the injection well side. In this study, the 11m radius GREG increased geothermal lifetime the most out of all the other tested radii, seeing geothermal lifetime increase of 20 years, to a final lifetime of 81 years, compared to the control model, which sees a lifetime of 61 years. The same 11m radius GREG on the injection side results in a slightly lower geothermal lifetime increase of 16 years more than the control, to 77 years. EOS production temperature is 2.83 degrees higher than the control for the injection side placement of this GREG, and 3.22 degrees for the production side placement.

While these results exhibit significant increases in production temperature, lifetime increases, and function-

ality of the GREGs in their purpose, it remains unrealistic to install 11m radius structures several kilometers into the subsurface, as this has never been done before. Therefore, it is important to consider the results of smaller radius GREGs, such as the 0.5m, 0.25m and 0.1m. For the injection side, and the production side placement, the 0.1m radius GREGs increased geothermal lifetime by only 2 years and 3 years more than the control study, respectively, which pertained to EOS production temperature increases of 0.20 degrees, and 0.43 degrees. However, upon closer inspection, a valuable characteristic is revealed by these smaller dimensioned GREGs, as shown in Figure 5.8, which shows thermal flux of each GREG by radius, by the end of the simulation:

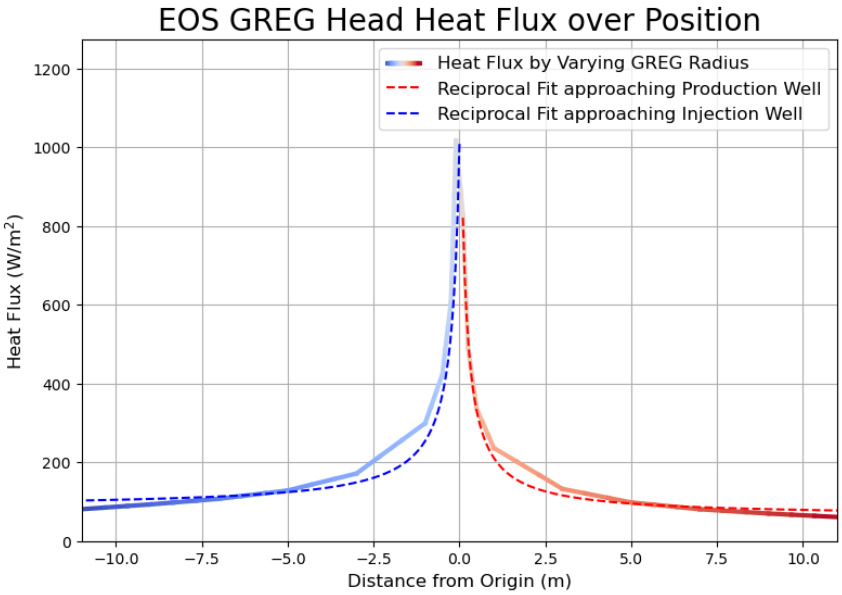

Figure 5.8: Final EOS heat flux of GREG compared to different tested radii.

Evidently, as radius decreases, heat flux per unit area increases nonlinearly. This result is due to the shorter contact time with the cold plume and the hot exterior wall of the GREG, as shorter-radius GREGs have less surface area to contact the incoming thermal breakthrough plume with. In larger-dimensioned GREGs, heat transfer along the boundary levels off due to the high contact time of the thermal breakthrough plume along the large radius of the GREG, allowing the contact water to approach the temperature of the GREG for a longer period of time. As the difference in temperature between the plume and the GREG approaches zero, so does the heat transfer. Shorter-radius GREGs therefore take advantage of this consistently high temperature difference, and are able to output more heat per unit surface area in less time, and while alone, these smaller-dimensioned GREGs may not have a significant impact on the production temperature and final geothermal lifetime, but if considering an array of these structures, they may be the better performing GREGs, with the added advantage of them being all that more feasible for installation several kilometers into the subsurface.

$$q_{Production}[\frac{W}{m^2}] = \frac{166.24[\frac{W}{m}]}{r_{GREG}[m] + 0.119[m]} + 62.67[\frac{W}{m^2}] \tag{5.7}$$

$$R^2 = 0.9964 \tag{5.8}$$

$$q_{Injection}[\frac{W}{m^2}] = \frac{205.93[\frac{W}{m}]}{r_{GREG}[m] + 0.12[m]} + 84.40[\frac{W}{m^2}] \tag{5.9}$$

$$R^2 = 0.9959 \tag{5.10}$$

Additionally, the results shown in Table 5.3 raise an important question in what initially seems to be a discrepancy in the results, and highlight an unexplained phenomenon. This can be seen when comparing the total energy output over the lifetime of the geothermal plant, to the lifetime extension. The geothermal plant power production is 8,716.67 kW, which corresponds to a yearly energy output of approximately 76,358 MWh. Therefore, one can reasonably assume that adding this amount of energy into the geothermal reservoir may linearly increase lifetime by a year. However, the data suggests that this is not true, which can be seen in the energy production from the GREG versus the added lifetime. The 11m radius GREG placed at the production side achieved a 20 year lifetime increase with 177,779 MWh of added energy the the geothermal reservoir, amounting to a yearly energy input by the GREG of 8,889 MWh/year. At the injection side, using the same GREG, we find that the yearly input of energy is more than doubled, to 18,836 MWh/year, yet, the geothermal lifetime is diminished by comparison, and even so, the lifetime of the utility is extended with much less than the benchmark value of 76,358 MWh per added year of lifetime. Why does this happen?

There are two reasons why this may happen; the first of which is obstruction. The simple act of placing the GREG in the reservoir may result in added geothermal lifetime attributed to the simple fact that the GREG may significantly obstruct the incoming thermal breakthrough plume, to the point of keeping the cold water away for a period of time that cascades into a significant amount of added lifetime. Therefore, the lifetime increase is not only attributed to the heat flux out of the GREG, but also, its obstructive component.

However, this also fails to fully explain the reason why one placement benefits the lifetime extension more than the other. However, when observing the flows in the model, one important finding is the initial advance of the thermal breakthrough. At approximately year 17 is when thermal breakthrough begins to have an effect on the production temperature, and becomes more visually apparent in the simulated years after that. Prior to surrounding the production well entirely, at around this time, a finger of cold water extends from the injection well directly to the production well, which gradually grows in size. However, in the case of the GREG being placed at the production side, this thin finger of colder water, while under the control scenario may have a drastic effect on the thermal breakthrough of the system, is completely obstructed by the implementation of the GREG, especially if it is of high radius, as shown in Figure 5.9.

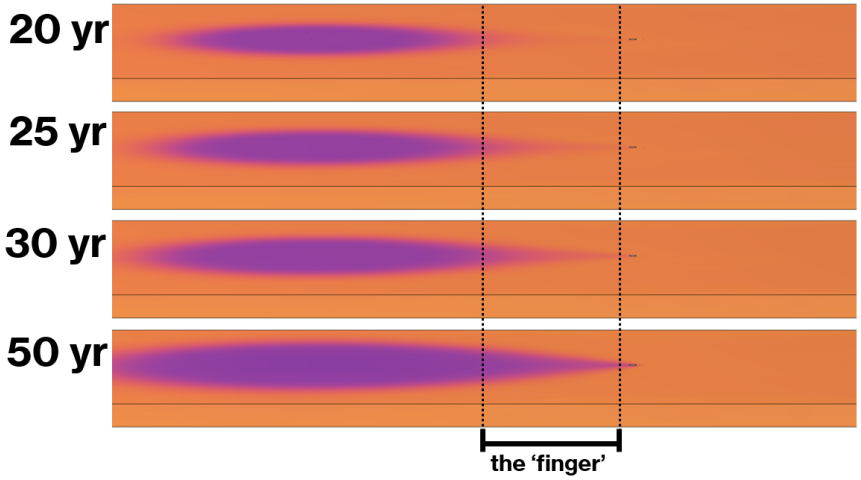

Figure 5.9: "The Finger" phenomenon, possibly explaining higher resulting lifetimes for GREG placement by the production well, over the injection well.

A well-placed GREG may be able to take advantage of this initial finger of cold water at its most concentrated point, which is right before the production well, and surrounds the boundary layer of the GREG, optimizing the angle of attack for reaheating this initial portion of the breakthrough plume. This may also explain why the GREG placement in the center of the domain was not incredibly beneficial to the geothermal lifetime, as most of the thermal breakthrough plume essentially bypassed the GREG, seen in Figure 5.10.

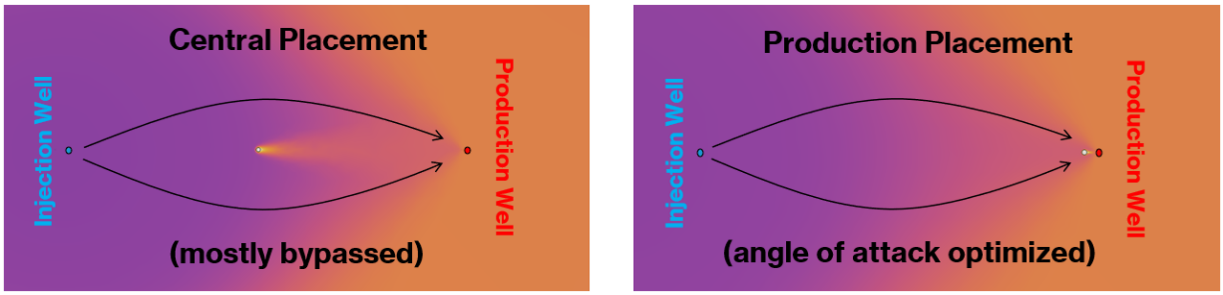

Figure 5.10: Thermal breakthrough plume at year 40 bypassing GREG in central placement (left) compared to production side placement which optimizes reheating of the plume at its most concentrated point (right).

According to these results, the placement of the GREGs will now be limited to the production well side, as this maximizes lifetime of the geothermal utility, based on what has been observed. Subsequent studies will also only consider shorter-radius GREGs of 0.5m, 0.25m, and 0.1m, given the feasibility constraint in any dimensions exceeding these. Additionally, their high heat output per unit area makes them interesting to study further.

Table 5.3: Radius Analysis Summary of Results

GREG Radius (m)	Lifetime (yr)	Lifetime Change (yr)	Lifetime Heat Flux (W/m^2)	Lifetime Power Output (kW)	Lifetime Energy Output (MWh)	EOS Heat Flux (W/m^2)	EOS Power Output (kW)	EOS Production Temperature (°C)	EOS Production Temperature Change (°C)
No GREG (control)	61	NA	NA	NA	NA	NA	NA	61.291	NA
-11	77	16	69.3	478.7	301379	80.9	558.7	64.13	2.834
-9	76	15	79.2	447.8	277727	93.1	526.1	63.91	2.621
-7	73	12	90.4	397.3	236558	107.3	471.7	63.55	2.259
-5	70	9	107.0	336.1	191350	128.4	403.1	63.12	1.833
-3	68	7	141.0	265.7	146499	171.5	323.1	62.66	1.364
-1	65	4	244.9	153.8	81356	299.3	187.9	62.02	0.733
-0.5	64	3	346.1	108.7	56718	422.6	132.7	61.79	0.503
-0.25	64	3	499.6	78.4	40980	606.3	95.2	61.66	0.369
-0.1	63	2	839.7	52.7	27181	1017.4	63.9	61.49	0.198
0.1	64	3	595.8	37.4	15497	827.9	52.0	61.72	0.431
0.25	64	3	350.7	55.1	22578	489.9	76.9	61.91	0.619
0.5	66	5	243.4	76.4	32229	336.2	105.6	62.08	0.788
1	67	6	170.4	107.0	45995	236.4	148.5	62.40	1.111
3	72	11	98.0	184.5	84616	132.4	249.4	63.17	1.875
5	75	14	74.9	235.1	113014	98.1	308.1	63.58	2.290
7	78	17	63.1	277.4	139518	80.7	354.9	63.99	2.701
9	80	19	55.4	313.4	162366	69.8	394.8	64.30	3.009
11	81	20	49.2	339.8	177779	61.0	421.3	64.51	3.216

**Negative radii pertain to GREG placement near injection well, while positive radii represent GREGs placed near the production well*

Research Objective Review

This concludes the first section of study regarding the static experimentation, which aimed to fulfill the first research objective. In this first part of the study, the performance of the GREG was narrowed down iteratively, answering the question as to how this idea could be optimized.

1. The first study, known as the Temperature Analysis detailed how geothermal lifetime and GREG power output was set to change over different static temperature settings, which would represent the equalized GREG temperature according to the final depth of the GREG. Perhaps unsurprisingly, this study revealed that lifetime increases with set GREG temperature, and that there is a linear relationship between GREG power output into the reservoir and temperature setting of the GREG.
2. The second study, known as the Position Analysis showed that the placement of the GREG in the underburden is extremely important, as it was able to maximize lifetime of the geothermal system much more than what was tested in the Temperature Analysis. Furthermore, it revealed that the domain has a lopsided nature in performance, and placement of the GREG near the production side dispproportionately benefits geothermal lifetime extension compared to any other tested distance.
3. The third study, known as the Radius Analysis, exhibited the benefits of having smaller versus larger GREG structures in terms of radial dimension. The findings show that larger GREGs capitalize on high surface areas, while shorter-radius GREGs see nonlinear benefits in heat flux per unit surface area. Additionally, using this data and the data from the Position Analysis, conclusions were drawn as to why GREG placement at the production side benefited geothermal lifetime more than other placements, which had to do with the onset of thermal breakthrough, as well as the obstructive capacity of the GREG.

With this information, preliminary optimization of the model has been executed, which aimed to investigate placement and dimensioning of GREGs, among other properties, to maximize doublet lifetime. The subsequent study aims to fulfill the second research objective, which is to find out how effectively the underburden would provide heat to the geothermal reservoir via the GREG, through transient heat transfer.

5.3. Dynamic GREG Model Results

In the previous section, an analysis as to the benefits of temperature, position, and dimensioning of GREGs was provided. This section aims to explore the transferability of the heat from the underburden into the reservoir through the GREGs. The model is once again run for a simulation time of 200 years for every trial. The two most consequential differences between these simulations and the previous ones, are the addition of the underburden layer, which contains all the heat resources, and the removal of the temperature boundary condition from the GREGs. This will allow for the measurement of production temperature, fluxes and GREG head temperature as a direct consequence of what heat resources are available in the underburden.

The dimensioning and conditions of this model take from the insights of the previous study, which is to say that the favorable conclusions reached previously, which most feasibly maximized geothermal lifetime, are employed in this study. This means that the GREG placement should be studied near the production well, in order to analyze the most significant increases in geothermal lifetime. Additionally, radii tested are 0.5m, 0.25m and 0.1m, due to their dimensions being the most relatively feasible for installation by current drilling standards. The study will proceed by testing singular GREGs, with varying the thermal conductivity of the material.

A mesh refinement analysis will follow, re-running the previous analysis under both a coarser mesh, and a finer mesh for the GREG. This portion of the study aims to increase confidence and reliability in the results.

Following this, a mesh size will be decided on, and the final depths and lengths of the GREG will be probed, querying the performance of the GREGs when subjected to the lower and hotter depths of 5km. At a final depth of approximately 4km, the GREGs were exposed to temperatures nearing 140°C. At a test depth of approximately 5km, the GREGs will be exposed to temperatures of approximately 170°C. These GREGs will employ the favorable thermal conductivity determined in the previous portions of the study to measure overall heat transfer from the underburden into the reservoir.

5.3.1. GREG Thermal Conductivity Analysis

It is important to reiterate the need for high heat transfer rates for this concept, because without high heat transfer, the portion of the GREG exposed to the cold plume within the reservoir would cool down faster than it would heat up. High heat transfer rates and thermal conductivity would allow GREG heads to maintain a consistent temperature attributed to the underburden rather than assume the temperature of the cold plume. Therefore, the heat should have low resistance in traveling up the length of the GREG. One the way this could be achieved is through free convection. However, the modeling of this concept under this scale and dimensions presented significant difficulty given the limited computational power, such that in the place of assuming the GREG to be a fluid bounded by walls, the material itself was changed to be a solid of very high thermal conductivity. The thermal conductivities range logarithmically from 1 W/mK, to 1E10 W/mK. Figures 5.11, 5.12 and 5.13 show the production temperature and power output results of each tested radius, between 0.5m (green), 0.25m (pink), and 0.1m (blue), with color intensity increasing with thermal conductivity.

Production Temperature

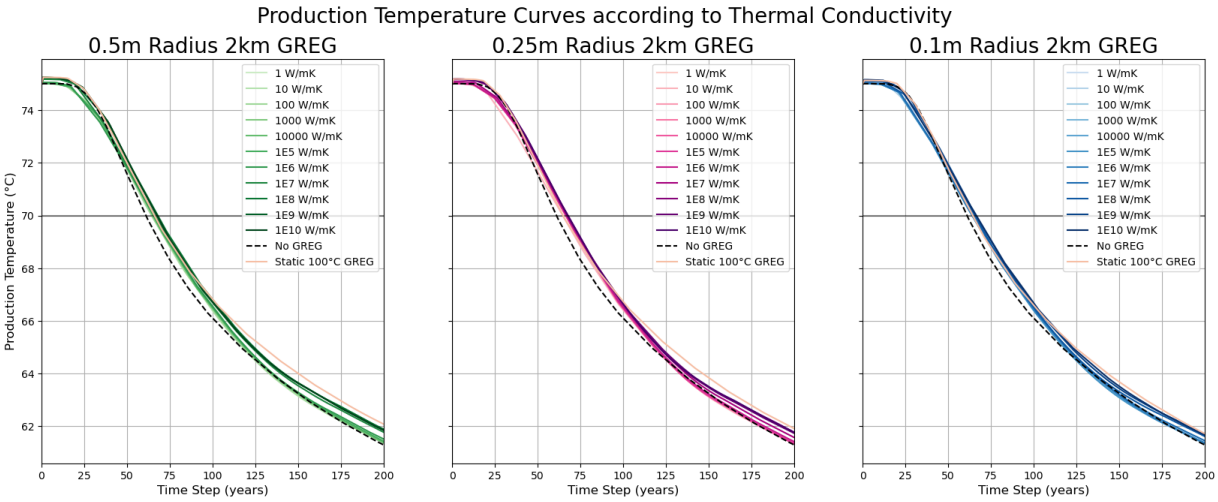

Figure 5.11: From left to right: production temperature results for tested thermal conductivities for 0.5m Radius GREG (left), 0.25m Radius GREG (center), and 0.1m Radius GREG (right)

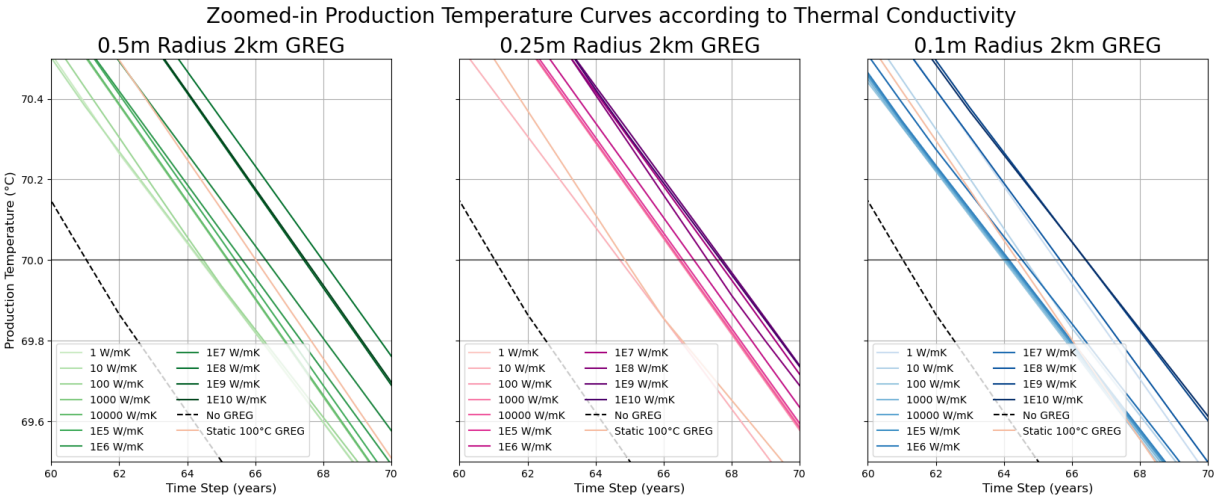

Figure 5.12: From left to right: zoomed-in production temperature results around lifetime threshold for tested thermal conductivities for 0.5m Radius GREG (left), 0.25m Radius GREG (center), and 0.1m Radius GREG (right)

As seen in Figures 5.11 and 5.12, the best performing thermal conductivities applied to the 0.5m radius GREG were those of 1E8, 1E9 and 1E10 W/mK, which was expected, due to them having the highest heat transfer capability. These settings each achieved a geothermal lifetime extension of 6 years compared to the control for GREG radius of 0.5m, for a final lifetime of 67 years. In terms of geothermal doublet lifetime, these three thermal conductivity settings significantly outperformed the 100 degree Celsius temperature-set GREG of 0.5m radius placed at the production side of the reservoir from the static studies, by almost 2 years, denoted by the light orange contour in Figures 5.11 and 5.12.

For the 0.25m radius 2km long GREG, the highest thermal conductivities of 1E7, 1E8, 1E9, and 1E10 W/mK extended geothermal lifetime by 6 years compared to control when testing the 0.25m radius GREG, for a final lifetime of 67 years. All thermal conductivities for the 0.25m GREG outperformed the lifetime of the static 100 degree Celsius GREG of the same dimensions and placement, with the exception of the 10 W/mK setting.

For the 0.1m radius GREG, the highest lifetime extension was seen in the thermal conductivity settings of 1E9 and 1E10 W/mK, resulting in a lifetime increase of 5 years when compared to the control, for a total of 66 years. Lower thermal conductivity settings tested did not increased geothermal lifetime by more than this amount, and resulted shorter geothermal lifetimes at lower thermal conductivities at the range tested. Higher thermal conductivities ranging from 1E6 to 1E10 outperformed the lifetime gains from the static 100 degree Celsius 0.1m radius GREG in the radius analysis.

It should be mentioned that meshing for the underburden in the 0.1m radius trial failed at these dimensions. The element sizes were modified arbitrarily and retried, until a stable meshing was found, with the least amount of change to the formatted meshing design determined at the beginning of the experiments. Changing the maximum element size in the swept mesh from 0.5m to 1m resulted in a stable mesh.

A key insight to these results is that the added benefit of increasing thermal conductivity of the material reaches a plateau past a certain point, and the extension of geothermal lifetime is only marginally changed as a result. This can be seen in the two distinct clustering regions of production temperature contour lines for the 0.5m GREG radius, to the right of the No-GREG curve. Initially, geothermal lifetime increases marginally along the logarithmic increases of thermal conductivity till after 1E7 W/mK - from there, production temperature curves see a significant jump at k = 1E8 W/mK, landing them on the higher cluster of production temperature curves, after which logarithmic increases in thermal conductivity once again start to see less significant changes in production temperature and geothermal lifetime increase. Upon closer inspection, the data also suggests that the highest thermal conductivity material does not in fact yield the highest doublet lifetime, as thermal conductivity setting of 1E8 W/mK surpasses the 1E9 and 1E10 W/mK curves. The rest of the trials generally seem to follow hierarchal increases in lifetime in response to increases in thermal conductivity.

Clustering for the 0.25m radius GREG was less obvious when referring to the production temperature curves, however, slight clustering was observed between the three highest thermal conductivity settings of 1E8, 1E9 and 1E10 W/mK as they passed the 70-degree threshold. This means that there is only marginal benefit in lifetime increase from logarithmic increases of thermal conductivities at this range, similar to the data seen from the 0.5m radius, 2km-long GREG.

For the 0.1m radius GREG, clustering was less obvious, similar to the 0.25m radius GREG results. The plateau in geothermal production lifetime increase is seen between the 1E9 and 1E10 W/mK thermal conductivity settings. There is also a noticeable gap between these thermal conductivities, and the 1E8 W/mK setting. The distinction between these results and the other tested radii, is that for the 0.1m trials, there is noticeable space between the two highest thermal conductivities tested, which mean that the plateau is not as pronounced, and there may be more benefit in thermal conductivity increases from 1E10 W/mK in this GREG dimensioning than in the other tested dimensions.

Thermal Power Output

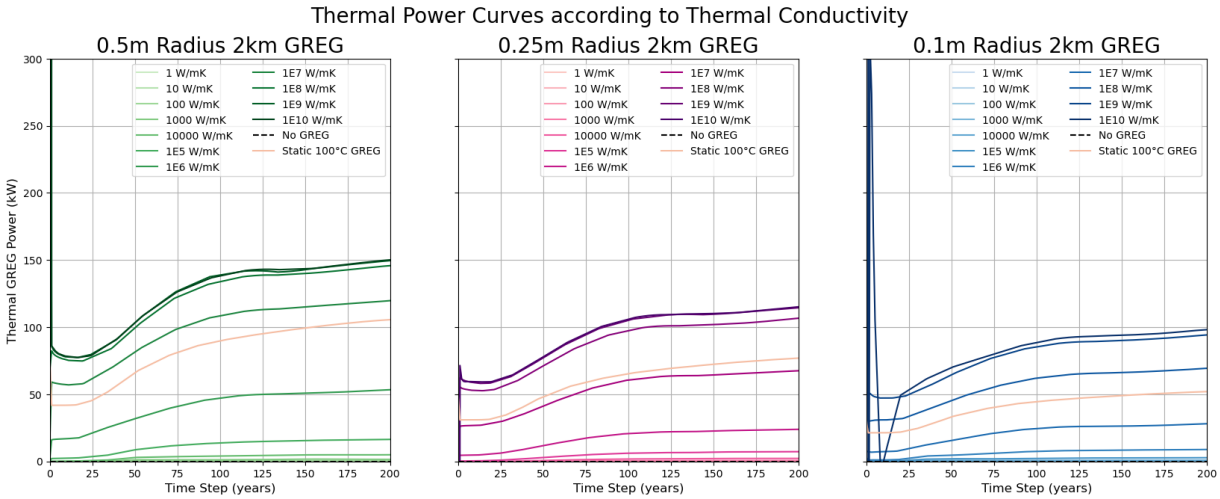

Figure 5.13: From left to right: thermal power results according to changes in thermal conductivity, for 0.5m Radius GREG (left), 0.25m Radius GREG (center), and 0.1m Radius GREG (right)

The clustering of data from the 0.5m radius GREG study seen in the production temperature curves is also reflected in the thermal power curves, once again showing thermal conductivity settings of 1E8, 1E9 and 1E10 W/mK grouping together along the length of the study. These curves do not however exhibit the marginal surpassing of higher thermal conductivity setting curves by lower thermal conductivity settings as seen in the production temperature curves, following an expected hierarchal pattern. There is very little difference between the thermal conductivity settings of 1E9 and 1E10 W/mK, which leads to the suspicion that upwards heat transfer rate is no longer the limiting factor of this system. What this means is that the rate of heat trickling into the bottom of the GREG may become limited by the thermal conductivity of the underburden, resulting in a long lasting slow trickle of of heat into and out of the system, and a balance between energy in and energy out. This could potentially mark what may be possible in a natural convection scenario if it is assumed to transfer heat at a rate equal to or greater than the high thermal conductivity setup. By the time the doublet in this case has reached its lifetime, power outputs were approximately 119.9 kW and 119.4 kW, for thermal conductivity settings of 1E9 and 1E10 W/mK, respectively, and approximately 149.5 kW and 150.1 kW by end of simulation. Results for energy in (through GREG bottom) and energy out (through GREG head) are provided in Figure 5.14, showing that the GREG in the model reaches an equilibrium point in energy transference at some point prior to 50 years. Data pertaining to thermal input through the bottom of the GREG was less stable as thermal conductivities increased. However, this data shows an increase in heat transfer equilibrium level depending on the radial size of the GREG.

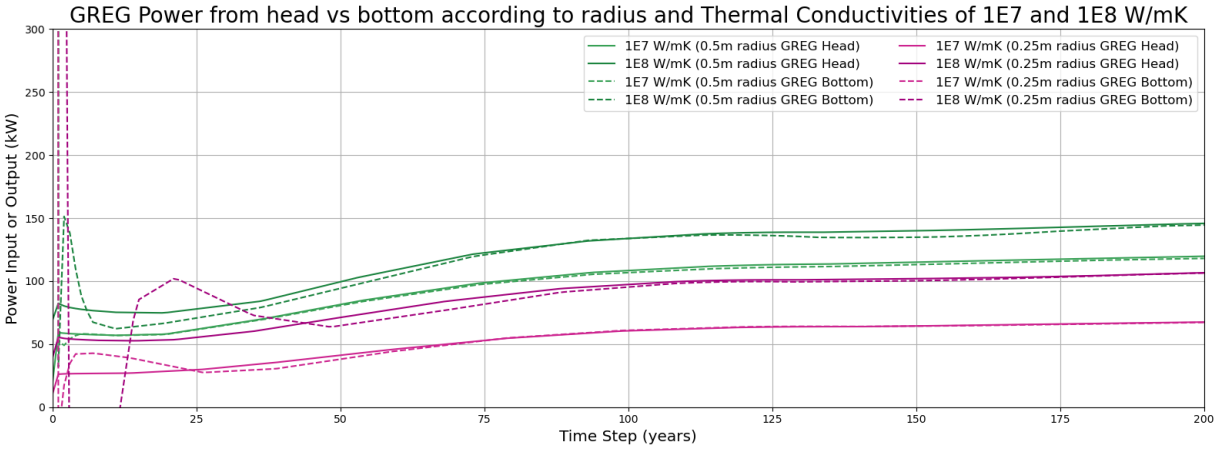

Figure 5.14: Comparison of power curves for heads and bottoms of 0.5m radius and 0.25m radius GREGs, using thermal conductivities of 1E7 and 1E8 W/mK. The results for the 0.1m radius GREG were not plotted due to highly oscillatory data.

Thermal power results for the 0.25m radius GREG proved similar to those of the 0.5m radius GREG, showing a similar shape in thermal power output evolution from the GREG head. Once again, power output increases were seen with thermal conductivity increases. As with the 0.5m radius GREG study, there was little difference between the settings of 1E9 and 1E10 W/mK, reinforcing the idea that at this range, the increases in power output due to increases in thermal conductivity plateau. While the shapes of the curves were similar, the total power outputs for the shorter-radius GREG was generally decreased. However, if the heat flux rate is considered, the 0.25m radius GREG achieves a higher output per square meter, matching the results from Section 5.2.3. Once again, this means that the shorted-dimensioned GREGs transfer heat at an increased rate when compared to their larger counterparts. Power outputs for 1E9 and 1E10 W/mK resulted in 89.5 and 90.4 kW by lifetime, respectively, and 114.4 and 115.1 kW by EOS.

All data suggest that there is a direct correlation between high GREG thermal conductivity, and higher power output rates, which also applies to the smallest radius GREG of 0.1m. The thermal conductivities which resulted in the highest power outputs were once again the 1E9 and 1E10 W/mK thermal conductivity settings, which were outputting at rates of 73.1 and 76.4 kW, respectively, by lifetime, and by EOS, were outputting at 94.2 and 98.1 kW, respectively. These power outputs are once again less than those of the larger 0.25m radius GREG, and almost half of what was seen from the 0.5m radius GREG. The advantage

of a GREG of these dimensions, however, is that in terms of installation potential, it lands in feasible territory, as perforations of this radius have been made at this depth. Additionally, while the total output surface is significantly less than that of a 0.5m radius GREG, it confirms the previous finding of higher output efficiencies per unit of surface area. The simulation for the 1E10 W/mK thermal conductivity setting, however, produced erratic data during the beginning of the simulation, as seen in Figure 5.13, resulting in oscillations in the beginning of the simulation. Therefore, the information from this contour may not be as viable as the rest.

Additionally, the data for thermal power output, for all GREG radii tested followed a logistic, S-shaped trend along the logarithmic increases of thermal conductivity, as seen in Figure 5.15.

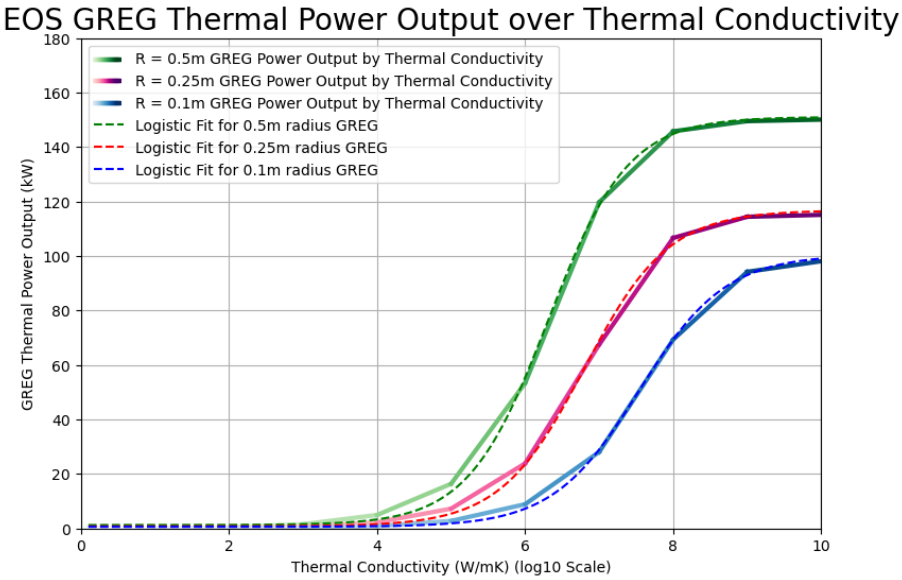

Figure 5.15: EOS GREG Head Power Output vs varying Thermal Conductivities.

The relationship between GREG head power output and thermal conductivity can be described by the following equations, for each of the GREG radii:

$$Q_{0.5m}[kW] = \frac{149.82}{1 + e^{-1.85(log_{10}TC - 6.31)}} + 1.26 \tag{5.11}$$

$$R^2 = 0.9995 \tag{5.12}$$

$$Q_{0.25m}[kW] = \frac{116.10}{1 + e^{-1.76(log_{10}TC - 6.80)}} + 0.75 \tag{5.13}$$

$$R^2 = 0.9994 \tag{5.14}$$

$$Q_{0.1m}[kW] = \frac{99.96}{1 + e^{-1.72(log_{10}TC - 7.54)}} + 0.60 \tag{5.15}$$

$$R^2 = 0.9995 \tag{5.16}$$

GREG Head Temperature

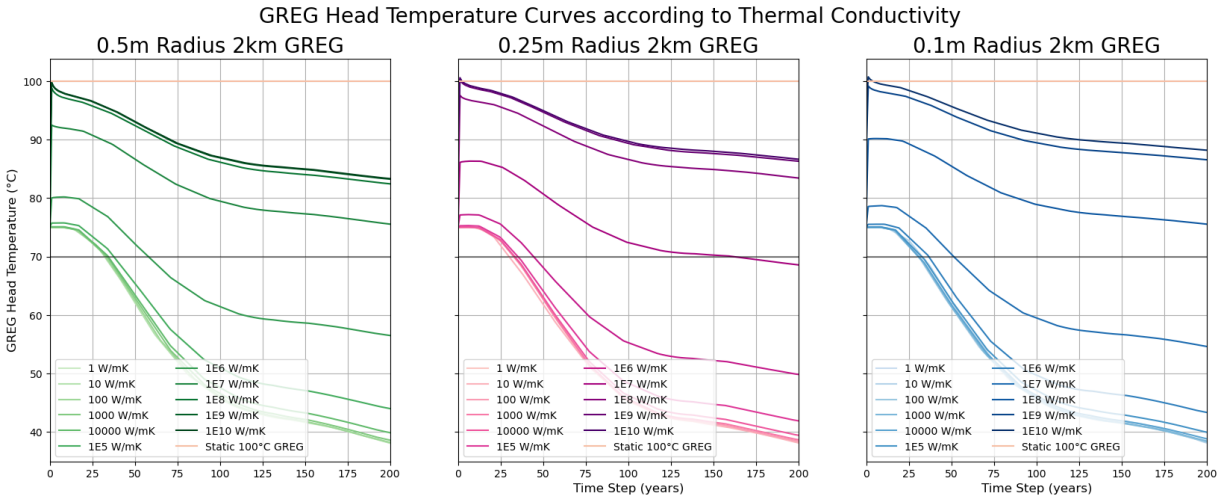

Figure 5.16: From left to right: GREG head temperature results according to changes in thermal conductivity, for 0.5m Radius GREG (left), 0.25m Radius GREG (center), and 0.1m Radius GREG (right)

GREG head temperature increases corresponded with thermal conductivity increases in every case, following the expected hierarchal pattern. The head of the GREG saw the highest temperatures at thermal conductivity settings of 1E9 and 1E10 W/mK, corresponding to approximately 90.5°C and 90.6°C by lifetime, respectively, and 83.3°C and 83.4°C by EOS for the 0.5m radius GREG study. For the 0.25m radius GREG study, this translated into 92.5°C and 92.8°C by lifetime for the same two thermal conductivities, respectively, and by EOS, 86.3°C and 86.7°C. Finally, for the 0.1m radius GREG, the head temperature resulted in 92.4°C and 93.1°C by lifetime, and 86.6°C and 88.2°C by EOS. These were surprising results, due to an intrinsically higher surface area-to-volume ratio, usually relating to higher rates of heat dissipation [26]. This was not exactly the case, as smaller dimensioned GREGs saw higher head temperatures sustained throughout the simulation time of 200 years when compared to their larger counterparts.

Tables 5.4, 5.5 and 5.6 summarize the information from the thermal conductivity study, which pertained to 2km-long GREGs, ranging from radii of 0.5m, 0.25m, and 0.1m, respectively, at material thermal conductivities ranging logarithmically from 1E0 W/mK to 1E10 W/mK:

Table 5.4: Thermal Conductivity Analysis Summary of Results for 0.5m radius GREG

Thermal Conductivity (W/mK)	Lifetime (yr)	Lifetime Change (yr)	Lifetime GREG Head Temperature (°C)	Lifetime Heat Flux (W/m^2)	Lifetime Power Output (kW)	Lifetime Energy Output (MWh)	EOS Heat Flux (W/m^2)	EOS Power Output (kW)	EOS Production Temperature (°C)	EOS Production Temperature Change (°C)
No GREG (control)	61	NA	NA	NA	NA	NA	NA	NA	61.291	NA
0.5m Radius GREG										
1.00E+00	64	3	55.82	0.0	0.0	-38	0.1	0.0	61.37	0.079
1.00E+01	64	3	55.93	0.7	0.2	31	0.4	0.1	61.37	0.08
1.00E+02	64	3	56.09	1.8	0.6	115	1.5	0.5	61.37	0.076
1.00E+03	65	4	56.47	4.0	1.3	283	4.9	1.5	61.38	0.084
1.00E+04	65	4	57.16	10.7	3.4	879	15.8	5.0	61.39	0.097
1.00E+05	65	4	59.72	34.3	10.8	3251	52.2	16.4	61.43	0.138
1.00E+06	65	4	68.02	119.6	37.6	14697	170.0	53.4	61.51	0.222
1.00E+07	66	5	83.79	295.9	93.0	41554	381.3	119.7	61.77	0.481
1.00E+08	67	6	89.85	368.7	115.8	53060	464.3	145.8	61.89	0.597
1.00E+09	67	6	90.47	381.7	119.9	55055	476.3	149.5	61.85	0.556
1.00E+10	67	6	90.57	380.2	119.4	55031	478.0	150.1	61.85	0.558

Table 5.5: Thermal Conductivity Analysis Summary of Results for 0.25m radius GREG

Thermal Conductivity (W/mK)	Lifetime (yr)	Lifetime Change (yr)	Lifetime GREG Head Temperature (°C)	Lifetime Heat Flux (W/m^2)	Lifetime Power Output (kW)	Lifetime Energy Output (MWh)	EOS Heat Flux (W/m^2)	EOS Power Output (kW)	EOS Production Temperature (°C)	EOS Production Temperature Change (°C)
No GREG (control)	61	NA	NA	NA	NA	NA	NA	NA	61.291	NA
0.25m Radius GREG										
1.00E+00	66	5	55.82	-1.1	-0.2	-159	-0.4	-0.1	61.33	0.037
1.00E+01	64	3	56.12	-0.8	-0.1	-136	-0.1	0.0	61.36	0.066
1.00E+02	66	5	55.85	-0.3	0.0	-128	1.1	0.2	61.33	0.034
1.00E+03	66	5	55.99	1.6	0.3	-52	4.4	0.7	61.33	0.037
1.00E+04	66	5	56.42	7.4	1.2	188	14.3	2.3	61.33	0.042
1.00E+05	66	5	57.87	26.9	4.2	1084	46.3	7.3	61.35	0.061
1.00E+06	66	5	63.07	98.1	15.4	5156	152.2	23.9	61.42	0.125
1.00E+07	67	6	77.31	314.4	49.4	21002	430.2	67.5	61.57	0.282
1.00E+08	67	6	89.90	529.2	83.1	37768	679.3	106.7	61.77	0.478
1.00E+09	67	6	92.52	569.8	89.5	41268	728.9	114.4	61.73	0.440
1.00E+10	67	6	92.79	575.7	90.4	41753	733.3	115.1	61.77	0.476

Table 5.6: Thermal Conductivity Analysis Summary of Results for 0.1m radius GREG

Thermal Conductivity (W/mK)	Lifetime (yr)	Lifetime Change (yr)	Lifetime GREG Head Temperature (°C)	Lifetime Heat Flux (W/m^2)	Lifetime Power Output (kW)	Lifetime Energy Output (MWh)	EOS Heat Flux (W/m^2)	EOS Power Output (kW)	EOS Production Temperature (°C)	EOS Production Temperature Change (°C)
No GREG (control)	61	NA	NA	NA	NA	NA	NA	NA	61.291	NA
0.1m Radius GREG										
1.00E+00	63	2	55.85	1.0	0.1	51	0.8	0.1	61.33	0.040
1.00E+01	65	4	55.89	1.2	0.1	43	0.9	0.1	61.39	0.103
1.00E+02	63	2	55.98	1.8	0.1	79	1.6	0.1	61.33	0.039
1.00E+03	63	2	56.18	4.1	0.3	132	4.7	0.3	61.33	0.041
1.00E+04	63	2	56.51	11.2	0.7	265	14.4	0.9	61.34	0.047
1.00E+05	63	2	57.24	31.0	1.9	689	44.1	2.8	61.35	0.054
1.00E+06	64	3	58.85	85.7	5.4	1815	141.7	8.9	61.35	0.058
1.00E+07	64	3	66.44	298.4	18.7	6790	447.2	28.1	61.46	0.167
1.00E+08	65	4	82.99	823.2	51.7	22436	1104.4	69.4	61.60	0.312
1.00E+09	66	5	92.36	1164.2	73.1	33434	1500.2	94.2	61.66	0.370
1.00E+10	66	5	93.90	1216.9	76.4	33968	1562.4	98.1	61.64	0.349

5.3.2. GREG Mesh Refinement Analysis

The availability of the previous results opened the possibility of executing a mesh refinement study on the GREG to see how the transfer of heat reacts under a finer mesh. Therefore, the elements within the GREG domain and the boundary shared between the GREG and the reservoir and underburden were adjusted. These changes would be exacted through the adjustment of the amount of cross-sectional elements within the GREG. Based on these changes, the resulting mesh from the reservoir and the underburden would also adjust at the boundary.

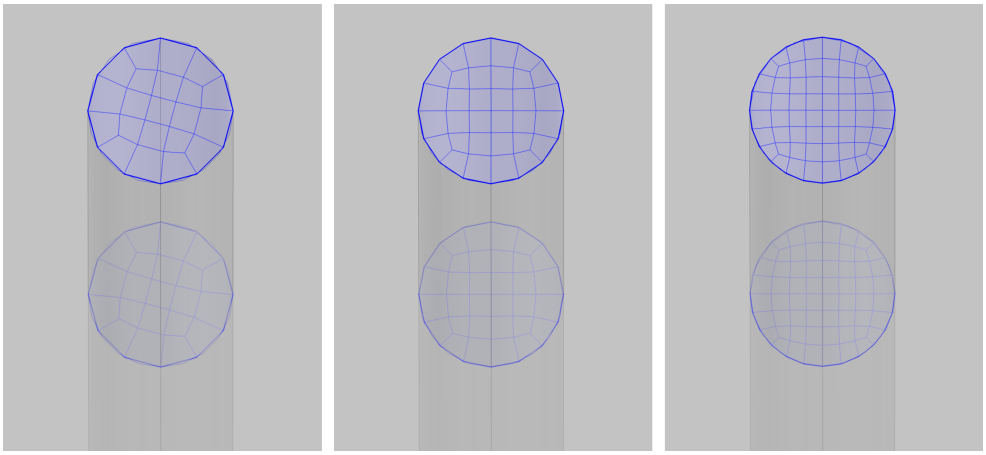

Figure 5.17: From left to right: 21 mesh element model, 32 mesh element model (original), 60 mesh element model.

Two additional mesh sizes were tested on the 0.5m radius GREG face boundary. The faces therefore captured 21 and 60 elements per face, which were swept down the entire length of the GREG, same as the tested 32-element setup. A visualization of all tested meshes is offered in Figure 5.17. The thermal

conductivity study was then repeated for thermal conductivities of 1E7, 1E8, 1E9 and 1E10 W/mK on the 0.5m radius GREG.

Production Temperature

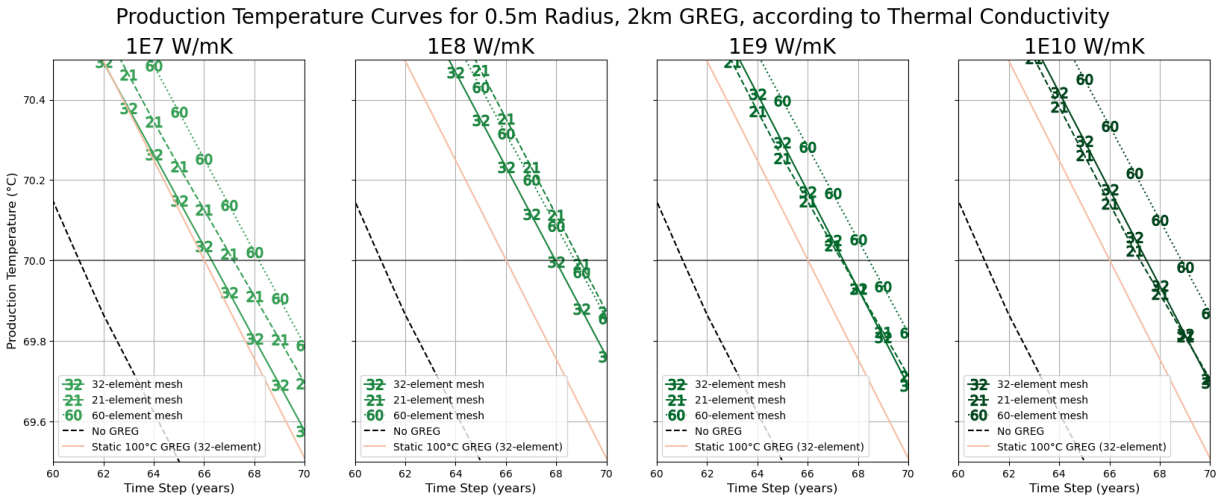

Figure 5.18: Closeup view of geothermal production lifetime extension from different tested face meshes, of 21, 32 and 60 elements per GREG face, for the same four tested thermal conductivities, from left to right, of 1E7, 1E8, 1E9, and 1E10 W/mK.

The data suggests that the mesh plays a significant role in lifetime determination of the geothermal utility. Figure 5.18 shows how the production temperature results and lifetime extensions differ according to what mesh is used. The finer mesh of 60 elements resulted in the highest lifetime extension, for a total of 68 years across all thermal conductivities tested. Thermal conductivity of 1E7 W/mK presented the most drastic distribution, exhibiting a lifetime change spanning two years across the 3 meshes tested.

Thermal Power Output

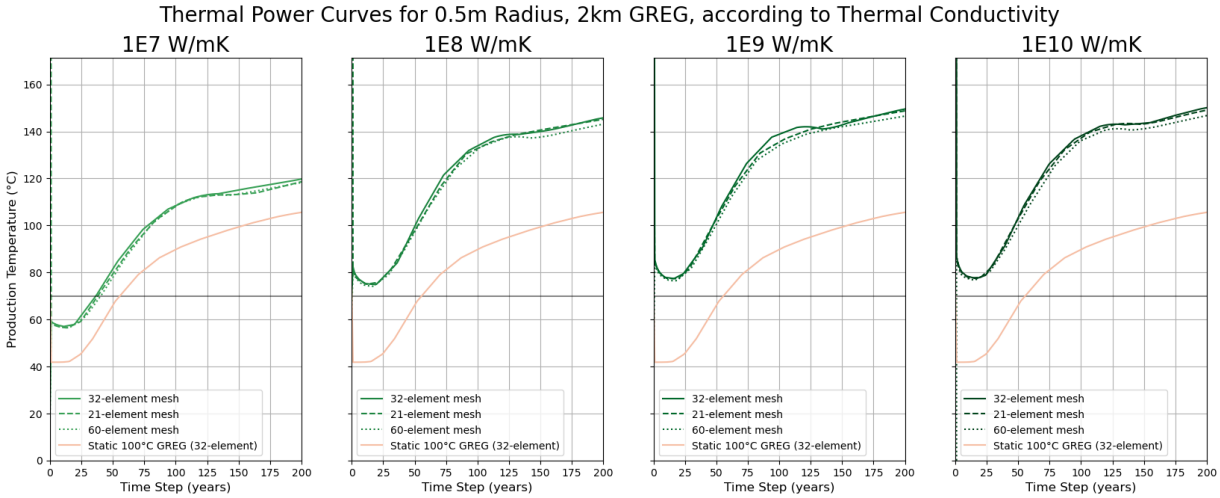

Figure 5.19: Thermal power output curves from different tested face meshes, of 21, 32 and 60 elements per GREG face, according to thermal conductivities of 1E7 (left), 1E8 (center left), 1E9 (center right), and 1E10 W/mK (right).

GREG Head Temperature

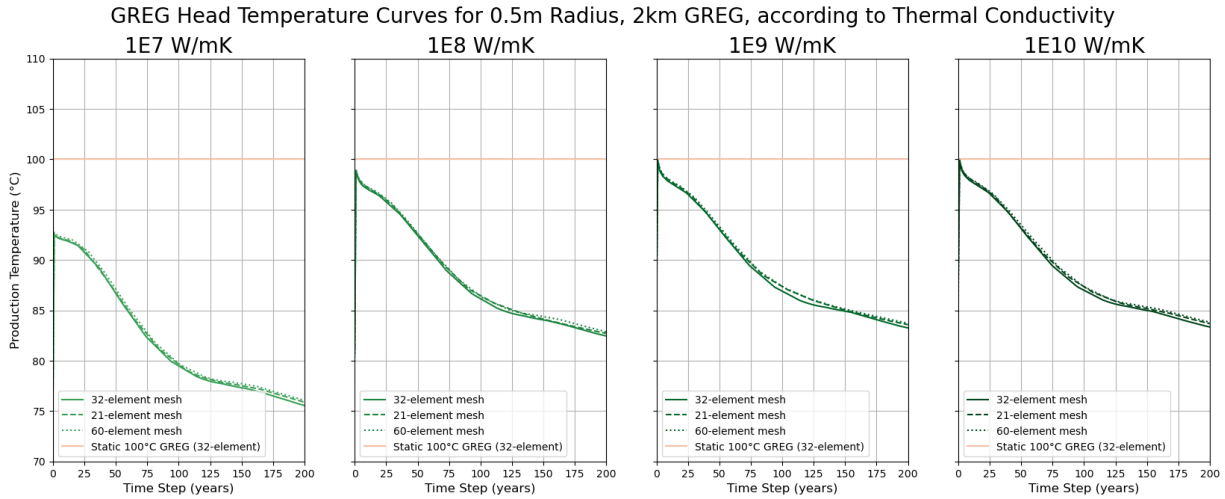

Figure 5.20: GREG head temperature curves from different tested face meshes, of 21, 32 and 60 elements per GREG face, according to thermal conductivities from left to right, of 1E7, 1E8, 1E9, and 1E10 W/mK.

Figure 5.19 shows changes in thermal power output according to differences in cross-sectional GREG meshing. The results indicate that the power output does not deviate as significantly when refining or coarsening the mesh. The main takeaway is that the finer 60-element mesh appears to reduce the power output values compared to the other mesh sizes, while the 32-element mesh seems to score slightly higher in this regard. Similar to the power curve results, the results for GREG head temperature also show minimal deviations between the tested mesh sizes, as seen in Figure 5.20. A summary of the results is shown in Table 5.7

Table 5.7: Mesh Refinement Analysis Summary of Results

Mesh Size	Lifetime (yr)	Lifetime Change (yr)	Lifetime GREG Head Temperature (°C)	Lifetime Heat Flux (W/m2)	Lifetime Power Output (kW)	Lifetime Energy Output (MWh)	EOS Heat Flux (W/m2)	EOS Power Output (kW)	EOS Production Temperature (°C)	EOS Production Temperature Change (°C)
No GREG (control)	61	NA	NA	NA	NA	NA	NA	NA	61.291	NA
Thermal Conductivity (1E7 W/mK)										
21 Mesh Elements	67	6	83.79	292.9	92.0	41551	377.7	118.6	61.77	0.477
32 Mesh Elements	66	5	83.79	295.9	93.0	41554	381.3	119.7	61.77	0.481
60 Mesh Elements	68	7	83.94	292.1	91.7	41909	376.6	118.2	61.76	0.464
Thermal Conductivity (1E8 W/mK)										
21 Mesh Elements	68	7	89.93	363.4	114.1	53662	462.3	145.2	61.85	0.559
32 Mesh Elements	67	6	89.85	368.7	115.8	53060	464.3	145.8	61.89	0.597
60 Mesh Elements	68	7	90.02	360.0	113.0	53250	455.8	143.1	61.85	0.56
Thermal Conductivity (1E9 W/mK)										
21 Mesh Elements	67	6	90.64	376.6	118.3	54820	473.8	148.8	61.85	0.561
32 Mesh Elements	67	6	90.47	381.7	119.9	55055	476.3	149.5	61.85	0.556
60 Mesh Elements	68	7	90.71	372.1	116.8	54985	466.7	146.5	61.84	0.548
Thermal Conductivity (1E10 W/mK)										
21 Mesh Elements	67	6	90.71	378.2	118.8	54923	474.8	149.1	61.86	0.571
32 Mesh Elements	67	6	90.57	380.2	119.4	55031	478.0	150.1	61.85	0.558
60 Mesh Elements	68	7	90.91	369.7	116.1	54919	467.3	146.7	61.86	0.570

5.3.3. GREG Final Depth Analysis

It is important to study the depth at which these GREGs can operate. In theory, the deeper the GREG is installed, the more it is exposed to higher temperature zones, and the more surface area it will have to capture this heat, hypothetically equalizing the GREG head to a higher temperature overall, and consequently, resulting in a higher heat flux from it. This would help ensure the longevity of the GREG, and its capacity to heat up the incoming cold water plume over longer periods of time.

The GREGs tested at deeper depths should also be paired with high thermal conductivities, once again, reflecting what may be possible with natural convection. Based on the previous findings, there is a positive correlation between higher GREG thermal conductivities, and the extension of geothermal lifetime. For the 0.5m and the 0.25m radius GREGs, the 1E9 and 1E10 W/mK thermal conductivity settings exhibited

similar results. For the 0.1m radius GREG, both of these thermal conductivity settings resulted in a lifetime extension of 5 years, however, the 1E10 W/mK result seemed to oscillate in the thermal power output charts, and therefore should not be used. This result, however, seemed to level off at a similar trend to the 1E9 W/mK power curve, which exhibited much more stable data. The additional 5 years of geothermal lifetime was also retained for both of these trials. Therefore, for this study, the length of the GREGs of radii of 0.5m, 0.25m, and 0.1m are extended to 3km, for a final depth of 4950m. Thermal conductivity of 1E9 W/mK is applied to them, due to this trial offering the maximum lifetime extension, and the most stable results under the previous study, represented by the solid colored lines in the subsequent figures. The results from the 2km-long GREG trials with the same 1E9 W/mK thermal conductivity are represented as the dashed colored lines as reference points. A 32-element GREG face mesh was used for all tested GREG radii, as the 0.25m and 0.1m radius GREGs could not be meshed under the finer 60-element mesh with the same parameters mentioned in Section 4.1.2. Additionally, the swept mesh module for the 0.1m radius GREG had to be changed to a maximum element size of 1m for the mesh to successfully discretize the domain. Once again, the black dashed line represents the control scenario, in which no GREG is present, which results in a final lifetime of 61 years. The orange line represents the result from the radius analysis pertaining to the GREG of the same radius, with a temperature boundary condition set at 100°C, from the static experiments.

Production Temperature

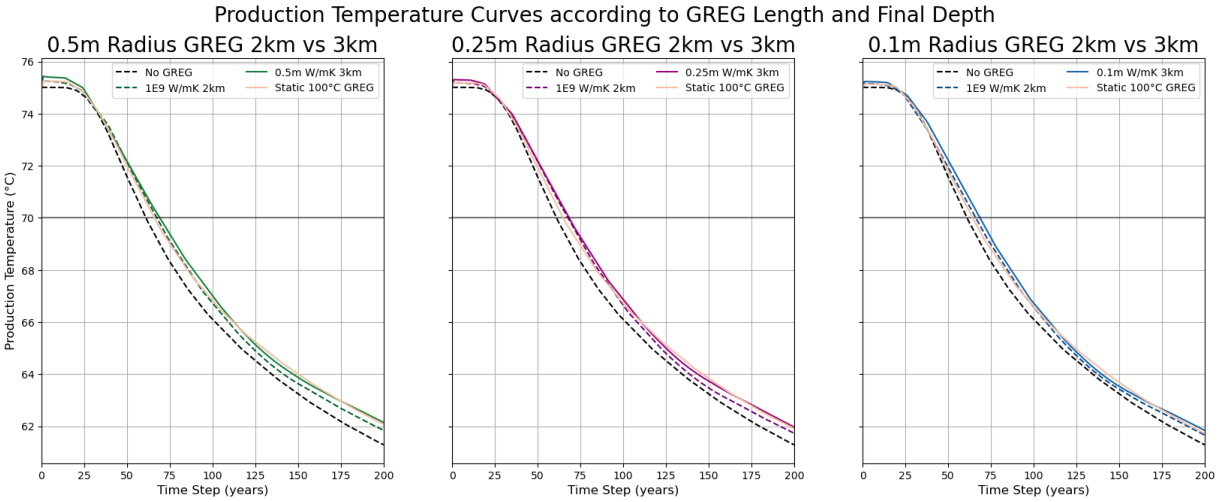

Figure 5.21: From left to right: production temperature results for tested GREG radii of 0.5m (left), 0.25m (center), and 0.1m Radius GREG (right), at lengths of 2km and 3km, and thermal coonductivity of 1E9 W/mK.

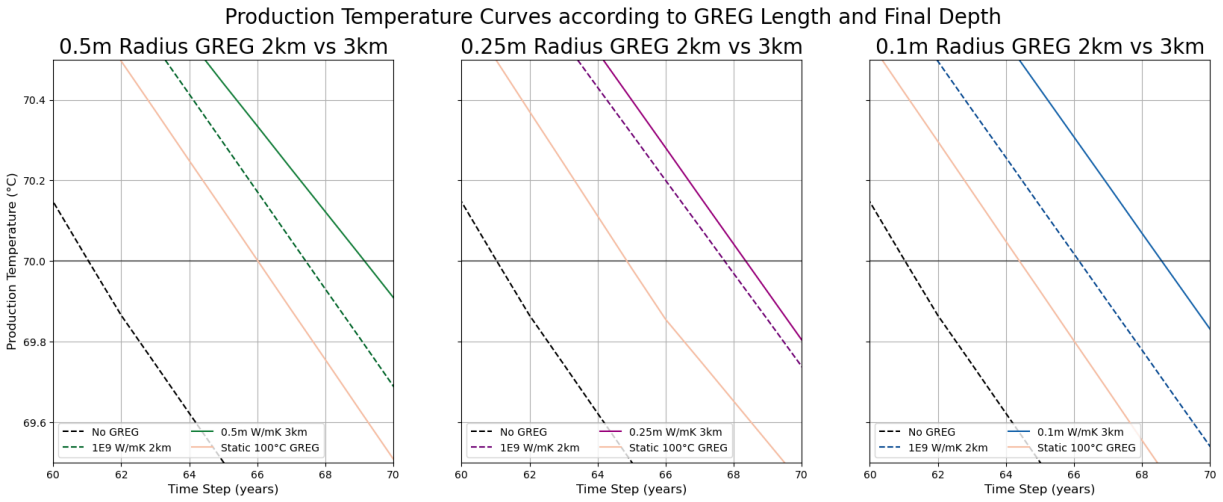

Figure 5.22: Closer look at the production temperature curves for the 3km GREGs of, 0.5m radius, 0.25m radius, and 0.1m radius (left, center, and right, respectively) as they pass the 70 degree Celsius threshold, compared to their 2km-long counterparts.

According to the results shown in Figures 5.21 and 5.22, the increase in length of the GREG to 3km increased production temperature and geothermal lifetime for every tested radius. A 2-year increase in lifetime was seen in the 0.1m and the 0.5m radius GREGs when comparing with the 2km trial, for final lifetimes of 68 and 69 years. The extension of the 0.25m radius GREG by an additional kilometer only resulted in a 1-year lifetime increase, compared to the 2km trial.

Once again, the 0.1m radius trial domain could not be successfully meshed using the same format as the 0.25m and the 0.5m radius GREGs. Therefore, the maximum element size for the swept mesh node was changed to 1m from 0.5m, as in the thermal conductivity experiments.

Thermal Power Curves

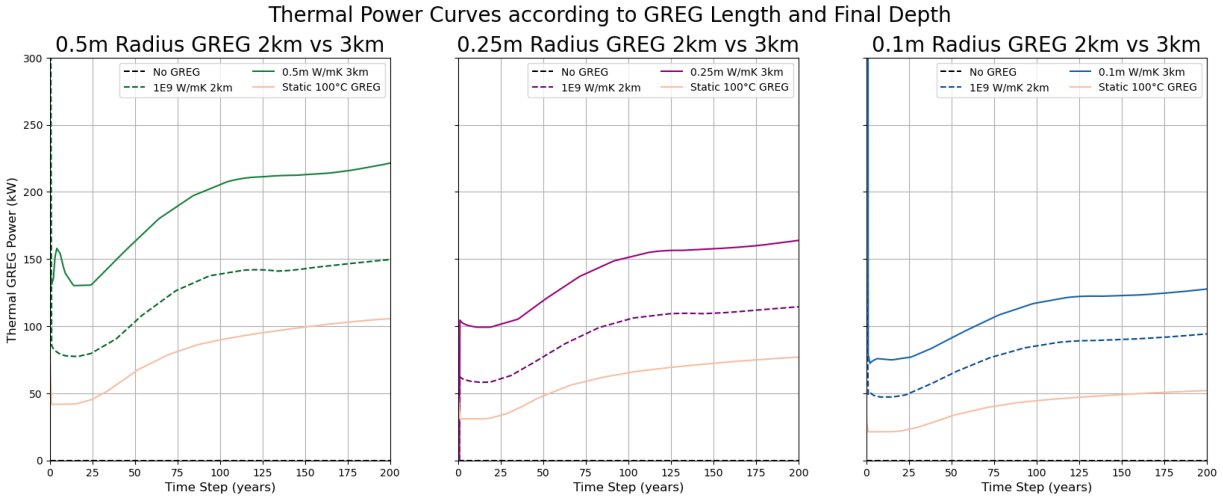

Figure 5.23: From left to right: thermal power results according to changes in final depth and length of GREG, for 0.5m Radius GREG (left), 0.25m Radius GREG (center), and 0.1m Radius GREG (right)

Power output for the 0.5m radius 3km GREG was less stable in this study, as observed in the data, when compared to the 2km length GREG of the previous study, showing a slight oscillation in thermal power output at the beginning of the simulation. Results indicate that extending the GREG by an additional kilometer resulted in a general increase of power output by over a 53% increase from the 2km iteration

by lifetime, from 119.9 kW, to 184.3 kW. The 0.25m radius 3km GREG also saw significant increases in power output compared to the 2km long GREG, however, were slightly dampened compared to the changes seen from the 0.5m radius GREG, seeing a 50% increase in power output through the extension of the GREG by an additional kilometer, from 89.5 kW, to 134.2 kW by lifetime. The 0.1m radius GREG in the 3km trial saw a 40% increase in power output compared to its 2km long counterpart, increasing from 73.1 kW to 102.5 kW by lifetime.

The general takeaway from these trials is that increasing the depth and length does significantly increase power output of the GREG. The lifetime benefit however, does not necessarily scale with these increases, as seen in Figure 5.22. Additionally, heat flux and power output benefits from longer and deeper GREGs are more significant in the larger radius GREGs. The shorter radius GREGs seem to have lower output increase benefits. This suggests that aspect ratios pertaining to length and radius of GREGs play an important role in their upward heat conductance.

GREG Head Temperature

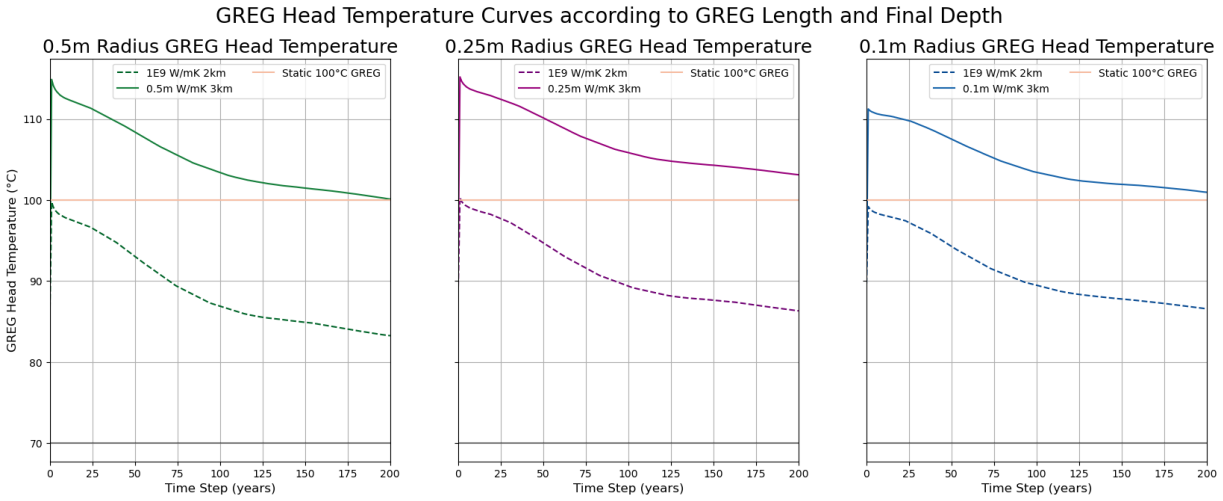

Figure 5.24: From left to right: GREG head temperature results according to changes in final depth and length of GREG, for 0.5m radius (left), 0.25m radius(center), and 0.1m radius (right) GREGs.

For every radius GREG tested in the depth analysis, the GREG head saw a significant increase in temperature. By the time the geothermal lifetime was reached, the GREG head was at a temperature 13.4 degrees higher than that of the 2km trial. For the 0.25m and 0.5m radius trials, this temperature increase was slightly higher, at over 15.5 degrees higher for the 3km trials for both radii settings. The head temperatures peaked at the beginning of the simulation for all three trials, at 111.3°C, 115.2°C, and 114.9°C, for the 3km-long GREGs of 0.1m, 0.25m, and 0.5m radius. From this point, temperatures level off as thermal breakthrough takes hold, to 105.8°C, 108.3°C and 106.2°C by lifetime, for 3km-long GREGs of 0.1m, 0.25m, and 0.5m radius, respectively. By end of simulation, however, the model suggests that the temperature of the GREG head still remains at a temperature of at least 100°C for each of the GREG radii tested, which means that after 200 years, they are still very capable of thermal output. A summary of these findings is offered in Table 5.8:

Table 5.8: Depth Analysis Summary of Results

Tested GREG Length (km)	Lifetime (yr)	Lifetime Change (yr)	Lifetime GREG Head Temperature (°C)	Lifetime Heat Flux (W/m2)	Lifetime Power Output (kW)	Lifetime Energy Output (MWh)	EOS Heat Flux (W/m2)	EOS Power Output (kW)	EOS Production Temperature (°C)	EOS Production Temperature Change (°C)
No GREG (control)	61	NA	NA	NA	NA	NA	NA	NA	61.291	NA
0.5m radius GREG										
2km	67	6	90.47	381.9	119.9	55055	476.3	149.5	61.85	0.556
3km	69	8	106.16	586.8	184.3	93152	705.2	221.4	62.15	0.855
0.25m radius GREG										
2km	67	6	92.52	569.8	89.5	41268	728.9	114.4	61.73	0.440
3km	68	7	108.27	854.8	134.2	67039	1043.6	163.9	61.97	0.677
0.1m radius GREG										
2km	66	5	92.36	1164.2	73.1	33434	1500.2	94.2	61.66	0.37
3km	68	7	105.80	1631.9	102.5	51105	2032.2	127.6	61.84	0.55

Research Objective Review

This concludes the second section of study regarding the dynamic experimentation, which aimed to fulfill the second research objective, which was to probe the heat transfer capabilities of the underburden, to support the power output of the GREG over long periods of time, under the application of the optimal settings determined in the static experiments.

1. The first of the dynamic studies, known as Study 4, or the Thermal Conductivity Analysis, showed how high rates of thermal conductivity could speed up heat transfer from the underburden into the geothermal reservoir. It was noted that increasing thermal conductivities were correlated with increased geothermal lifetimes. Additionally, GREG power output was maximized with increases in thermal conductivity, until benefits plateaued. The underlying assumption is that natural convection could potentially transfer heat faster than any material applied with the thermal conductivities tested. The hope is that produced data from this study could potentially mirror what may be possible from a natural convection experimental setup, while avoiding characteristically high computational costs. Additionally, it was found that the underburden was successfully able to sustain average elevated temperatures above 80°C in the GREG head for 200 years, even as its reservoir surroundings dropped to temperatures in the low sixties over this amount of time, due to thermal breakthrough.
2. The second of the dynamic studies, known as Study 5, or the Mesh Refinement Analysis, aimed to improve the confidence in the results, by re-running the Thermal Conductivity analysis under different meshes. Deviations were determined to be minimal regarding power outputs and head temperatures, however, had the potential to change geothermal lifetime results by up to two years with the meshes tested.
3. The third of the dynamic studies, known as Study 6, or the Final Depth Analysis, aimed to probe the effects of final depth, and extended length of the GREG deeper into the underburden, so that it may take better advantage of the thermal gradient, and reach high quality temperatures to see how this reflected in the geothermal lifetime. It was discovered that increase in GREG length by an additional kilometer did increase the lifetime by 1-2 years, depending on the radial dimension used, which was marginal. The head temperatures and power outputs, however, seemed to reflect a significant elevations according to this change, once again, speaking to the amount of high quality heat that may be provided by the underburden.

With this investigation, the amount of heat transfer that is possible and dependent on the underburden's thermal resources has been explored. The findings conclude that high amounts of heat provisions do exist in the underburden, and they could potentially be used to extend the lifetime of conduction dominated geothermal systems.

6

Discussion

This section details concepts related to the implementation of the GREGs. Section 6.1 discusses the applicability of the GREGs within a geothermal system to meet consumer heating demand. Section 6.2 discusses the economics of GREG installation, offereing some insight into produced energy, levelized cost of heat, and structure specification.

6.1. System Integration

There is currently a global shift to integrate more sustainable practices into daily life, as the energy transition is exacted not only by industry, but by the consumer. One notable shift is to update the insulation level of homes and buildings for the purposes of reducing heat losses and therefore energy consumption, with the added benefit of saving the consumer money. The application of the GREGs presented in this study for the extension of geothermal lifetime could therefore be analyzed within this context, seeing what effect changing anthropogenic behaviors has on the reach of geothermal heat.

The direct consequence of increasing building insulation rates is a decreased heating demand from the same pool of customers. As a result, the geothermal utility has two avenues of response, which would be either to retain the same consumers and decrease geothermal production rates, or to increase the consumer pool, while keeping the production rate constant.

The Case for Reducing Flowrates

This approach is purely hypothetical, however, may provide an interesting approach in seeing how the geothermal lifetime changes according to an unchanging consumer pool. Keeping the same consumer pool has a few notable benefits, and disadvantages. If it is assumed that the thermal power from geothermal is used only to service energielabel 'G' consumers at 380 kWh/m^2, the yearly consumer pool is equal to 200,942 m^2 of consumer space. The benefit of keeping the same consumer pool the same through increasing insulation practices, is that the original 200,942 square meters of consumer space will now require a reduced power demand from the geothermal utility. This would translate into reduced pump rates, and consequently, a slower progression of thermal breakthrough, increasing the lifetime of the base geothermal doublet model. With the GREGs included, increases of doublet lifetime could possibly weigh more due to increased breakthrough plume contact time around the GREGs, attributed to the lower groundwater velocities.

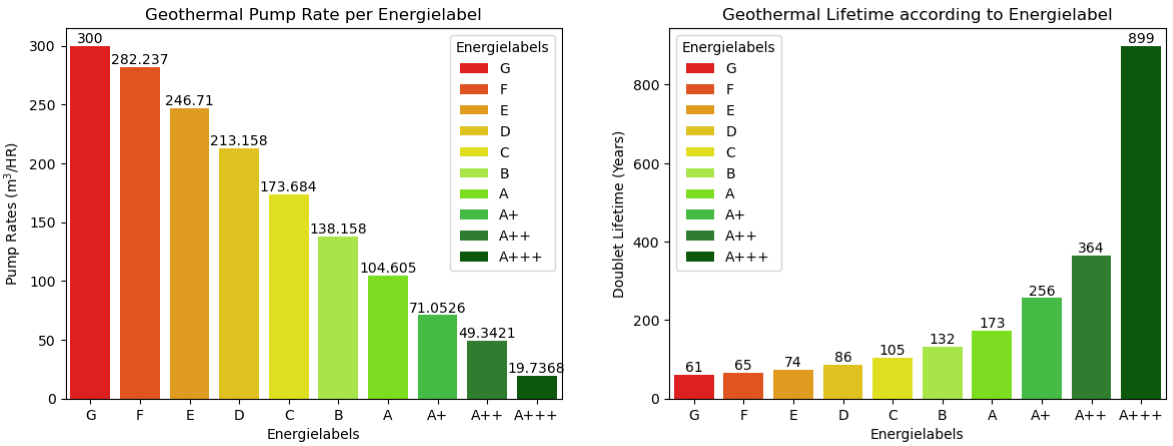

Figure 6.1: Required geothermal flowrates to satisfy 200,942 m^2 of floor space heat demand (left), and corresponding geothermal lifetimes according to new pump rates (right).

One red flag in this approach is that these utilities are designed to operate at a certain preferred flowrate, which maximizes pumping efficiency. Any deviation in this pump rate could significantly decrease pump efficiency, resulting either in sub-profitable energy production, or the necessary investment in a smaller pump or impeller [27]. Additionally, reduced flowrates would also affect the pressure differences in the subsurface between the production and injection wells needed to successfully drive the geothermal production. Reducing these flowrates over time may affect the necessary pump head needed for operation. Finally, as insulation rates in buildings increase, the necessity of high heat resources drops. In this case, additional investment in heat exchangers may be required for converting high temperature flows, into lower temperature flows as low temperature consumers cannot efficiently use high temperature district heating [28].

The Case for Increasing the Consumer Pool

With regard to possible geothermal lifetime extension, there is none for this case, as production rates essentially stay the same, and the full power output of the geothermal utility is used. What would change in this scenario is the economics of the GREGs. In this case, the consumer can be regarded once again as a unit area of floorspace. BENG-2 indicates that energielabel 'G' consumers require at least 380 kWh per year for every square meter of floor space, making it the least energy-efficient consumer on the scale. On the other hand, energielabel 'A' consumers take up at the very most, 160 kWh of energy per year, per square meter, and at the very least, 105 kWh per year, per square meter [16]. When considering the full power output of 8716.67 kW from the modeled geothermal utility, we once again find that the 200,942 square meters of therotical energielabel 'G' floorspace would consume the energy given from the geothermal production, which would translate to approximately 477,238 square meters under the least energy-efficient energielabel 'A' consumers, and triple, to 727,219 square meters per year for the highest energy efficiency energielabel 'A' consumers. Considering even higher energy efficiency homes and constructions has the potential to nonlinearly increase the geothermal customer base beyond this point.

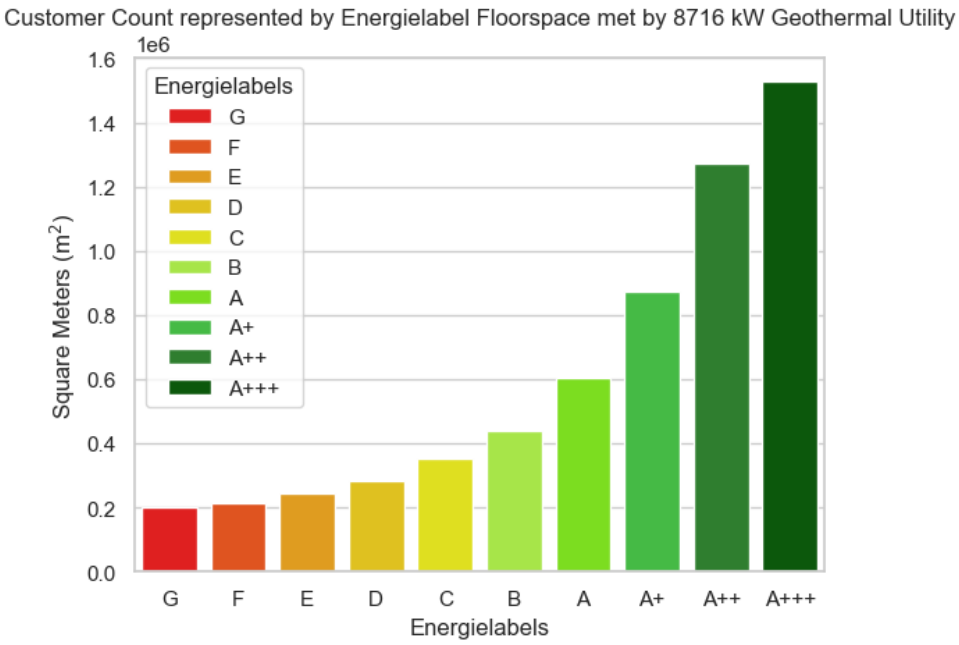

Figure 6.2: Amount of Customers that can be Serviced by the Geothermal Utility according to Floorspace per Energielabel (averaged by range of kWh/m^2).

In other words, while the extension of geothermal lifetime under the modeling of experimental GREGs is promising (providing an extra 381,791 MWh of additional energy, and therefore providing for the same consumers over an extended period of time), its performance also pails in comparison to changes that can be made in terms of retrofitting existing constructions and boosting their energy efficiency. Geothermal energy, as well as all other energy used for heating becomes much more far-reaching through the lens of improving building insulation in this regard. Therefore, this analysis can be extended to consider current and projected Dutch housing stock to analyze how the constantly changing built environment will improve the reach of geothermal energy, including with it, the role that GREGs may play in this landscape.

There are nearly 8.3 million homes in the Netherlands, of which approximately 5.1 million have subscribed to the Energielabel system, characterizing each household by its energy efficiency [29]. The current distribution of Dutch housing stock by energielabel values is shown in Figure 6.3.

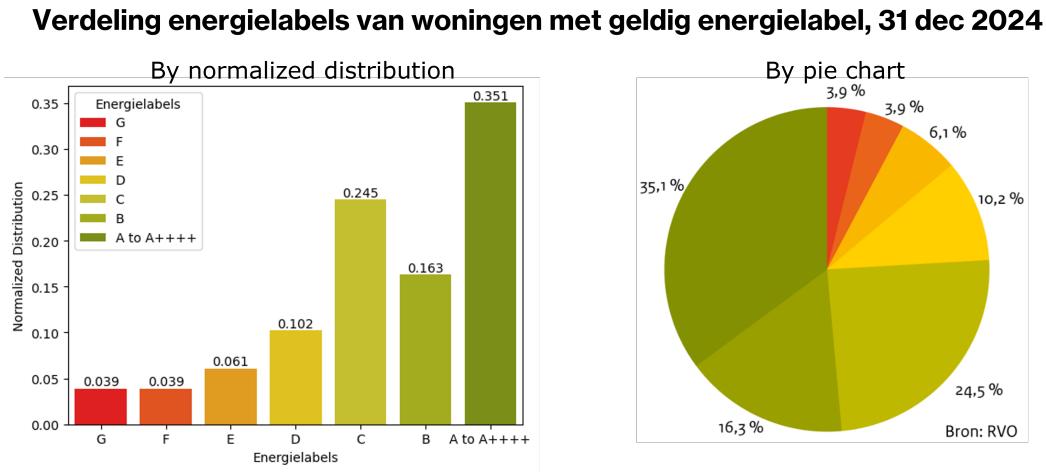

Figure 6.3: Distribution of Energy Labels for Homes with Valid Energy Labels. Source: RVO.

In order to visualize the role played by the GREGs, it is important to first characterize how the initial

geothermal model would service the current heating demand; in the current scenario, the median energy consumption per square meter of floor space of the Dutch housing stock is 186 kWh/year, according to ABN Amro, which is within the 'B' energielabel level [30]. A similar value of 186.75 kWh/m^2/year was calculated using this distribution of housing by energielabel, along with calculated average heating demands per level, which is shown in Table 6.1.

Table 6.1: Normalized Data applied to average BENG Energielabel Energy Demands per square meter

Energielabel	X: Fraction of housing stock	Energy usage per year (lower bound)	Energy usage per year (upper bound)	Average Energy usage per year (kWh/m^2)	X(kWh/m^2)
G	0.039	380	NA	402.5	15.70
F	0.039	335	380	357.5	13.94
E	0.061	290	335	312.5	19.06
D	0.102	250	290	270	27.54
C	0.245	190	250	220	53.90
B	0.163	160	190	175	28.53
A	0.351	0	160	80	28.08
				Sum	186.75

**Higher energielabel 'A' levels that result in a negative energy demand are excluded from this analysis. Average energielabel G heating demand is calculated as half of the difference between the upper and lower bounds of energielabel F, additional to the lower bound of energielabel G.*

Another important design consideration is to containerize the distribution of consumers according to the type of heat distribution which they would require. According to the Amsterdam Heat Guide, networks are able to distribute High-Temperature (HT), Medium-Temperature (MT), and Low-Temperature (LT) heating. HT heating can apply to all buildings according to this guide, however, for the extension of this analysis, HT heating will be reserved for the least energy-efficient constructions of energielabels 'E' through 'G' for the model neighborhood [31]. MT heat is therefore applied to constructions from energielabel 'D' through 'B', and finally, LT heat is routed to energielabel 'A' category consumers. There is also the existence of ultra-low temperature heat (ULT) which can be provided to constructions of energielabels higher than 'A', however, to simplify the model this level is excluded from the study. Each of these heating levels comes with an operating range of temperature levels, for supply and return flows - for this discussion, the following temperatures are used to meet the neigborhood model demands as described in Table 6.2.

Table 6.2: Initial LT, MT and HT Heat Dispatch, Supply, and Return Temperatures

Heat Supply	Supply Temperature (°C)	Return Temperature (°C)	Applicable Energielabel Constructions
HT	90	70	E, F, G
MT	70	40	B, C, D
LT	40	20	A to A++++

Given that the HT supply requires 90 degree flows, a consideration must be made for the design of the system, as the geothermal utility outputs at a maximum temperature of 75°C. Therefore, to service this demand, a heat pump must be implemented which will help satisfy that demand, as the geothermal utility is unable to produce 90°C heat for Energielabel 'E' through 'G' constructions. With this consideration in mind, the initial production temperature of 75°C is used to draft the initial conditions of the model neighborhood, presented in Table 6.3.

Table 6.3: Model neighborhood consumer distributions, along with power demands at a production temperature of 75°C

Energielabel	Initial demand to satisfy (m^2)	Adjusted demand to satisfy (m^2)	Adjusted fraction of housing stock	Average energy usage ($kWh/m^2/yr$)	Adjusted energy demand (kWh/yr)	New Power Demand (kW)	Power Demand from Geothermal (kW)	Power Demand from Heat Pump (kW)
HT								
G	15946	15946	0.032	402.5	6418454	732.7	183.2	549.5
F	15946	15946	0.032	357.5	5700863	650.8	162.7	488.1
E	24942	24942	0.050	312.5	7794348	889.8	222.4	667.3
MT								
D	41706	52742	0.105	270	14240244	1625.6	1625.6	0
C	100177	126683	0.252	220	27870341	3181.5	3181.5	0
B	66648	84283	0.168	175	14749563	1683.7	1683.7	0
LT								
A	143518	181493	0.362	80	14519465	1657.5	1657.5	0
Sum	408884	502036				10421.6	8716.7	1704.9

This approach uses the total yearly geothermal energy production of approximately 76,358,029 kWh, 100% of which is assumed to supply a neighborhood bearing a similar distribution of energielabeled households. It also assumes zero heat losses at the heat exchanger, and that the heat transferred through the network is assumed to be able to supply temperatures equal to those of the production well. Only a portion of the geothermal energy will route into the HT heating. The rest of the demand is met via the heat pump. The stipulation that this energy demand only applies to a geothermal production temperature of 75°C is important, because according to the results of the study, the production temperature is set to deviate from this value, mostly due to thermal breakthrough, decreasing it over time. Therefore, while the necessary power to the heat pump is initially about 1,705 kW, this value will increase as the geothermal production temperature gradually drops and approaches the cutoff temperature, making the utility less able to contribute to the satisfaction of HT demand, and leading to the heat pump requiring more power, and a surplus of lower grade heat that will be dispatched to MT and LT consumers, again, assuming the full 8716.67 kW of geothermal power is used. The amount of MT and LT consumers therefore becomes a variable, and the total amount of energy delivered by the system exceeds the 8716.67 kW provided by the geothermal, as new energy enters the system via the heat pump. Additionally, under this scenario, the amount of HT consumers remains constant. The initial 75 degree condition is used as a starting point to calculate the initial MT and LT demand, which sit at approximately 6491 and 1657 kW, respectively, and slightly deviates from the initial housing stock distribution. Seeing as the HT demand is static, the flow out of the HT consumer is considered constant, as this demand is always met. The MT consumer is therefore provided with the exiting flow from the HT consumer, and an additional flow directly from the geothermal plant/heat exchanger at 70°C. This flow then continues to fulfill the LT consumer, and exits at an average temperature of 32.34°C. The flowrate through the heat exchanger is initially 51.71 kg/s, however, this gradually increases over time as the geothermal utility is able to provide less heat to the HT consumer. An overview of the system integration is offered in Figure 6.4, which shows the initial design setup of the serviced consumers:

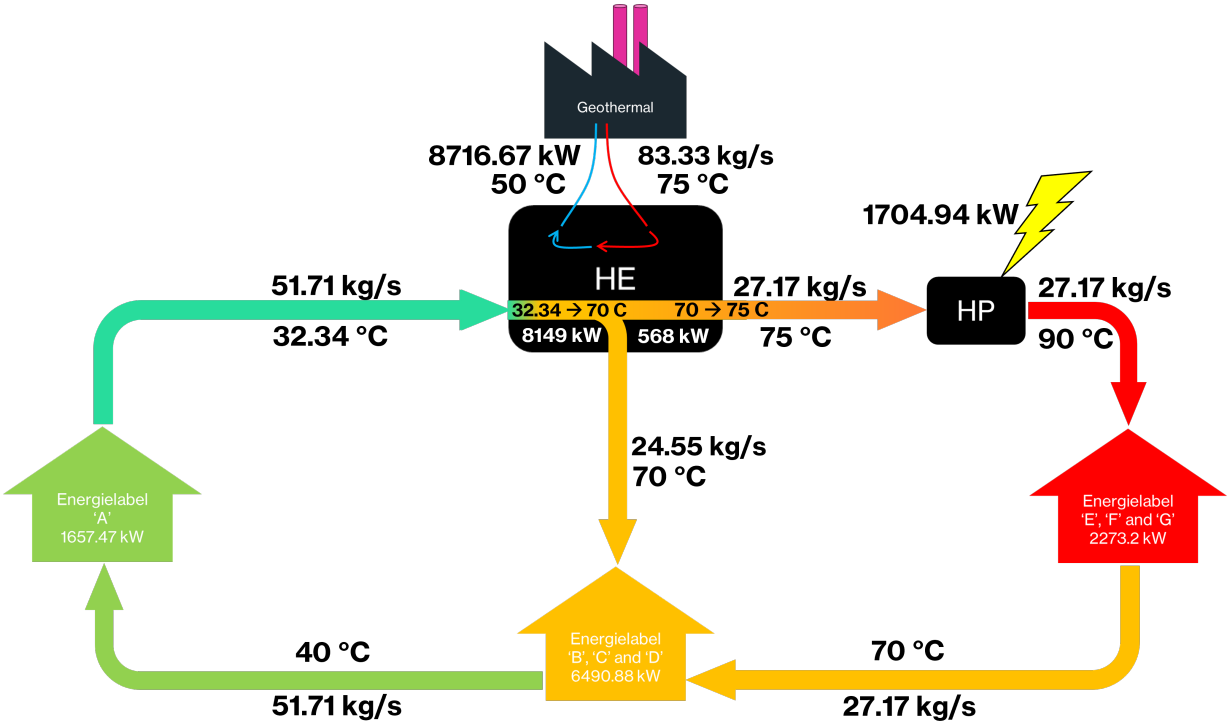

Figure 6.4: Customer base serviced by the Geothermal Utility and Heat Pump according to Energielabel, at t = 0.

**The complete mass flow of 51.71 kg/s exiting from the MT consumers (energielabel 'B', 'C', and 'D') in this figure enters the LT consumer node as a simplification. In reality, this flow can be split into two separate flows, in which approximately 19 kg/s enters the LT consumer node and exits with a 20 degree difference, while the remaining 40-degree flow is routed back to the HE, where it reconverges with the 20-degree branch, averaging to a final temperature of approximately 32.34°C.*

While the amount of MT and LT consumers fluctuates throughout the model, the ratio between them always stays the same. Additionally, the MT and LT consumers will always accept heat at 70°C, and 40°C in this analysis, respectively. Therefore, the initial condition of 75°C production temperature is used to calculate initial flowrates and resulting temperatures according to Figure 6.4. Geothermal heat use is assumed to charge return water in two steps: first, charging the whole 51.71 kg/s flow to the cutoff temperature of 70°C, and second, to charge 27.17 kg/s of this flow to the production temperature of that year, which in the initial case, is 75°C, and routed to the heat pump for additional charging to 90°C. The remaining 70°C flow is routed directly to the MT consumer at 70°C. The investment of geothermal power input into the HT dispatch is regarded as charging above 70°C, and passes off the initial charging to 70°C to be counted at the MT consumer. The MT consumer dispatch therefore counts both incoming flows as what was charged by the geothermal utility to the full 70°C. Finally, the input of LT heat from the geothermal utility is counted from the temperature difference across the LT consumer. A short summary of calculations according to production temperature at 75°C, and 70°C is offered in Table 6.4.

Table 6.4: Demand fluctuation table at two production temperature extremes of 75°C, and 70°C

	Heat Supply	Power (kW) at T_{prod} = 75 °C	Power (kW) at T_{prod} = 70 °C
HT			
	Geothermal	568.31	0
	HP	1704.94	2273.25
MT			
	Geothermal	6490.99	6943.71
LT			
	Geothermal	1657.37	1772.96
Total Geothermal		8716.67	8716.67
Total System		10421.61	10989.92

Under the initial conditions, the total flowrate through the MT consumer is 51.71 kg/s with a 30-degree temperature difference, from 70°C to 40°C, servicing approximately 6491 kW. At the cutoff temperature of 70°C, however, the flowrate through the MT consumer would be about 55.32 kg/s, with the same temperature difference, servicing approximately 6944 kW, with a flowrate once again exiting at 40°C. Afterwards, the LT consumer receives this 40°C flowrate, and brings it down to a final temperature of 32.34°C in both of the scenarios discussed in Table 6.4, servicing approximately 1657 kW and 1773 kW at geothermal production temperatures of 75°C and 70°C respectively. Charging the 55.32 kg/s flowrate back up to 70°C from 32.34°C results in the full geothermal output of 8716.67 kW, however, which would leave the heat pump to address the full recharge from 70°C to 90°C past this point for the HT consumer. In both cases, the full thermal power from the geothermal utility is used, and the resulting consumer pool, mass flowrates, and heat pump power investment become variables that speak to the energetic efficiency of a Dutch model neighborhood bearing HT heating consumers.

The production temperatures from the modeling results were therefore input into this system integration model, showing how the geothermal production temperature affects the distribution of different level heat flows, and how the consumer pool reacts to these changes. This allows for the measurement of demand servicing before and after the introduction of GREGs, along with the total dispatch of energy over lifetime of the project. Specifically, the results from the control model and the dynamic model using the 0.1m radius GREG of 2km length, with a thermal conductivity of 1E9 W/mK are used. The results are summarized in Table 6.6.

However, the current distribution of Dutch housing is not to remain constant, as ABN Amro predicts that by 2030, the Netherlands will have its average energy consumption drop to approximately 164 kWh/m^2/year, which would bring the housing stock average close to an 'A' level energielabel. Figure 6.5 shows this projection as a continuation of the current scenario.

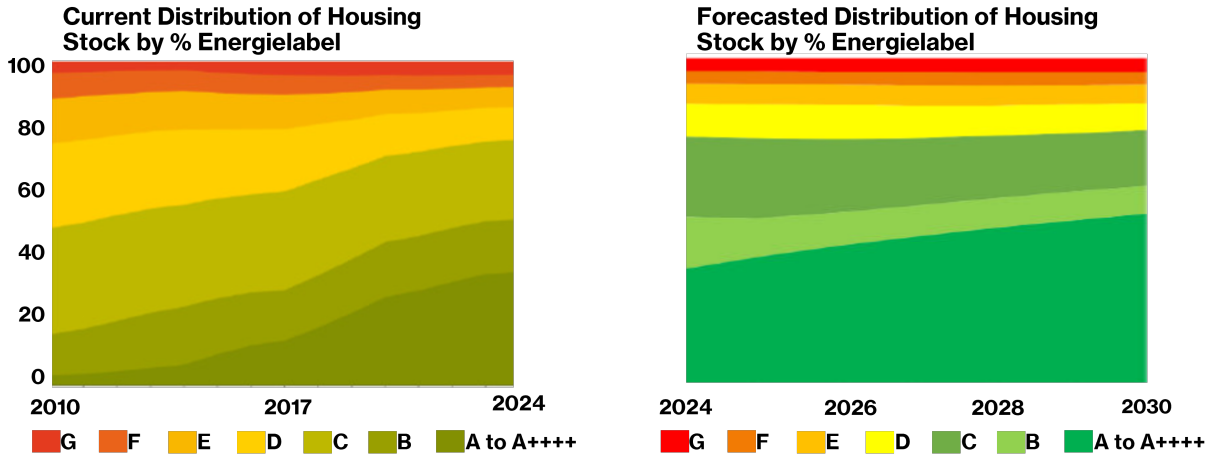

Figure 6.5: Current Distribution of Energy Labels for Homes with Valid Energy Labels (left) and Forecasted Distribution of Energy Labels for Homes in 2030 (right). Source: ABN Amro.

Additionally, the Netherlands plans to have 'F' and 'G' energielabels completely phased out by this point, with strong encouragement to upgrade energielabel 'E' buildings to at least a 'D' level [32]. Therefore, a slightly liberal estimate is taken for a scenario beyond 2030, in which the Dutch housing stock is limited to energielabels 'A++++' through 'D'. This scenario would discount the need for HT district heating, as well as the heat pump to charge the water to 90°C.

Table 6.5: 'Beyond 2030' energy demand table

Energielabel	X: Fraction of housing stock	Average Energy usage per year (kWh/m2)	X(kWh/m2)	Demand to be satisfied by 8716.7 kW Geothermal utility (m2)	Demand to be satisfied by 8716.7 kW Geothermal utility (kWh/yr)
MT					
D	0.105	270	28.26	59040	15940723
C	0.174	220	38.37	98400	21647895
B	0.116	175	20.35	65600	11479944
LT					
A	0.605	80	48.37	341118	27289467
Sum			135.35	564157	76358029

Using the provided data, a consumer base is drafted as seen in Table 6.5. In this case, the average Dutch housing stock achieves the 'A' level, at approximately 135 kWh/m^2, which will be used for the new demand scenario. The geothermal utility retains the same cutoff temperature of 70°C, and initially produces heat at 75°C, as before, however, the MT consumer is assumed to take 70°C heat, so in this setup the heat exchanger outputs into the system at 70°C with no losses. Once again, the model is set to provide the full 8716.67 kW of thermal power to the consumer pool, only servicing MT and LT consumers, as seen in Figure 6.6.

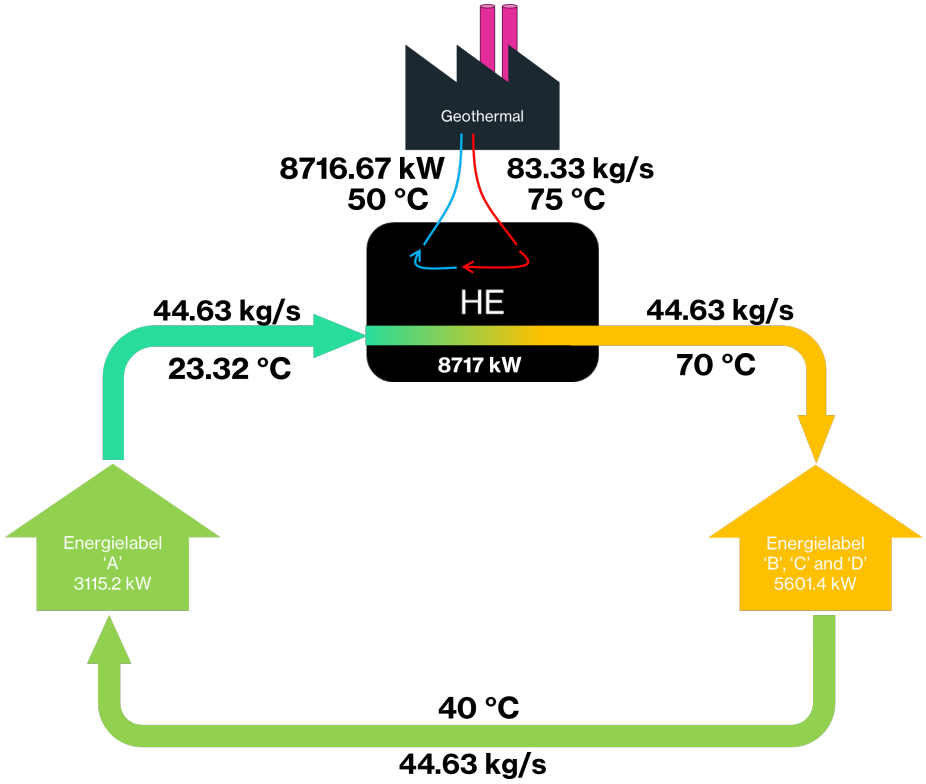

Figure 6.6: 'Beyond 2030' possible customer base serviced by the Geothermal Utility according to Energielabel.

Construction of this model begins with calculating the mass flowrate through the MT consumer using the demand information in Table 6.5. Based on this, the flowrate of approximately 44.63 kg/s is calculated assuming a 30 degree temperature difference from the flow incoming 70 degree flow to meet the 5601 kW demand. The same process is used to address the LT consumer pool. As in the previous scenario, the outflow from the LT consumer is assumed to be a mix of two different flows, of which one actually passes through the consumer and is returned back to the heat exchanger at 20°C, and the other that bypasses this consumer entirely, returning to the heat exchanger at 40°C, however, is simplified as a weighted average flow exiting at 23.32°C. These setups can then be used to model the net gain from the GREGs as in the previous experimentation and discussion point under a new context/scenario. It is important to note, that in this scenario, the consumer base is not a variable, as production temperature is no longer a limiting factor in servicing different types of demand prior to the cutoff temperature. The production temperature data from the 2km long 0.1m radius GREG is used again, from the dynamic simulations, at a thermal conductivity of 1E10 W/mK. The results from this are summarized in Table 6.6.

Table 6.6: Summary of Results

	Serviced Demand (MWh)	
Test Case	Current Scenario	Projected Scenario
Control		
From Geothermal	4734196	4734196
From Heat Pump	1017616	0
Total	5751812	4734196
0.1m GREG (2km)		
From Geothermal	5115987	5115987
From Heat Pump	1107046	0
Total	6223033	5115987
Added Geothermal Output	381791	381791
Heat Pump Output Difference	89430	0

There are two very important takeaways from this analysis - the first is that lifetime geothermal output does not change between demand scenarios, however, does change between the test cases. The second main takeaway is that while the current scenario does meet more demand, it does so through the intervention of a heat pump. The geothermal output seen in the control model is equal to 4,734,196 MWh, and within the current scenario, forces an additional 1,017,616 MWh of electricity investment into running the heat pump, potentially implying the use of fossil fuel sources. The added geothermal output from the implementation of GREGs is equal to 381,790 MWh over the additional 5 years of doublet lifetime. This test case also requires an additional 89,430 MWh of energy to be used in the heat pump over the additional years. Once again, this energy is dispatched to service HT consumers, which are less energetically efficient. This energy production and use information is broken down by square meter of floor space heat demand serviced, pertaining to each level of heat dispatch to properly analyze how many consumers are met, according to Table 6.7.

Table 6.7: Current Scenario Detailed Serviced Heat Demands from Control Model

Heat Supply (Control)	Lifetime Energy Consumption (MWh, % of Total)		Lifetime Geothermal Energy Demand (MWh)	Lifetime Heat Pump Energy Demand (MWh)	Weighted Average Energy Demand (kWh/m^2)	Average Serviced Yearly Demand (m^2, % of Total)	
HT	1234647	21.47%	217031	1017616	350.38	56835	11.12%
MT	3598379	62.56%	3598379	0	215.62	269173	52.65%
LT	918786	15.97%	918786	0	80.00	185239	36.23%
Total	5751812		4734196	1017616	181.46	511247	

The analysis indicates that an average of 511,247 m^2 of consumer space heating demand is serviced per year when taking the entire lifetime of the control model into account, and averaging out the demands by weight of each energielabel within the model neighborhood. In the current scenario the MT and LT consumer pools are variable, however, they can be averaged throughout the lifetime of the utility, amounting to a neighborhood yearly energy demand of approximately 181.5 kWh/m^2. The most important conclusion that can be drawn from Table 6.7 is that while the HT consumer only accounts for about 11.1% of the consumer pool, it also is responsible for the consumption of 21.5% of the system's energy, most of which enters via the heat pump, which is not only bought energy, but could potentially be sourced from fossil fuels. Given the disproportionate amount of energy consumption per unit area of this type of consumer, it is easy to draw the conclusion that retrofitting HT consumers with better infrastructure and insulation to increase housing stock energy efficiency should be of the utmost priority, as a home with this energy demand easily takes up the energy demand of more than 4 energielabel 'A' homes according to this model neighborhood. The analysis probing the implementation of the GREG also sees similar results, as seen in Table 6.8.

Table 6.8: Current Scenario Detailed Serviced Heat Demands from GREG Model

Heat Supply (Control)	Lifetime Energy Consumption (MWh, % of Total)		Lifetime Geothermal Energy Demand (MWh)	Lifetime Heat Pump Energy Demand (MWh)	Weighted Average Energy Demand (kWh/m^2)	Average Serviced Yearly Demand (m^2, % of Total)	
HT	1334215	21.44%	227145	1107070	350.38	56835	11.10%
MT	3894456	62.58%	3894456	0	215.62	269580	52.66%
LT	994385	15.98%	994385	0	80.00	185520	36.24%
Total	6223056		5115986	1107070	181.43	511934	

The amount of consumers is not significantly changed between the two models, however, the energy dispatch from the geothermal utility over lifetime is extended, by the 381,790 MWh brought on by the GREG, which represents an extension of serviced demand to the original consumer base by 5 years.

The projected scenario, beyond 2030 is not affected by HT consumers, and is reduced to only MT and LT consumers. This analysis is simpler, as there is no need to account for the energy invested in the heat pump, and therefore, the MT and LT consumers stay constant. Table 6.9 shows these changes.

Table 6.9: Projected Scenario Detailed Serviced Heat Demands from Control Model

Heat Supply (Control)	Lifetime Geothermal Energy Consumption (MWh, % of Total)		Weighted Average Energy Demand (kWh/m^2)	Average Serviced Yearly Demand (m^2, % of Total)	
MT	3043847	64.29%	220.00	223156	39.57%
LT	1690349	35.71%	80.00	340796	60.43%
Total	4734196		135.40	563952	

As previously mentioned, this scenario excludes the HT consumer. The analysis indicates that a total consumer space of 563,952 m^2 is serviced in the projected scenario, with the control model alone, which is approximately 10.3% more demand by unit area compared to the control model in the current scenario. The disproportionality is once again seen in the weighted average energy demand per unit area of this neighborhood, as one can conclude that an MT consumer home here takes up enough energy to supply heat to almost 3 LT homes of the same area. This means that while retrofitting MT constructions is not as beneficial as retrofitting HT constructions, they still hold significant improvement potential in increasing the efficiency of the Dutch housing stock.

Table 6.10: Projected Scenario Detailed Serviced Heat Demands from GREG Model

Heat Supply (Control)	Lifetime Geothermal Energy Consumption (MWh, % of Total)		Weighted Average Energy Demand (kWh/m^2)	Average Serviced Yearly Demand (m^2, % of Total)	
MT	3289318	64.29%	220.00	223156	39.57%
LT	1826668	35.71%	80.00	340796	60.43%
Total	5115986		135.40	563952	

The implementation of the GREG does not have an effect on serviced yearly consumer space by unit area, as the rates of servicing MT and LT consumer pools does not change between the years prior to the 70 degree cutoff temperature. Simply, the effect of this implementation is a longer lifetime, or 5 additional years of geothermal production at full capacity.

The main conclusion which can be drawn from this analysis is that the Dutch housing stock is energetically dragged down from an efficiency standpoint by HT and MT consumers, which consume approximately three to four times more energy than the average LT consumer in this model. The energy produced by the geothermal utility is therefore better used when dispatched to LT consumers, and would be considered an effective allocation of resources. Over the lifetime of the geothermal utility, this approach would be capable of providing heat to approximately 954,475 m^2 of consumer space per year according to this model, rather than the 511,934 m^2 from the current scenario, or the 563,952 m^2 from the projected scenario. This approach however, would imply additional capital expenditures related to in increased connections to the utility. Due to this, low efficiency consumers may be the most favorable to service, due to the sale of the same amount of heat, with the least amount of connections, essentially making them 'cash cows'. Reducing the size of the system in this manner can also be economically favorable with regard to necessary equipment. However, excluding HT consumers from clean heat comes with the implication that they would continue to be responsible for the highest carbon emissions per unit area of the Dutch housing stock. A favorable approach may therefore be to incentivize the retrofitting of homes that are connected to the geothermal utility, increasing their energy efficiency through better insulation installations, to further the reach of clean heat and make it more accessible. In this way, the consumer base as a whole uses less and less heat, and it allows the district heating network to evolve gradually over time, satisfying more customers with less heat, and opening up additional opportunity for connections, furthering the mission of the energy transition.

6.2. Economics and LCoH

Thus far, the technicalities as to the implementation and functionality of GREGs have been explored. However, there would be significant costs associated with their implementation and installation. Conversely, their profitability associated with their functionality should also be explored. Therefore, it is necessary to detail the economic feasibility and return on this novel investment.

One of the main advantages to the design of GREGs is that they would essentially work as an add-on standalone element to a planned geothermal system, and they would require no intervention, or maintenance, as they would essentially run themselves. Therefore, the costs for heat pumps, drilling of geothermal wells, circulation pumps, and most of the operational expenditures of a geothermal project, up to the point of the control lifetime, may be circumvented under a very basic approach, as much of these expenses are already covered for by the geothermal project. Therefore the main costs associated with the installation of GREGs are the operational expenditures of running the geothermal project past the control model lifetime, and their drilling and installation expenditures. Their profitability could be determined by the amount of extra energy produced by the geothermal project due to their installation, which is weighed against their associated expenditures. However, it is also important to detail the cost of the system as a whole and compare it to the control scenario, as the lifetime extension of the GREGs may be maximized if they are installed at the inception of a geothermal project.

Therefore, for the determination of expenditures and profitability associated with GREGs, the 0.1m radius, 2km long GREG is used as an example, with the installation interval between 1950m and 3950m BLS, as seen in the dynamic studies, which will be compared to the control model scenario (no GREG) using Net Present Value (NPV) and Levelized Cost of Heat (LCoH) as economic indicators.

Given the details outlined in Section 2.2, regarding the installation procedure of the GREG, it can be assumed that the GREG follows nearly the same procedure of installation as a geothermal well casing, with the exception of plate welding at the top and bottom sections of the GREG. The majority of geothermal well installation costs are associated with the drilling and perforations into the crust [33]. Current drilling standards suggest that geothermal well perforations for casings up to 9 5/8 inches in diameter (or approximately 25 cm) are possible up to a depth of 10,000 meters [34], large and deep enough for the installation of the 0.1m radius, 2km long GREG, at a final depth of 3950m BLS. Therefore, the following equations are offered for the calculation of drilling costs, according to [35] and [36], respectively:

$$GeothermalWellCost_{2014} = 1.72 \times 10^{-7} \times MD^2 + 2.3 \times 10^{-3} \times MD - 0.62 \tag{6.1}$$

$$GeothermalWellCost_{2012} = S \times (0.2 \times MD^2 + 700 \times MD + 25000) \times 10^{-6} \tag{6.2}$$

where MD is the measured depth of the geothermal well in meters, geothermal well cost is in millions of U.S. dollars for [35], and millions of Euros in [36], and S is a scaling factor applied according to marken conditions [35] [36]. Using 3950 m as an input, we find that in 2014, the cost of completing one geothermal well was approximately 11.149 million dollars, according to Equation 6.1, which is assumed to include material cost, casing, and development of the well. After adjusting for inflation this value amounts to about 15.162 million dollars, or approximately 13.191 million euros in November 2025. Using Equation 6.2, which is also assumed to cover well development, results in a well cost of 8.866 million euros when using the default scaling factor of S = 1.5, as seen in [36], or 11.791 million euros when accounting for inflation since 2012. Updated formulas pertinent to November 2025 prices considering inflation and USD to Euro conversion rates from [35] [36] are offered as Equations 6.3 and 6.4, respectively:

$$GeothermalWellCost_{2025} = 1.36 \times 0.87 \times (1.72 \times 10^{-7} \times MD^2 + 2.3 \times 10^{-3} \times MD - 0.62) \tag{6.3}$$

$$GeothermalWellCost_{2025} = 1.33 \times S \times (0.2 \times MD^2 + 700 \times MD + 25000) \times 10^{-6} \tag{6.4}$$

It should be noted that these formulas may not accurately reflect drilling costs of today, as they are based on data and pricing from projects completed more than a decade ago. It is also possible that the relative

cost of drilling has not been maintained since this data was recorded, and depending on the country, these rates can rise and fall. Subsurface features to perforate also play a significant role in pricing, as some places are more difficult and therefore more expensive to drill than others. Additionally, the researchers in the study found difficulty in locating data relating to geothermal drilling costs due to the confidential nature of the industry [35].

To reiterate, the reason for investigating the drilling cost of a geothermal well is to extrapolate the information so that it may be used to roughly estimate the cost of installing a 0.1m radius GREG of 2km length, as the perforation dimensions would in theory clear these dimensions. Averaging the costs calculated using Equations 6.3 and 6.4, we find that the installation of a 2km long GREG to a depth of 3950 meters BLS, is approximately 12.491 million euros if drilling starts from the surface.

As an alternative to starting from the surface, the wellbore from the geothermal production site could possibly be dual-purpose, so that upon completion of the production well perforation of a new geothermal project, this pathway can serve as a starting position to drill the rest of the way down to 3950 m BLS for the installation of GREGs. This way, there is a cost saving in the initial 2km of drilling required for every installed GREG, as the first two kilometers already come included with the geothermal production well. Using the production well bore as a starting point would employ directional drilling to branch out from a distance above the top of the geothermal reservoir layer, which should be high enough to be able to straighten out by the beginning of the top of the geothermal reservoir, at a horizontal distance of 20 meters away from the original production bore, in the direction of the injection well. For example, in the study, the top of the reservoir is at 1950m BLS, in which case as an arbitrary example, the bore branching out of the production bore could start at a kick-off-point (KOP) of 1850m BLS, and be straighened out by 1950 m BLS, allowing for clearance enough for the GREG head to intercept the entire thickness of the geothermal reservoir, at a distance of 20 meters away from the production bore. This approach would imply additional costs attributed to directional drilling generally being more expensive than vertical drilling per unit length [37], however, if the drilling distance from 1850 m BLS to 1950 m BLS is assumed to be vertical, the final installation cost would have saved approximately 4.498 million euros, resulting in a final cost of approximately 7.993 million euros per GREG, when averaging between Equations 6.3 and 6.4.

Since the GREG model is to be compared to the control model, the cost of the geothermal utility must also be determined. Equations 6.3 and 6.4 are used to find the cost of the geothermal wells for this modeled project, which amounts to 5.145 million euros per well of 2050m measured depth, for a total of 10.290 million euros for the doublet. Other expenditures include the price of replacing pumping equipment, pump power, and operational expenditures. Pump efficiency is assumed to be 100% under the ideal scenario. Heat and electricity price are assumed to be 60, and 100 €/MWh, respectively, and the pump cost is assumed to be 500,000€, to be replaced every 5 years [25]. To calculate the final NPV, a 7% discount rate is also used, and it is assumed that operational expenditures are equal to 5% of the capital expenditures associated only with the geothermal doublet installation, since no operational expenditures are planned for the GREG. Using this information, the cash outflow can be calculated. A summary of parameters is provided in Table 6.11:

Table 6.11: Preferable Economic Parameters

Doublet CAPEX (€)	GREG CAPEX (€)	Pump OPEX (€)	Geo OPEX (% of Doublet CAPEX)	Pump Lifetime (yr)	Pump Efficiency (%)	Heat Price (€/MWh)	Electricity Price (€/MWh)	Annual Discount Rate (%)
10289954	7993000	500000	5	5	100	60	100	7

The expenditures are also dependent on pump rate, which is dependent on the pressure difference measured between the production well and the injection well. Pressures for injection and production were probed in the 2km long 0.1m radius GREG trial from the thermal conductivity dynamic study. Figure 6.7 denotes the evolution of the pressure at these two locations:

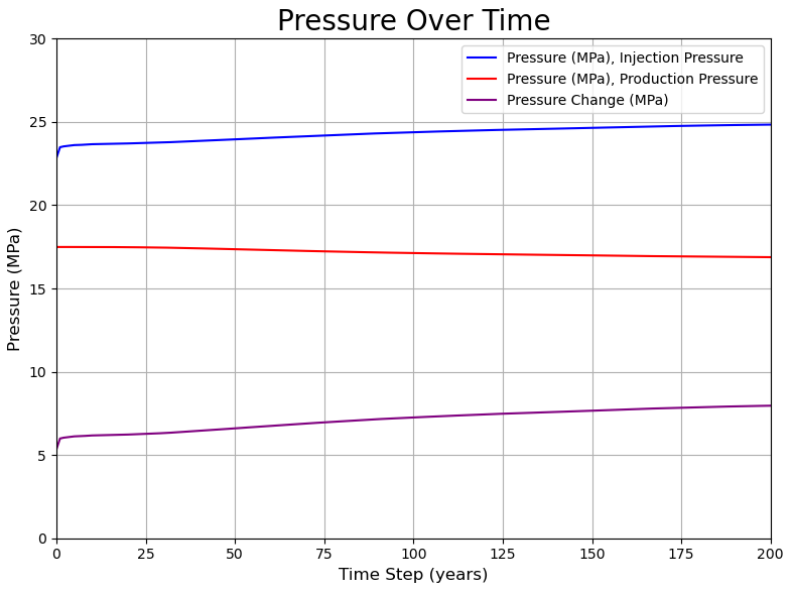

Figure 6.7: Pressure change between injection and production wells over simulation time.

The injection and production pressures fluctuated over time, affecting the pressure change between them. Therefore, pump power also changes over time. However, as a simplification, pressure difference was assumed to be the average pressure difference along the production lifetime, resulting in 6.354 MPa and 6.388 MPa, for the control scenario, and the implemented 0.1m radius 2km long GREG scenario, respectively. Pump power was therefore calculated according to Equation 6.5 using the average pressure change between these two values.

$$P_{Pump} = \frac{Q\Delta P}{\eta} \tag{6.5}$$

The final pump power only considers the pressure difference between the injection well and the production well, requiring a constant electrical power demand of 531 kW, amounting to a yearly cost in electricity of approximately 465,156€, assuming an electricity price of 100€/MWh. Once again, capital expenditure is only considered to be the drilling cost of the doublet, since the GREG will not require maintenance or operation. The produced energy every year does not change, resulting in a yearly cash inflow of approximately 4,581,481€, at a heat cost of 60€/MWh. Equations 6.6 and 6.7 are used to calculate Net Present Value (NPV) and Levelized Cost of Heat (LCoH), according to the cash inflows, outflows and energy produced:

$$NPV = \sum_{t=0}^{n} \frac{CF_t}{(1+r)^t} \tag{6.6}$$

$$LCoH = \frac{CAPEX + \sum_{t=o}^{n} OPEX_t}{\sum_{t=0}^{n} \frac{MWh_{produced,t}}{(1+r)^t}} \tag{6.7}$$

The results indicate that the net present value of the control project levels off at approximately 42.2 million euros, while the model which includes the GREG levels off at approximately 34.5 million Euros. The difference between these two values is approximately 7.993 million euros, which is the value of the additional up-front cost of the project which includes the GREGs. The reason for this is that the yearly operational expenditure for both projects is exactly the same, with the only difference being the additional years of accrued operational cost. Capital cost, however, is increased from 10.3 million euros to 18.3 million euros with the implementation of the GREG technology. Higher up-front costs are much more difficult to recover, and for this reason the GREG is not immediately more profitable under the current

setup and discount rate. The GREG scenario only becomes profitable at a discount rate of approximately 1%, which is not realistic. However, this does build up the case for later implementation of GREGs - if they were to be installed a few years after the drilling of the geothermal doublet, this would increase the NPV of the technology, and its economic feasibility. LCoH for the control is calculated at 23.28€/MWh till the end of year 61. For the GREG scenario, the LCoH is calculated at 30.16€/MWh.

This analysis does not take into consideration several variables which may also affect the economics of this study. For example, corrosion potential of GREG casing material may be quite high, due to dissolved substances in the geothermal reservoir and/or saturated underburden, such as dissolved carbon dioxide and brine, which are known to corrode commonly used casing material such as carbon steel over time [38]. Therefore, higher upfront costs may be attributed to the investment of higher quality GREG casing to resist corrosion. Additionally, if the GREG is unable to resist the chemistry of the subsurface over the duration of 66 years, operational expenditures in replacing the structure may also arise, aside from the necessary abandonment of the structure at the end of the geothermal lifetime. This may narrow down the applicability of GREGs to subsurface regions which are more chemically inert.

6.3. Future Work

This study served to develop the foundation for a new technology, which would provide energetic security by increasing lifetime of geothermal projects. Thus far, a general overview and approach has been provided, however, there remains much to be explored.

Modeling Natural Convection within the GREG

The researcher's main grievance is that this study could not be executed under a convective model, as this required a high level of computational resources that could not be secured. A significant amount of time and effort went into modeling this concept under the scope of natural convection as the main transport method of heat. Initially the GREG was considered to be a 2000 meter long hollow rectangle filled with water, with an arbitrary width of 5 meters, which included an aluminum wall of 1 meter thickness. This was modeled using a 2D COMSOL model, with laminar flow and heat transfer physics. The 2D domain also ultimately failed to correctly grasp the reservoir groundwater flows and subsequent heat transfer. After 2 weeks of simulating the convection problem, only about 430 hours of simulation time were recorded.

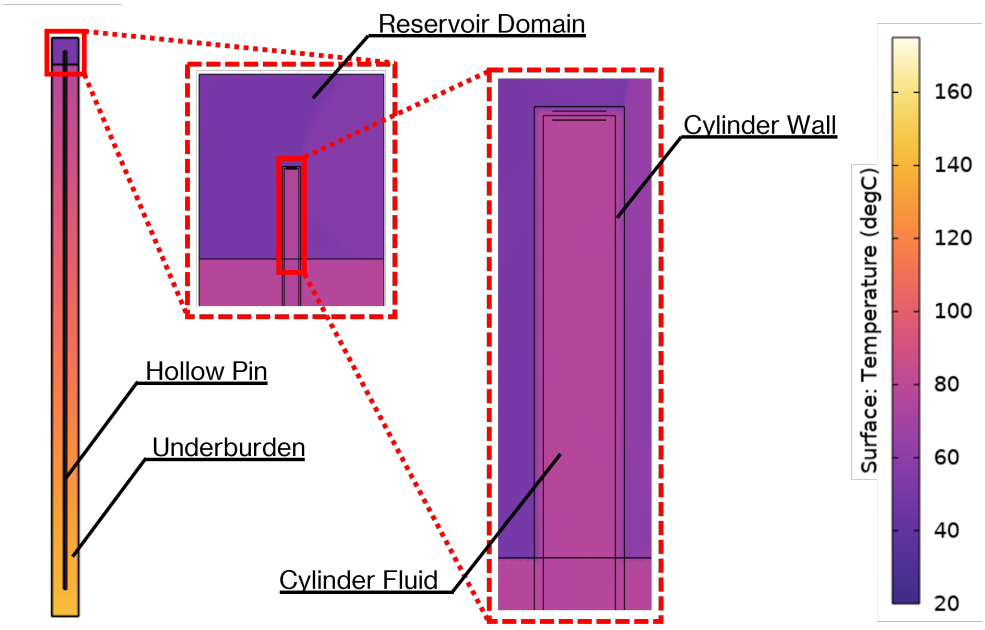

Figure 6.8: Summary of the 2D GREG model - before it was referred to as a GREG, it was simply called a pin.

A 2D axisymmetric COMSOL template model that probes natural convection does exist, and served as a good starting point, as it worked. This experiment, however, largely carried the same limitations of

groundwater flow modeling that the original 2D model had. The one benefit to this approach was its ability to output 3D results at a 2D computational cost. However, this computational cost was still exorbitant, and the model could not be extended to a height past 3 meters, as it would fail after this point. Essentially, it could not be applied to the GREG either. The solver's ability to work out the Navier-Stokes equations also seemed to be related to aspect ratios of the modeled fluid vessel.

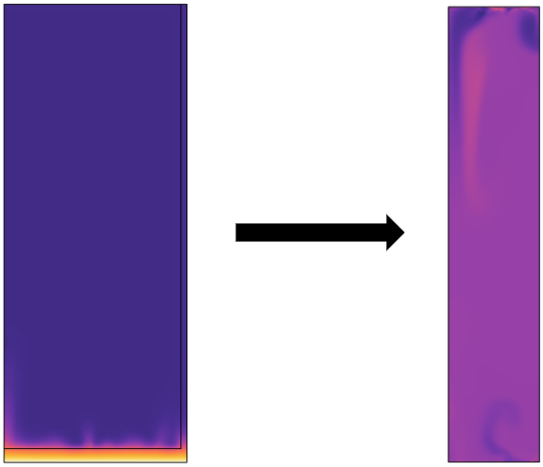

Figure 6.9: Slightly modified working glass cup model template (left) compared to repurposed working model using turbulent module at a height of 1m (right).

Up until this point, laminar flow had been assumed. However, eventually it was determined that the experimental setup would actually result in turbulent flows within the GREG. The laminar flow physics module in this example was replaced with the turbulent flow physics L-VEL module, which in some instances ran, but ultimately stopped working at slightly larger scales.

Several other methods were tried, such as testing 3D models, changing the solver type (which is supposedly better for large scale models), changing the amount of Newtonian iterations, and testing different boundary conditions. Most new tested models failed, and a select few never advanced to the first time step, which could mean that they were not broken, but would take a very long time to resolve.

The main takeaway, however, is that more computational ability is likely required to perform this kind of modeling. Students who are to undertake CFD studies should be properly briefed on the subject, and given the computational resources to pursue higher level studies such as these. This experimentation is lacking from truly yielding results pertaining to a more true performance of GREGs in a geothermal reservoir. The main advance that could be made for this study, is to model the dynamic studies using fluid dynamics-physics on GREGs that are fluid-filled, to capture the transient heat transfer between the underburden, the GREG and the reservoir, which operates through natural convection.

Alternatively, a scaled down model could be produced which would estimate the transient heat transfer between the underburden and the geothermal reservoir. It should be noted that in the experiments performed in this study, increasing thermal conductivity reached a plateau in geothermal lifetime benefits, and the underlying assumption is that natural convection would transfer heat faster than the GREGs under the tested high thermal conductivities. In this case, the material properties of the reservoir and the underburden became the limiting factors in the uptake and output of heat via the GREG. Running a natural convection model on GREGs would therefore serve to confirm or reject that assumption.

Alternative Setups

This study performed using conduction mainly focused on a geothermal system which exceeded a lifetime of 60 years. However, there are many more variables which may play a significant role in the geothermal lifetime:

- At a well spacing of 1km, GREGs added 5 years of geothermal lifetime. How would their performance change if the well spacing is increased or decreased from this level? It could be that the lifetime

increase is dependent on the projected lifetime of the geothermal utility, which is very dependent on well spacing. Would the added lifetime by GREGs be a set value, or would they scale with this projected lifetime?

- Subsurface conditions such as conductivity and heat capacity of the porous matrix of the underburden, as well as the geothermal reservoir play a significant role in transference of heat through the system. As subsurface properties change from place to place, this should be more closely studied - performance of GREGs may change via sensitivity analysis playing on these variables. Increasing/decreasing heat capacities and thermal conductivities of these materials could potentially affect results in significant ways. Additionally, the tested setup assumed that the underburden was a solid. How would changing this to a saturated porous material, which is more realistic, change the performance of the GREGs?
- The entire study was executed through thermally segregating of the reservoir and the underburden layer, using a thermal insulation boundary condition. The reason for this was to study the effect of tranferability of heat through the GREGs, unfettered by inter-layer communication. This of course, is unrealistic, and a more realistic model should be developed that takes these phenomena into account. A small trial was done which removed the thermal insulation between these two layers, and showed an equal lifetime increase in both the control model, and the GREG model (using 0.1m radius, 2km-long, 1E9 W/mK thermal conductivity setting trial). The lifetime change therefore remained at 5 years. This should be probed and confirmed.
- The production temperature charts seen in every study seem to indicate that the slope intensity settles over the long term. Could it be possible to design an array of GREGs around the production well that would make a geothermal system in a conduction-dominated reservoir last forever, through a leveling of production temperature above the cut-off point? A short analysis was done using the static model and it showed that this has potential - however, this result would be more valuable using the dynamic model. When attempting this on the larger dynamic model, however, adding multiple GREGs often broke the mesh, which remains unsolved. Additionally, the mesh should be better standardized under the single-GREG scenario, and experimentation may greatly benefit from finer absolute and relative tolerances.

Geometries

Obstruction of the geothermal breakthrough path plays a significant role in increasing the geothermal project lifetime, and this is a concept that while not incredibly pertinent to this study, should be considered further. This consideration of different geometries taking better advantage of flow path obstruction than a cylinder may result in additional insights regarding geothermal lifetime extension. However, there is a limit to this concept, and the differences in pressure between the production well and the injection well should be considered if testing different geometries.

Another angle to this concept would be to model the applicability of heat dissipation fins to the GREG. In this way, heat transfer into the geothermal reservoir could potentially be accelerated, resulting in immediate heat gains which could potentially benefit the geothermal production temperature and dependent lifetime. Installation procedure should be carefully considered, however, as a finned structure at this depth may be more difficult to install, and may result in higher implementation costs and capital expenditures.

7

Conclusion

The aim of this study was to explore a novel method of addressing thermal breakthrough, a subsurface phenomenon that limits the longevity of geothermal doublet production. This method was explored by modeling the behavior of long cylindrical structures that transfer heat into the geothermal reservoir, called Geothermal Reservoir Enhancing Geometries (GREGs), from the underburden. The majority of this study focused on optimization of the dimensions, placement and physical properties of GREGs, to maximize their capability in reheating thermal breakthrough for the purposes of maximizing doublet lifetime. The results indicate that geothermal system lifetime is mostly maximized when the GREG is placed near the production well. Additionally, increases in GREG temperature increase doublet lifetime, as well as radial dimension, although large structures are not technically feasible for deep subsurface installation. Conversely, more feasible, shorter radii GREGs exhibited nonlinear increases in heat flux per unit surface area. These results served to fulfill the first research objective, which was to find optimal GREG sizing and dimensions, which when applied to a modeled geothermal system, would maximize its lifetime.

Review of transient heat transfer under the scope of GREGs was limited to applying a range of thermal conductivities to the GREGs, testing them at different final depths and lengths within the model domain, and running a mesh refinement analysis to gain confidence in the data. Results show that GREGs tend to perform better with increases in thermal conductivity, indicated by higher fluxes and longer geothermal lifetimes. Additionally, increasing depth of GREGs has a slight benefit in geothermal lifetime increase, however, as later discussed, does not immediately warrant the additional economic cost. The energy stored within the underburden does however sustain performance of the GREGs throughout 200 years of simulated time, which fulfills the second research objective, that aimed to see what rates of heat output the underburden could sustain. The most technically feasible trial was able to increase the modeled geothermal utility lifetime by approximately 8.2%.

Economics of the novel means were also discussed, and it was determined that additional heat as a consequence of implemented GREGs could result in an additional 381,791 MWh of energy output from the geothermal utility during its extended lifetime. LCoH pertaining to a geothermal utility employing one singular 2km-long GREG of 0.1m radius amounted to approximately 30.16 €/MWh, which considered, drilling, material costs associated with the implementation of this technology, geothermal plant operational expenditures, electricity prices, heat prices, pump replacements, and a discount rate of 7%. Without the GREG, the control geothermal utility LCoH amounts to approximately 23.38€/MWh, however, loses 5 years in lifetime compared to the model which includes the GREG.

The extension of geothermal lifetime was also investigated within the context of changing projected heat demands. New projected consumers of heat would be more efficient in thermal energy use, as new constructions and buildings come equipped with higher rates of insulation. Lifetime of the control geothermal project was found to significantly increase when assuming the same consumer pool upgrading its insulation levels and reducing the necessary pump rates from the utility. However, when considering current vs projected scenarios, and a variable consumer demand, the addition of the GREG resulted in servicing the same geothermal utility consumer pool for 5 additional years. It also helped outline the necessity of retrofitting older, less energy efficient buildings which would make direct connections to the geothermal facility with improved insulation practices, which are projected to develop over the coming decades.

References

[1] World Meteorological Organization. *Weather-related disasters increase over past 50 years, causing more damage but fewer deaths*. 2021. URL: https://wmo.int/media/news/weather-related-disasters-increase-over-past-50-years-causing-more-damage-fewer-deaths#:~:text=The%20number%20of%20disasters%20has,deaths%20decreased%20almost%20three%2Dfold..

[2] U.S. Department of Energy. *Electricity Generation*. URL: https://www.energy.gov/eere/geothermal/electricity-generation#:~:text=Geothermal%20power%20plants%20draw%20fluids,reinjected%20back%20into%20the%20reservoir..

[3] U.S. Department of Energy. *Geothermal Basics*. URL: https://www.energy.gov/eere/geothermal/geothermal-basics#:~:text=Deep%20underground%2C%20the%20presence%20of,more%20about%20geothermal%20electricity%20generation..

[4] Anna Billerbeck et al. "Perception of district heating in Europe: A deep dive into influencing factors and the role of regulation". In: *Energy Policy* 184 (2024), p. 113860. DOI: https://doi.org/10.1016/j.enpol.2023.113860. URL: https://www.sciencedirect.com/science/article/pii/S0301421523004457.

[5] John W. Lund. "Direct Utilization of Geothermal Energy". In: *Energies* 3.8 (2010), pp. 1443–1471. DOI: 10.3390/en3081443. URL: https://www.mdpi.com/1996-1073/3/8/1443.

[6] BBC. *Geothermal energy*. URL: https://www.bbc.co.uk/bitesize/articles/zp362v4#zt9phcw.

[7] Mohammed Adil Sbai et al. "Analyzing the relationship between doublet lifetime and thermal breakthrough at the Dogger geothermal exploitation site in the Paris basin using a coupled mixed-hybrid finite element model". In: *Geothermics* 114 (2023), p. 102795. DOI: https://doi.org/10.1016/j.geothermics.2023.102795. URL: https://www.sciencedirect.com/science/article/pii/S0375650523001499.

[8] Violaine Gascuel et al. "Deep geothermal doublets versus deep borehole heat exchangers: A comparative study for cold sedimentary basins". In: *Applied Energy* 361 (2024), p. 122826. DOI: https://doi.org/10.1016/j.apenergy.2024.122826. URL: https://www.sciencedirect.com/science/article/pii/S0306261924002095.

[9] Mukhtar A. Kassem et al. "Navigating risk in geothermal energy projects: A systematic literature review". In: *Energy Reports* 13 (2025), pp. 696–712. DOI: https://doi.org/10.1016/j.egyr.2024.12.052. URL: https://www.sciencedirect.com/science/article/pii/S2352484724008667.

[10] Qitao Zhang et al. "Downhole flow control: A key for developing enhanced geothermal systems in horizontal wells". In: *Renewable Energy* 237 (2024), p. 121578. DOI: https://doi.org/10.1016/j.renene.2024.121578. URL: https://www.sciencedirect.com/science/article/pii/S096014812401646X.

[11] Sai Liu et al. "Review of Techniques to Mitigate Thermal Breakthrough in Enhanced Geothermal Systems". In: *Preprints* (May 2025). DOI: 10.20944/preprints202505.0422.v1. URL: https://doi.org/10.20944/preprints202505.0422.v1.

[12] Ladislaus Rybach et al. "At what time scale are geothermal resources renewable?" In: *Proceedings World Geothermal Congress* (Jan. 2000).

[13] Henry N. Pollack et al. "Heat flow from the Earth's interior: Analysis of the global data set". In: *Reviews of Geophysics* 31.3 (1993), pp. 267–280. DOI: https://doi.org/10.1029/93RG01249. URL: https://agupubs.onlinelibrary.wiley.com/doi/abs/10.1029/93RG01249.

[14] Ladislaus Rybach. "Geothermal Sustainability". In: *Geo-Heat Centre Quarterly Bulletin* 28 (Jan. 2007).

[15] Rijksdienst voor Rndernemend Nederland. *Energy label for commercial buildings*. URL: https://www.rvo.nl/onderwerpen/wetten-en-regels-gebouwen/energielabel-utiliteitsgebouwen.

[16] *energy label*. URL: https://www.joostdevree.nl/shtmls/energielabel.shtml#1.

[17] Ministerie van Volkshuisvesting en Ruimtelijke Ordening. *National Insulation Program*. URL: https://www.volkshuisvestingnederland.nl/onderwerpen/nationaal-isolatieprogramma.

[18] R.J.M Niessink. *Heat networks low temperature households (district heating)*. 2019. URL: https://energy.nl/data/heat-networks-low-temperature-households-district-heating/.

[19] D. Bonté et al. "Subsurface temperature of the onshore Netherlands: new temperature dataset and modelling". In: *Netherlands Journal of Geosciences - Geologie en Mijnbouw* 91.4 (2012), pp. 491–515. DOI: 10.1017/S0016774600000354.

[20] T.E Lokhorst A. Wong. *Geology of the Netherlands*. Routledge, 2007. URL: https://www.aup.nl/en/book/9789463728362/geology-of-the-netherlands.

[21] NLOG. *Geological Report TW OK II*. 2012. URL: https://www.nlog.nl/sites/default/files/2021-08/200331_bijlage_6_-_geologisch_rapport_wp_naaldwijk_i_gelakt.pdf.

[22] Innovation News Network. *Producing geothermal energy in the Delft Subsurface Urban Energy Lab*. 2023. URL: https://www.innovationnewsnetwork.com/producing-geothermal-energy-delft-subsurface-urban-energy-lab/32725/#:~:text=The%20geothermal%20project%20is%20at,via%20a%20large%20heat%20pump..

[23] Cees J.L. Willems et al. "Geology of the Upper Jurassic to Lower Cretaceous geothermal aquifers in the West Netherlands Basin – an overview". In: *Netherlands Journal of Geosciences* 99 (2020), e1. DOI: 10.1017/njg.2020.1.

[24] Alexandros Daniilidis et al. "Risk assessment of the Groningen geothermal potential: From seismic to reservoir uncertainty using a discrete parameter analysis". In: *Geothermics* 64 (Nov. 2016), pp. 271–288. DOI: 10.1016/j.geothermics.2016.06.014.

[25] Alexandros Daniilidis et al. "Interference between geothermal doublets across a fault under subsurface uncertainty; implications for field development and regulation". In: *Geothermics* 91 (2021), p. 102041. DOI: https://doi.org/10.1016/j.geothermics.2021.102041. URL: https://www.sciencedirect.com/science/article/pii/S0375650521000018.

[26] Michael Lewis. "Chapter 6 - Physical concepts". In: *Food Process Engineering Principles and Data*. Ed. by Michael Lewis. Woodhead Publishing, 2023, pp. 37–46. DOI: https://doi.org/10.1016/B978-0-12-821182-3.00030-3. URL: https://www.sciencedirect.com/science/article/pii/B9780128211823000303.

[27] Jianfeng Yu et al. "7 - Efficiency testing methods for centrifugal pumps". In: *Electrical Motor Products*. Ed. by Jianfeng Yu et al. Woodhead Publishing, 2011, pp. 125–172. DOI: https://doi.org/10.1533/9780857093813.125. URL: https://www.sciencedirect.com/science/article/pii/B9780857090775500074.

[28] C. Gürsan et al. "District heating with complexity: Anticipating unintended consequences in the transition towards a climate-neutral city in the Netherlands". In: *Energy Research Social Science* 110 (2024), p. 103450. DOI: https://doi.org/10.1016/j.erss.2024.103450. URL: https://www.sciencedirect.com/science/article/pii/S2214629624000410.

[29] Compendium voor de Leefomgeving. *Energielabels van woningen, 2010 t/m 2024*. 2025. URL: https://www.clo.nl/indicatoren/nl055611-energielabels-van-woningen-2010-tm-2024.

[30] Mike Langen. *Housing market monitor - Energy transition*. 2025. URL: https://www.abnamro.com/research/en/our-research/housing-market-monitor-energy-transition.

[31] Geemente Amsterdam. *The Amsterdam Heat Guide*. 2020. URL: https://openresearch.amsterdam/en/media/inline/2020/12/3/the_amsterdam_heat_guide.pdf.

[32] Anika Batenburg et al. *Unequal household vulnerability to high energy prices and the elusive quest for targeted policy support: Evidence from the Netherlands*. 2025. URL: https://publications.tno.nl/publication/34643908/dfEuw9ne/TNO-2025-R10499.pdf.

[33] B.R. van Dongen. *The economic potential of deep, direct use geothermal systems in the Netherlands*. 2019. URL: https://repository.tudelft.nl/record/uuid:4b1f0f67-f990-4e7e-a4be-104bdf07ebdc.

[34] Massechussets Institute of Technology Panel. *The Future of Geothermal Energy - Impact of Enhanced Geothermal Systems (EGS) on the United States in the 21st Century*. 2006. URL: https://www1.eere.energy.gov/geothermal/pdfs/future_geo_energy.pdf.

[35] Maciej Z. Lukawski et al. "Cost analysis of oil, gas, and geothermal well drilling". In: *Journal of Petroleum Science and Engineering* 118 (2014), pp. 1–14. DOI: https://doi.org/10.1016/j.petrol.2014.03.012. URL: https://www.sciencedirect.com/science/article/pii/S0920410514000813.

[36] J.-D. van Wees et al. "Geothermal aquifer performance assessment for direct heat production – Methodology and application to Rotliegend aquifers". In: *Netherlands Journal of Geosciences - Geologie en Mijnbouw* 91.4 (2012), pp. 651–665. DOI: 10.1017/S0016774600000433.

[37] JSM Civils PTY LTD. *Directional Drilling vs. Traditional Methods: Which is Right for Your Project?* 2024. URL: https://www.jsmcivils.com.au/resources/directional-drilling-vs-traditional-methods-which-is-right-for-your-project.

[38] TNO. *Corrosion in Dutch geothermal systems*. 2016. URL: https://www.nlog.nl/sites/default/files/2016.03.15_tno%202015%20r10160_corrosion%20in%20dutch%20geothermal%20systems_public.pdf.